To the Graduate Council:

I am submitting herewith a thesis written by Yaw Boateng-Poku entitled "Testing and Modeling of Subgrade Resilient Moduli for Tennessee Soils." I have examined the final copy of this thesis for form and content and recommend that it be accepted in partial fulfillment of the requirements for the degree of Master of Science, with a major in Civil Engineering.

Eric C. Drumm

Eric C. Drumm, Major Professor

We have read this thesis and recommend its acceptance:

William F. Kane

Accepted for the Council:

CW Minkel

Vice Provost
and Dean of The Graduate School

STATEMENT OF PERMISSION TO USE

In presenting this thesis in partial fulfillment of the requirements for a Master's degree at the University of Tennessee, I agree that the library shall make it available to borrowers under rules of the library. Brief quotations from this thesis are allowable without special permission, provided acccurate acknowledgment of the source is made.

Permission for extensive quotation from or reproduction of this thesis may be granted by my major professor, or in his absence, by the head of Interlibrary Services when, in the opinion of either, the propsed use of the material is for scholarly purposes. Any copying or use of the material in this thesis for financial gain shall not be allowed without my written permission.

Signature Yaw Boateng-Poku

Date July 29, 1988

TESTING AND MODELING OF SUBGRADE RESILIENT MODULI FOR TENNESSEE SOILS

A Thesis

Presented for the

Master of Science

Degree

The University of Tennessee, Knoxville

Yaw Boateng-Poku

August 1988

in memory of my father, and dedicated to my mother

ACKNOWLEDGEMENTS

The author is highly indebted to, and wishes to thank Dr. Eric C. Drumm for his sponsorship and supervision of his graduate studies and research. Without his advise, guidance, patience and criticism this thesis would not have been halfway what it is. The author also wishes to thank the Tennessee Department of Transportation for funding the research. Special appreciations and thanks are extended to Dr. William F. Kane who joined the Civil Engineering faculty at about the same time the author started the research, for his advice and words of encouragement, and also for serving on the author's committee. Special thanks go to Prof. A. B. Moore who was also involved in this research, for his advises and also for serving on the author's committee.

The author wishes to thanks Mr. Curtis Allin, the Civil Engineering laboratory technician for his paternal words of encouragement, readiness to share his knowledge, time and laboratory facilities. Special recognition is given to Ms. Teresa D. Johnson, who started and worked on the first phase of the research for this thesis. The author wishes to express his special appreciations to the Civil Engineering Department and staff, especially to those in Berry Hall, for renderir.g all assistances within their reach without hesitation to make the research and this thesis possible.

The author wishes to thank his family, Janice, Rika and Whitney for enduring the numerous hours the author had to work on this thesis. Special appreciation goes to his mother for her prayers for a guiding light for the author living far away from home.

ABSTRACT

A flexible pavement generally made up of three basic layer which are, the asphaltic concrete, the granular base and the subgrade soil. The subgrade layer has been found to contribute significantly to the total deformation of a pavement subjected to traffic wheel load. The resilient deformation of the subgrade layer has been found to a good indicator of the pavement performance. In order to accurately predicted the behavior of the in-service subgrade, the resilient modulus, a parameter obtained by the ratio of the deviator stress to the axial strain, has been accepted to indicate a soil's resilience response under repeated loading.

A laboratory testing program was implemented to determined the resilient moduli of widely used subgrade soils in the state of Tennessee. The tests were conducted according to the Tennessee Department of Transportation 207.04 specifications and the AASHTO T274 test method requirements. Standard laboratory tests were conducted to obtain the index properties of the soils. Using an X - Y plotter as data aquisition device, and cyclic triaxial test setup, repeated load tests were performed over a range of deviator stress to determine the resilient moduli of the selected soils.To characterize the resilient response of the soils, a plot of the resilient modulus versus deviator stress for each test specimen was obtained.

Modified hyperbolic equations were used to model the non-linear resilient modulus versus deviator stress response. Hyperbolic equations were also obtained for the stress-strain relationship for the unconfined compression test. Using the hyperbolic parameters from the repeated load tests as the dependent variables and the index properties and stiffness from the unconfined compression test as independent variables, regression equation were obtained for prediction of the measured curves. The breakpoint resilient modulus, E_{ri}, at 6 psi deviator stress, was also predicted for each measured curve selected since this indicator of resilient modulus is often in pavement design.

TABLE OF CONTENTS

CHAPTER PAGE

LIST OF TABLES

LIST OF FIGURES

FIGURE PAGE

CHAPTER I
INTRODUCTION

A flexible pavement is generally made up of three layers, which are asphaltic concrete, the granular base, and the subgrade soil. A schematic diagram of the multilayer system is shown in Figure I-1.

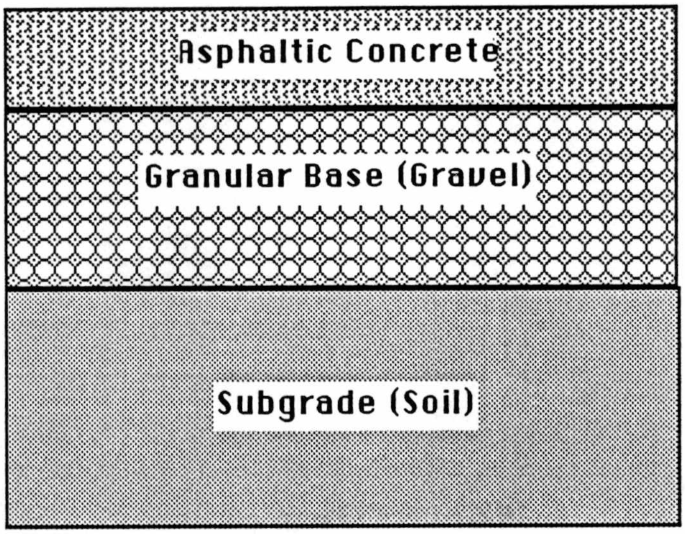

Figure I-1. Generalized Multilayer Pavement System .

The subgrade soil layer contributes significantly to the total deformation of the pavement system. The deformation of the in-service multilayer pavement system due to repetitive wheel loads is composed of two parts: the irrecoverable permanent, or plastic, deformation and the recoverable resilient, or elastic, deformation. For adequately designed flexible pavement, the major component of the deformation is the resilient component since the permanent or plastic deformation is very small (Robnett and Thompson, 1973). The resilient modulus characterize a soil behavior under repeated loading conditions. Until recently, the moduli of unbound flexible pavement materials have been treated as parameters of constant magnitude. Recent research in dynamic characterization has shown that many pavement materials are stress dependent

(Moossazadeh and Witczak, 1981). Due to the importance of the subgrade modulus in the overall performance of the flexible pavement, the most accurate assessment of modulus is essential to the successful design of a pavement system.

In order to accurately predict the pavement performance in service, analytical approaches based upon methods such as the multilayer linear elastic theory can be employed. The multilayer elastic theory incorporates the following assumptions (Yoder and Witczak, 1975):

1. Each layer is homogenous
2. Each layer has a finite thickness
3. Each layer is isotropic
4. Full friction is developed between layers at each interface
5. Surface shearing forces are not present at the surface
6. The stress solutions are characterized by two material properties for each layer. These are Poisson's ratio and the elastic modulus

Through the assumptions of isotropy, homogeneity and linear elasticity, the stress-strain behavior, the state of stress, strain, and displacement in any material can be evaluated. The resilient modulus, E_r, is a dynamic response parameter defined by the ratio of a soil's axial deviator stress (σ_d) to the recoverable axial strain (ε_r). This parameter is determined from laboratory dynamic or repeated triaxial loading tests. The axial stress (σ_1), is applied to the top of the sample simultaneously with a confining stress or chamber pressure (σ_3). The deviator stress is the difference between the axial and the confining stresses. The recoverable axial strain (ε_r), is also measured in the process. A schematic diagram of the cyclic loading and how the resilient modulus is obtained is shown in Figure I-2. The resilient modulus of cohesive materials generally decreases with increasing deviator stress and is referred to as "stress-softening" behavior;

the modulus of cohesionless materials increases with increasing deviator stress and is referred to as "stress-hardening" behavior.

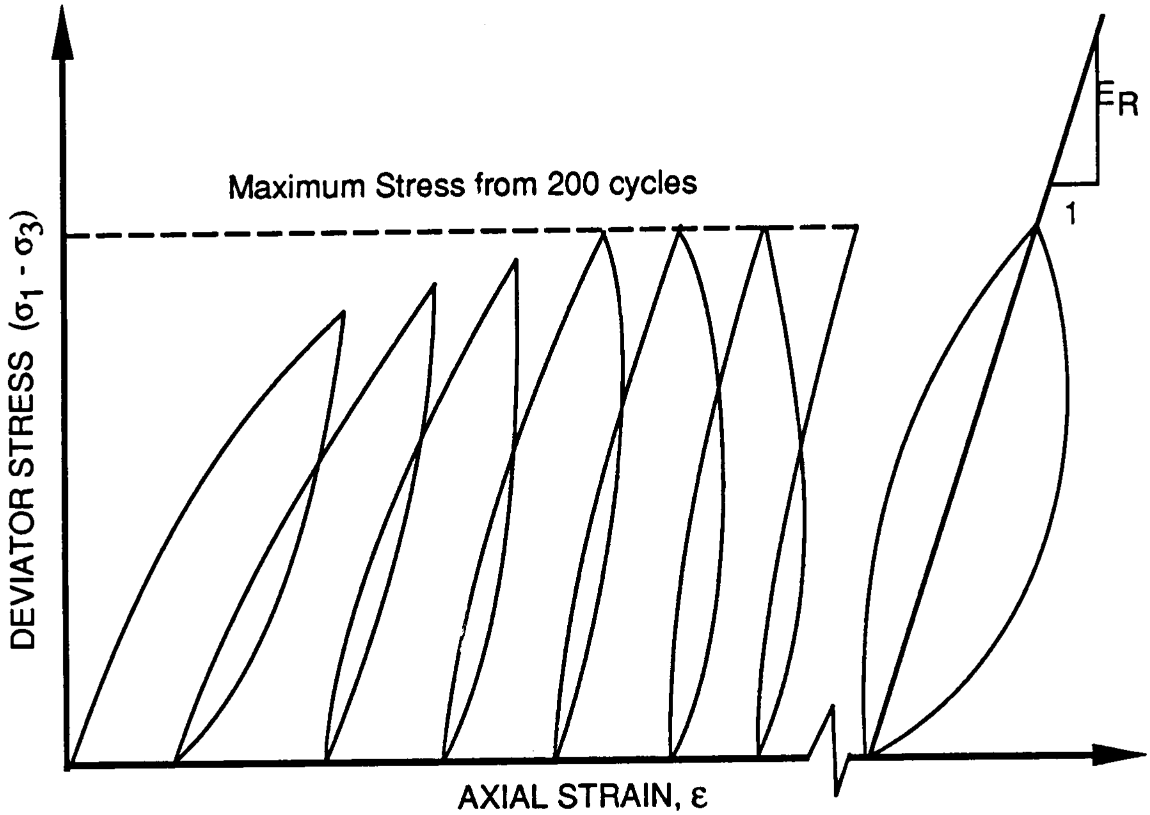

Figure I - 2. Schematic Stress-Strain Diagram For Repeated Load Triaxial Testing.

The results of the laboratory tests are used to determine the resilient modulus by the following equation:

$$E_r = \sigma_d/\varepsilon_r$$

Where E_r = the resilient modulus

σ_d = the deviator stress $(\sigma_1 - \sigma_3)$

ε_r = the recoverable or elastic strain

An early pavement design procedure recommended by the American Association of State Hghway and Transportation Officials (AASHTO) was based on the extensive American Association of State Highway Officials (AASHO) Road Test conducted in Ottawa, Illinois in the late 1950's and early 1960's. To make the flexible-pavement design equation obtained after the test applicable to a variety of environmental conditions, the concepts of a soil support (S) scale and a regional factor (R) were introduced. The latter was to account for the effect of various climatic conditions other than those found at the Road Test site. Due to the arbitrary manner in which the soil support (S) scale was introduced into the AASHTO design procedure, the input values could not be experimentally determined (Yoder and Witzcak, 1975).

The new American Association of State Highway and Transportation Officials (AASHTO) Design Guide now requires the use of the resilient modulus in pavement design as the method for evaluating soil support (AASHTO, 1986). The Design Guide, states that the resilient modulus can be used directly for the design of flexible pavements, but in the design of rigid or composite pavements it must be converted to a modulus of subgrade reaction (k-value). Each design agency using the Guide is advised to establish correlations between standard soil tests such as the California Bearing Ratio test (CBR) and triaxial strength tests to obtain the design resilient modulus as needed. The resilient modulus was selected to replace the soil support (S) value used in the early editions of the Design Guide for the following reasons (AASHTO, 1986):

1. Resilient modulus is a basic material property which can be used in the mechanistic analysis of multilayered systems for predicting roughness, cracking, rutting, faulting, etc.
2. It has been recognized internationally as the method for characterizing materials for use in pavement design and evaluation

3. Techniques are readily available for estimating the resilent modulus properties

The Design Guide suggest that agencies implement an experimental program to obtain reliable resilience results. A range of soil types, degrees of saturation, and densities should be examined critically in the testing program to identify their important effects. In the absence of test data on resilient modulus, the Guide reports suitable correlations for estimating the resilient modulus from tests such as the CBR, R-value, and soil index properties test results. A reported correlation between the Corps of Engineers CBR value, using dynamic compaction, and in situ modulus of soil is the following (Heukelom and Klomp, 1962):

$$E_r \text{ (psi)} = 1500 \times \text{CBR}$$

where E_r = resilient modulus

CBR = California Bearing Ratio

The range of the data from which this correlation was developed yielded E_r values from 750 to 1500 times CBR. This relationship is reasonable for fine-grained soils with a soaked CBR of 10 or less. Relationship has also been developed between the resilient modulus and the R-value (The Asphalt Institute, 1982):

$$E_r \text{ (psi)} = A + B \times (\text{R-value})$$

Where A = 772 to 1155

B = 369 to 555

R = regional factor

The AASHTO Guide proposes that for fine-grained soil with R-value less than or equal to 20, the following equation should be used until designers or agencies develop their own resilient modulus design data:

$$E_r\,(\text{psi}) = 1000 + 555 \times (\text{R-value})$$

E_r = resilient modulus

R-value = regional factor

It should be noted that these approximate relationships yield a singular value for resilient modulus that is independent of stress state. For completeness of design requirements for flexible pavements in the absence of other correlations, the Design Guide has provided the equations shown in Table I - 1 for unbound granular materials, that is base and subbase layer materials.

Table I - 1. AASHTO Equations for E_r for Unbound Granular Materials (after AASHTO, 1986).

θ (psi)	E_r (psi)
100	740 x CBR or 1000 + 780 x R
30	440 x CBR or 1000 + 450 x R
20	340 x CBR or 1000 + 350 x R
10	250 x CBR or 1000 + 250 x R

Where θ = sum of principal stresses

$= \sigma_1 + \sigma_2 + \sigma_3$

E_r = resilient modulus

CBR = California Bearing Ratio

R = regional factor

The sum of the principal stresses, θ, is a measure of the state of stress, which is a function of pavement thickness, load, and the resilient modulus of each overlaying layer (AASHTO, 1986).

The primary purpose of this study, conducted at the University of Tennessee, was to determine the resilient properties of soils widely used in the state of Tennessee as pavement subgrade materials. It was desired to obtain correlations between results of simpler tests and the resilient moduli of the soils. The simpler tests methods considered in the study are the Atterberg limits, Standard Proctor Test, and the unconfined compression test. This is in line with the AASHTO proposal that agencies using the Design Guide establish correlations between standard soil tests and the resilient moduli.

CHAPTER II

PREVIOUS RESEARCH

The need for proper design and evaluation of structural pavement has led to extensive research on the resilient properties of pavement materials. Attention was given to the resilient properties of subgrade materials after a landmark research study by the Washington Association of State Highway Officials revealed that for a typical flexible pavement, the subgrade layer contributes 60-70% of the pavement deflection under an 18 kips single axle load (WASHO, 1955). The American Association of State Highway Officials Road Test produced similar results (AASHO, 1962). The latter test showed that for a typical pavement subjected to an 18 kip single axle load, the deflection contributed by the subgrade is apprpximately two-thirds of the surface deflection. Field studies in Canada indicated that good performance beyond a period of 10 years is not obtained for flexible pavements carrying more than 1000 vehicles per day per lane if spring rebound deflections greater than 0.05 inch are experienced (Canadian Good Roads Association, 1967). The most commonly used laboratory test for subgrade evaluation, the California Bearing Ratio (CBR) Test, ASTM D1883 and AASHTO T193 procedures have been found inadequate for the subgrade support of fine-grained soils subjected to repeated, rapidly applied loads of short duration (Robnett and Marshall, 1973).

The Transportation Research Board's Committee on Strength and Deformation Characterization of Pavement Sections gives a practical guide for laboratory resilience tests (Barksdale, et al., 1975). A comparison shows that the AASHTO Design Guide method for the determination of resilient modulus, AASHTO T274-82 was adopted from the TRB's pioneering study. It was observed in the study that a compaction process that causes shearing deformation in a clay soil having a degree of saturation greater than 80% results in a dispersed (or parallel) clay structure. Clays having this structure exhibit greater deformation than the same clay soil with a flocculated (random) structure and lower degree of saturation when tested under the same conditions. Thus, compaction method and water content significantly affect the resilient response. General criteria to be used in the selection of the appropriate compaction conditions for clay soils are outlined as follows (Barksdale et al., 1975):

1. If the field compaction conditions and the in-service water content are both expected to remain less than the 80% saturation value, any of the standard impact, gyratory, kneading, or static procedures may be used to simulate the in-service condition.
2. If the field compaction conditions and the in-service water content are both expected to remain greater than the 80% saturation value, then the compaction process must be of the shearing type. An impact, gyratory, or kneading process must be used to simulate the dispersed structure in service.
3. If the the field compaction conditions will be at a water content less than 80% of the saturation water content and the in-service water content are expected to result in a degree of saturation greater than 80%, the static compaction process must be used to simulate the flocculated structure in service.

Granular soil specimens present difficulties in preparation and handling. However, if the granular soil has enough cohesion to permit handling, the methods described for cohesive soils can be used. Soil structure, has a small effect on most granular soils, except some silts which exhibit strength properties that depend on compaction conditions (Barksdale et al., 1975). Granular materials are easily compacted by use of a split mold mounted on the base of the triaxial cell with the samples compacted in layers of 1 to 1.5

inches thick using devices such as a vibrating hand operated air hammer. A vacuum is applied to prevent collapse of the sample before the mold is removed.

When a wheel load passes over an element of pavement material, there is a simultaneous increase in both the major and minor principal stresses. Only the variation in the major principal stress is considered essential in resilient modulus testing (Barksdale et al., 1975). Studies concluded that the actual stress pulse applied by a moving wheel load is close to a half sine in shape (Barksdale et al., 1975). However, triangular, sinusoidal, and half sine pulses can be used to simulate the actual in-situ stress provided care is taken in selecting the magnitude and duration of the pulse. No specific cyclic loading rate was found to be optimal. Environmental factors, such as spring and summer temperatures on conventional flexible pavement, dictate that the duration of the stress pulse changes with the element location, or point of loading, and the vehicular speed. A practical guide for selecting the duration of stress pulse when performing a resilience or repeated load test is provided (Barksdale et al., 1975).

The resilient modulus is affected by a wide spectrum of factors. There is no single value for the resilient modulus of a soil since the modulus is affected by many factors throughout the life of the pavement. For fine-grained soils, parameters such as degree of saturation and volumetric moisture content account for a substantial portion of the variability in the resilient properties (Marshall and Robnett, 1976). The resilient modulus of coarse-grained materials are affected by factors such as confining pressure, density, particle angularity or surface roughness, clay content, and degree of saturation (Hicks and Monismith, 1971). A summary of the factors effecting the resilient behavior of a material as reported by several researchers are as listed in Table II-1 (Thorton and Elliott, 1987).

All the factors listed are covered by the ASSHTO T274-82 test specifications and controlled by material properties with the exception of density and the degree of saturation. The latter two parameters depend on the researcher and the condtions the test is to simulate. A review of the Illinois test results showed that moisture content is very

Table II - 1. Factors Affecting the Resilient Modulus, Er
(after Thorton and Elliot, 1986).

Factor	Effects on Er
Stress duration	Er increases slghtly when the time of load application is reduced
Frequency	Er increases with increase frequency of load application
Grain size	Er, moisture content and density relation is dependent on soil type
Saturation	Er decreases with increasing degree of saturation
Confining pressure	Increases in the confining pressure result in large increases in Er
Deviator Stress	In coarse grain soils, deviator stress level has little effect on Er so long as the sample has little plastic deformation. For fine-grained Er decreases with increasing deviator stress

important. A considerable decrease in the resilient modulus from 11 ksi to 4 ksi resulted when the optimum moisture content was increased by 2%. Density was found not to be very crucial, although, higher densities were found to result in somewhat higher resilient moduli (Robnett and Marshall, 1973). From a study on Tilbury clay shown in Figure II - 1, it was deduced that 5 or 6 cycles of repeated load are sufficient to deterrmine the resilient modulus (Soderman et al., 1968).

In a research on lime-stabilized laterite, the ultimate unconfined compressive strength was found to increase when compression tests are performed after samples have been subjected to dynamic load applications (Akoto, 1986). Younger samples can have ultimate confined compressive strengths greater than older samples once they have been subjected to repeated loading before the determination of the unconfined compressive strength (Akoto, 1986). Samples subjected to dynamic tensile tests may have ultimate unconfined compressive strength greater than similar samples subjected to dynamic compressive loading (Akoto, 1986). The Tennessee Department of Transportation Specification 207.04 sets minimum values for the moisture content and dry density for field compaction conditions (TNDOT, 1981).

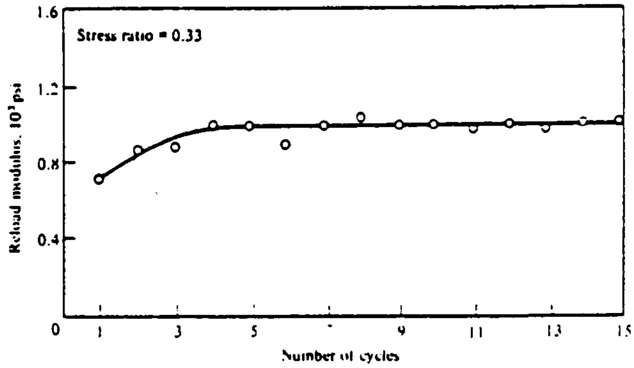

Figure II - 1. Variation in Reload Modulus with Number of Cycles (after Soderman et al., 1968).

Climatic factors have also been found to effect the resilient modulus of a subgrade. One of these factors is the amount of rainfall. Changes in subgrade moisture content cause changes in volume and in the strength characteristics of the subgrade soils. The influx of moisture during a rain results in an increase of pavement deflection and decrease in bearing capacity. Hypotheses postulated to explain the phenomena include a build up of hydrostatic pressure, capillary pressure, osmotic pressure, chemical reactions, and temperature gradients (Bandyopaddhyay and Frantzen, 1983). Research has been conducted to examine the feasibility of statistically relating the variation in subgrade modulus with the corresponding time history of precipitation in northeast Kansas. It was concluded that the extent of the variation in subgrade modulus will depend on the geotechnical properties of the subgrade soils and topography, as well as being directly affected by precipitation. The time required for the subgrade to reach its weakest state after a rainfall is quite long, and depending on local factors, might take as long as three weeks (Bandyopaddhyay and Frantzen, 1983).

Another climatic factor which immensely affects the resilient modulus of subgrade soil is the freezing and thawing cycle. In an Illinois study on effects of lime treatment on resilient modulus of fine-grained soils, it was found that one freeze-thaw cycle produce a large reduction in the resilient modulus of a subgrade soil (Robnett and Thompson, 1976), Figure II - 2. The decrease in the modulus is caused by the freezing of water, resulting in an increase volume and subsequent increase in void space. This produces larger strains and causes the reduction in the modulus. Studies on the effect of freezing and thawing on resilient modulus show a wide variation in the supporting capacity of subgrade materials in areas of seasonal frost. Analysis of data from one of such areas and laboratory repeated load tests have been conducted and the resilient characteristics successfully determined as function of imposed stresses, soil moisture tension, dry density, and temperature (Cole et al., 1981). Researchers at the U. S. Army Cold Regions Research and Engineering Laboratory have developed triaxial testing equipment to simulate the freeze-thaw recovery process in the laboratory that tests the soil at moisture tension levels several times that corresponding to field observations (Cole et al., 1985).

Research into factors affecting the results of cyclic triaxial testing in the laboratory has also been conducted and reported in the literature. The conventional earth platens, or the porous stones used at the ends of the specimen during testing, have been found to develop frictional forces (Sarby et al., 1980). The frictional forces restrain radial deformation and causes non-uniform loading of the specimen. One approach to overcome the problem is to test samples with a height-to-depth ratio of 2 to 3 so that specimen deformation is approximately uniform over the middle portion of the specimen. The other method is to use lubricated plattens so that lateral restraints are not developed (Sarby et al., 1980). In triaxial tests using lubricated plattens to determine the true elastic properties of soils, up to 80% of the the recorded axial deflection may be due to the compressibility of the free ends which is termed bedding errors (Sarby et al., 1980).

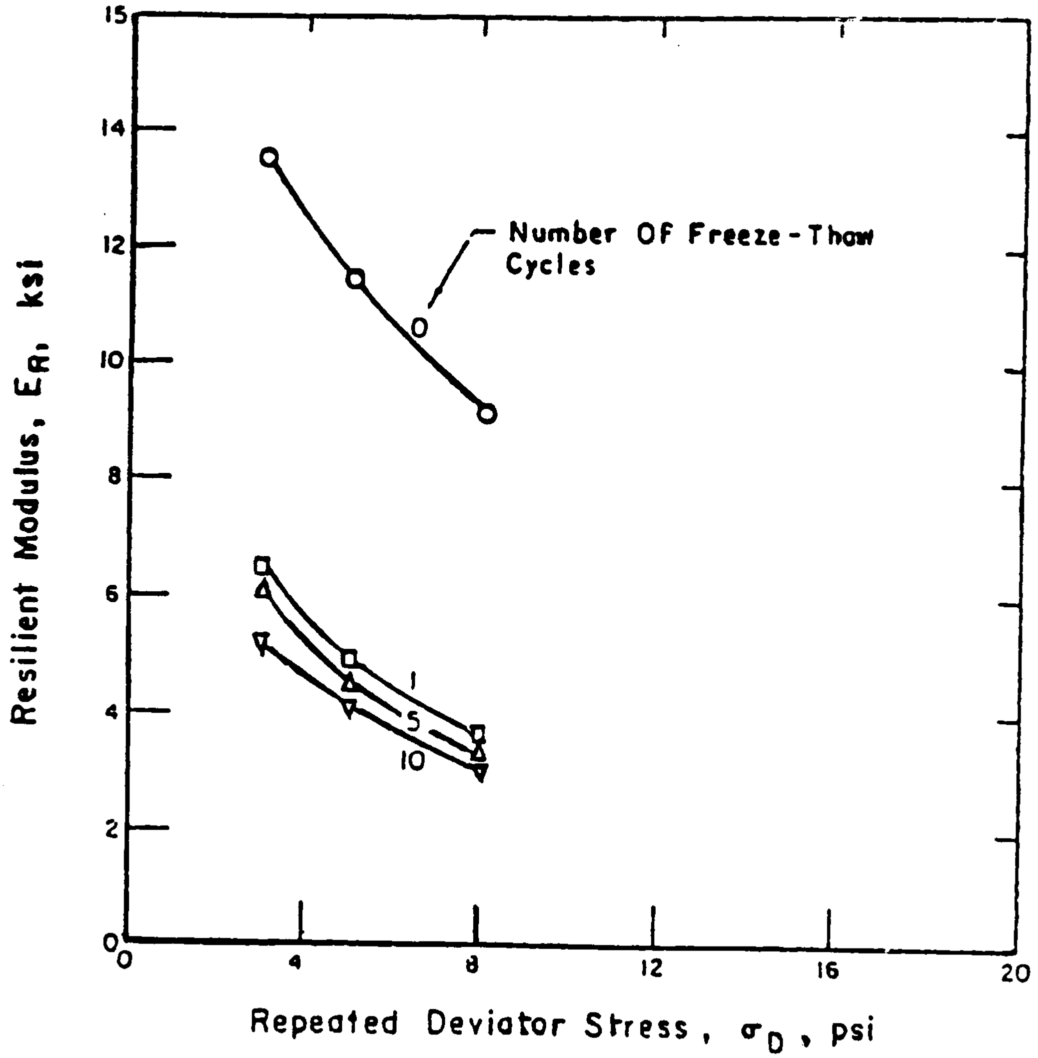

Figure II - 2. Effect of Freeze-Thaw Cycles on Resilient Modulus (after Thompson and Robnett, 1976).

The two factors causing bedding errors are the initial lack of fit between the samples surface and the lubricated platen, and penetration of the grease and disc layer by the constituent particles of the specimen. The magnitude of the bedding error is independent of the sample height and must be expressed as a deformation and not as a strain. After application of several cycles of the load, however, bedding deformation is totally recoverable (Sarsby et al., 1980). Other probems leading to bedding error may include the following (Costa Filho, 1985):

1. Nonuniformity of the surface of the specimen ends, such as the presence of asperities, irregularites, and so forth
2. Lack of flatness of the specimen ends
3. Nonparallelism of the specimen end surfaces
4. Tiliting or misalignment of the top cap

The dimetral test method (indirect tensile test) is being used more frequently to determine the resilient modulus and fatigue life of the asphaltic concrete mixtures and stabilized materials. Like the triaxial test solutions, the dimetral test solutions are based on the following assumptions (Hsu and Vinson, 1981).

1. The specimen is a linear elastic, homogeneous and isotropic material.
2. The stress solutions for a specimen subjected to dimetral load are valid for both plane stress and plane strain problems.
3. The strain solutions for a specimen subjected to dimetral load are valid for both plane stress and plane strain problems

Since the triaxial and the dimetral test methods assume an elastic layered theory to predict pavement response, Poisson's ratio has to be assumed or evaluated in the laboratory. Therefore, the problem of determining the critical conditions for design and pertinent material properties for each layer still remains (Barksdale et al., 1975). Many problems are associated with the reliability measurements of Poisson's ratio. However, pavement response is relatively insensitive to small and reasonable changes in in this parameter. Values of the resilient modulus in the dimetral load test are usually calculated based upon an assumed value for Poisson's ratio since variations of the ratio over a theoretical range of 0.2 to 0.5 only affect resilient modulus by about $\pm$ 25% (Hsu and Vinson, 1981).

Other suggested methods for determining the resilient modulus are the complex modulus test, flexural bending test, and the resonant column method. In 1980, the United States Army Corps of Engineers included procedures for cyclic triaxial testing in their Laboratory Soils Testing Engineering Manual (Department of the Army, 1970). The American Association of State Highway Transportation Officials' Pavement Design Guide recognizes the AASHTO Test Method T274-82 as the official laboratory test for the determination of reslient modulus (AASHTO, 1986). The American Society of Testing and Materials (ASTM) test method for resilient modulus is yet to be approved by committee (ASTM, 1985). The Asphalt Institute has incorporated an elastic-layered theory model in its pavement design by using subgrade resilient modulus as a design input (Asphalt Institute, 1981)

There are several models to characterize the resilience response of pavement materials. For granular soils exhibiting stress-hardening behavior, the resilient modulus is often approximted by the following equation:

$$E_r = k_1' \sigma_3^{k_2'}$$

or

$$E_r = k_1 \theta^{k_2}$$

where

σ_3 = confining pressure

θ = sum of principal stresses ($\sigma_1 + 2\sigma_3$)

k_1', k_2', k_1, k_2 = regression constants

The effective in-situ modulus of the granular layer in the field is a function of both the stress state and the shear strain induced in the layer by the magnitude of the surface loading (May and Witczak, 1981). The resilient modulus is influenced by the stress state, degree of saturation, and the degree of compaction (Gonzalo and Witczak, 1981). An analysis of nearly 100 data sets used to investigate whether or not general correlations exist between laboratory measured resilient modulus and laboratory measured CBR results, indicated that a very general, but variable, correlation does (Gonzalo and Witczak, 1981). However, since the resilient modulus test is stress dependent, the coefficient that relate Er to CBR must be stress dependent and not a unique or constant value.

A technique to predict permanent deformation of Florida quartz sand commonly found as subgrade material under repeated load laboratory tests using only static load triaxial test has been conducted (Pumphrey et al., 1981). It was concluded that increasing confining stress causes a slight or no increase in permanent strain for low stress ratios but a substantial decrease in this strain for large stress ratios. In all cases, permanent strain increases with increasing number of loading cycles. Resilient modulus increases slightly as the number of cycles becomes larger (Pumphrey et al., 1981). Permanent strain on laboratory sample may be predicted using a hyperbolic relationship found on a plot of normalized stress versus strain (Pumphrey et al., 1981).

The nonlinear stress-softening relationship between resilient modulus (ksi) and repeated deviator stress (psi) for fine-grained soils is often characterized by a bilinear relationship in terms of a " break point " deviator stress at which a significant change in the slope of the curve occurs. This relationship is shown in a pioneering study in Figure II - 3 (Terrel, 1972).

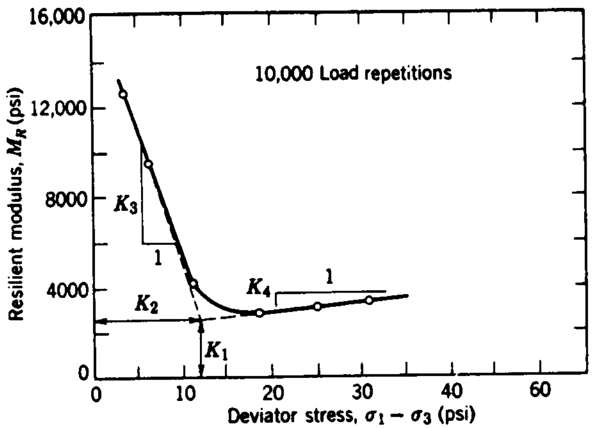

Figure II - 3. Typical Resilient Modulus Response for Fine-grained Soil (after Terrel, 1972).

$$M_r = K_2 + K_3 [(K_1 - (\sigma_1 - \sigma_3)] \text{ for } K_1 > (\sigma_1 - \sigma_3)$$
$$M_r = K_2 + K_4 [(\sigma_1 - \sigma_3) - K_1)] \text{ for } K_1 < (\sigma_1 - \sigma_3)$$

where M_r = resilient modulus

K_3, K_4 = slopes as shown in Figure II - 3

K_1, K_2 = the "breakpoint" deviator stress and resilient modulus respectively.

In the Illinois study, Figure II - 4 (Thompson and Robnett, 1976), the resilient modulus and the deviator stress corresponding to the intersection point of the bilinear relationship are designated as E_{Ri} and σ_{Di} respectively. The numerical value for the deviator stress for most of the curves in the study was found to occur at about 6 psi. Regression analyses were conducted using the data below and higher than the break point deviator stress as two distinct sets. The resulting bilinear models were used in a numerical analysis (Thompson and Marshall, 1976). A least squares curve fit computer program has been used to characterize the stress-softening behavior of each tested specimen by an exponential function (Johnson, 1986).

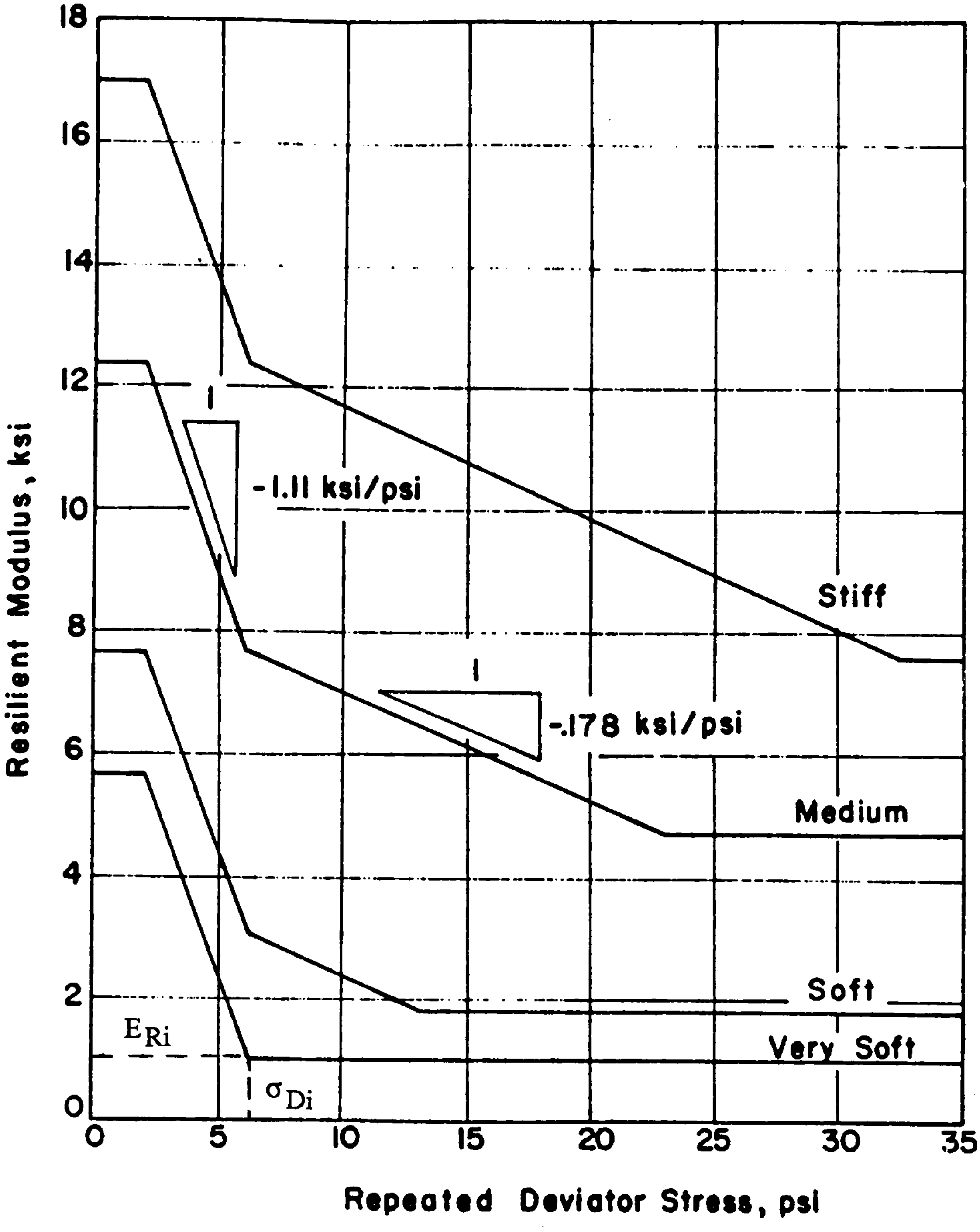

Figure II - 4. The Bilinear Model and the Breakpoint Resilient Modulus

(after Thompson and Robnett, 1976).

CHAPTER III

SELECTION AND COLLECTION OF SAMPLES

Soils types to test in the program were determined after a preliminary study of soils across the state (Highter and Moore, 1984). A map showing the General Soil Regions of Tennessee is shown Figure III-1. The complex and varied geology of Tennessee is demonstrated by the nine soil areas divided purely by physiographic regions. The soils of the Major Stream Bottom (A) and the soils of the Coastal Plain Region (C) have alluvial (water transported) soil origins. The soils of the Loess Region (B) have aeolian (air transported) soil origins. Finally, the other regions have residual (weathered in place) soils origin (Springler and Elder, 1980).

The Soil Conservation Service (SCS) has identified 376 different soils in Tennessee. Since each of the soils has a potential of being a highway subgrade soil, a selection process had to be instituted to sort out candidate soils for the laboratory testing program. The underlining selection criterion was how important a given soil map unit is as a subgrade material. "Importance" of each soil map unit was examined in three different ways (Highter and Moore, 1984):

1. The percentage of the total land area of Tennessee occupied by each soil map unit
2. The percentage of the total route miles (U. S. highways plus Interstates highway) traversing each soil map unit
3. The percent of the total of the product of average daily traffic and route miles (ADT multiplied by route miles) borne by each soil map unit

The priority soils were selected as listed in Table III-1 (Drumm and Moore, 1987). Sample collection constituted a major and important part of the project. Care was taken to obtain representative samples of each selected soil type. To ascertain that the correct sample for a specified soil type was collected, a particular city or landmark, such as a river located on the soil map, was selected and the soil sample obtained within the city limits or adjacent to the landmark. Enough samples at each site were collected for the index properties and the resilient modulus testing.

The samples were obtained from the cut embankment areas of the highways and far from the shoulders to assure that they were actually representative of the designated soil type. As is done in highway construction practice, the low strength agricultural soils were removed and discarded. The map of the State of Tennessee in Figure III-2 shows the approximate locations where the samples were obtained.

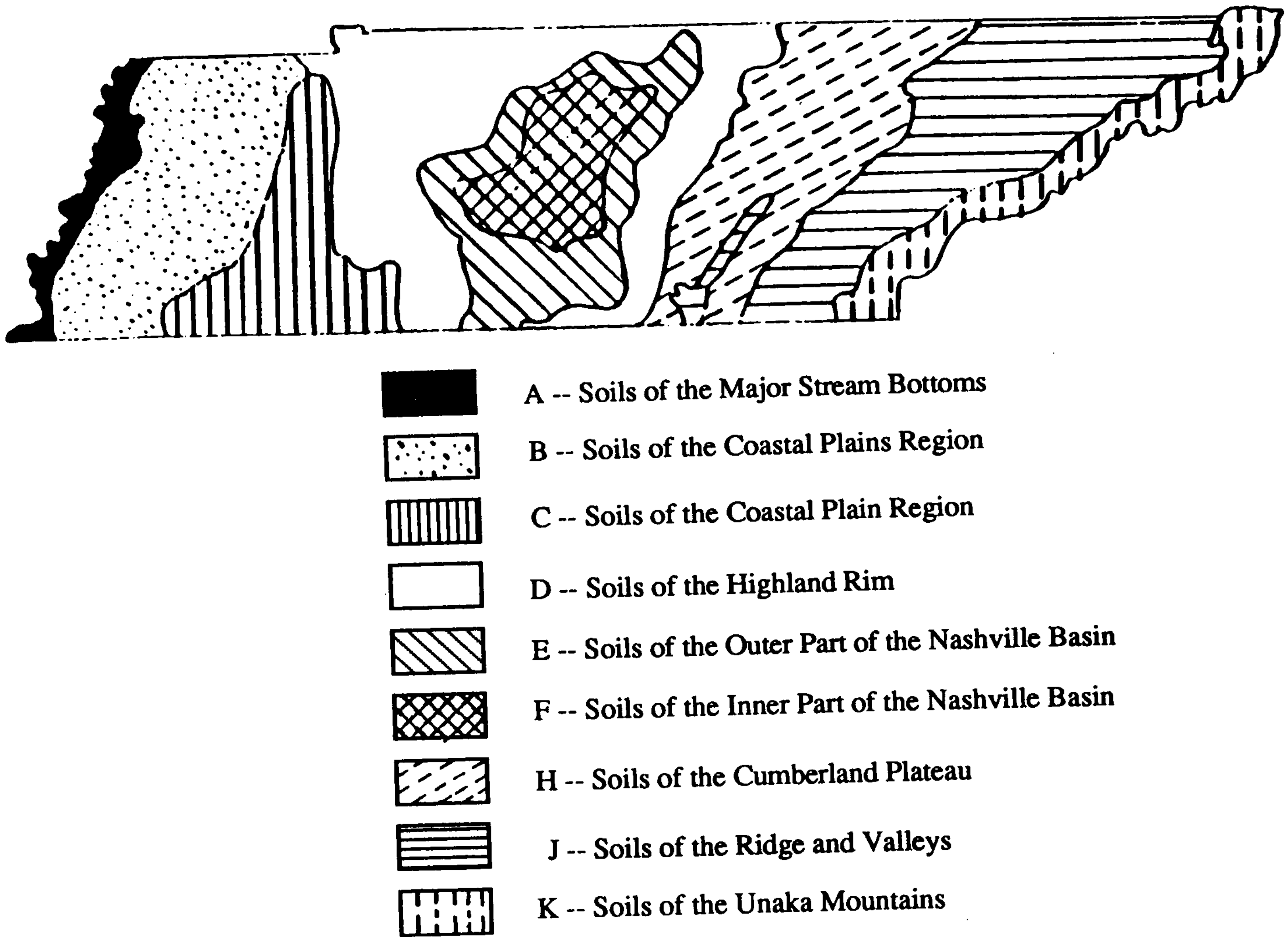

Figure III - 1. General Soil Regions Map of Tennessee (After Springler and Elder, 1980)

Table III - 1. Locations of Soil Samples for Resilient Modulus Testing.
(after Drumm and Moore, 1987)

SOIL TYPE	% BY ADT	COUNTY	LOCATION
J - 31	3.0	Loudon	I - 75 Around Little Tennessee River
H - 21	2.4	Campbell	I - 75 North of Jacksboro
H- 11	2.4	Cumberland	I - 40 Around Crossville
F - 11	4.4	Wilson	231 Around Lebanon North of I - 40
E - 21	5.5	Smith	I - 40 West of Caney Fork River
E -31	6.7	Sumner	31 - E Around Gallatin
D - 11	3.1	Benton	I - 40
C - 11	1.2	Henderson	22 Towards Lexington South of I - 40
B - 21	6.7	Haywood	I - 40 From Madison County Line to Hatchie River
A - 31	2.1	Haywood	I - 40 Adjacent to Hatchie River

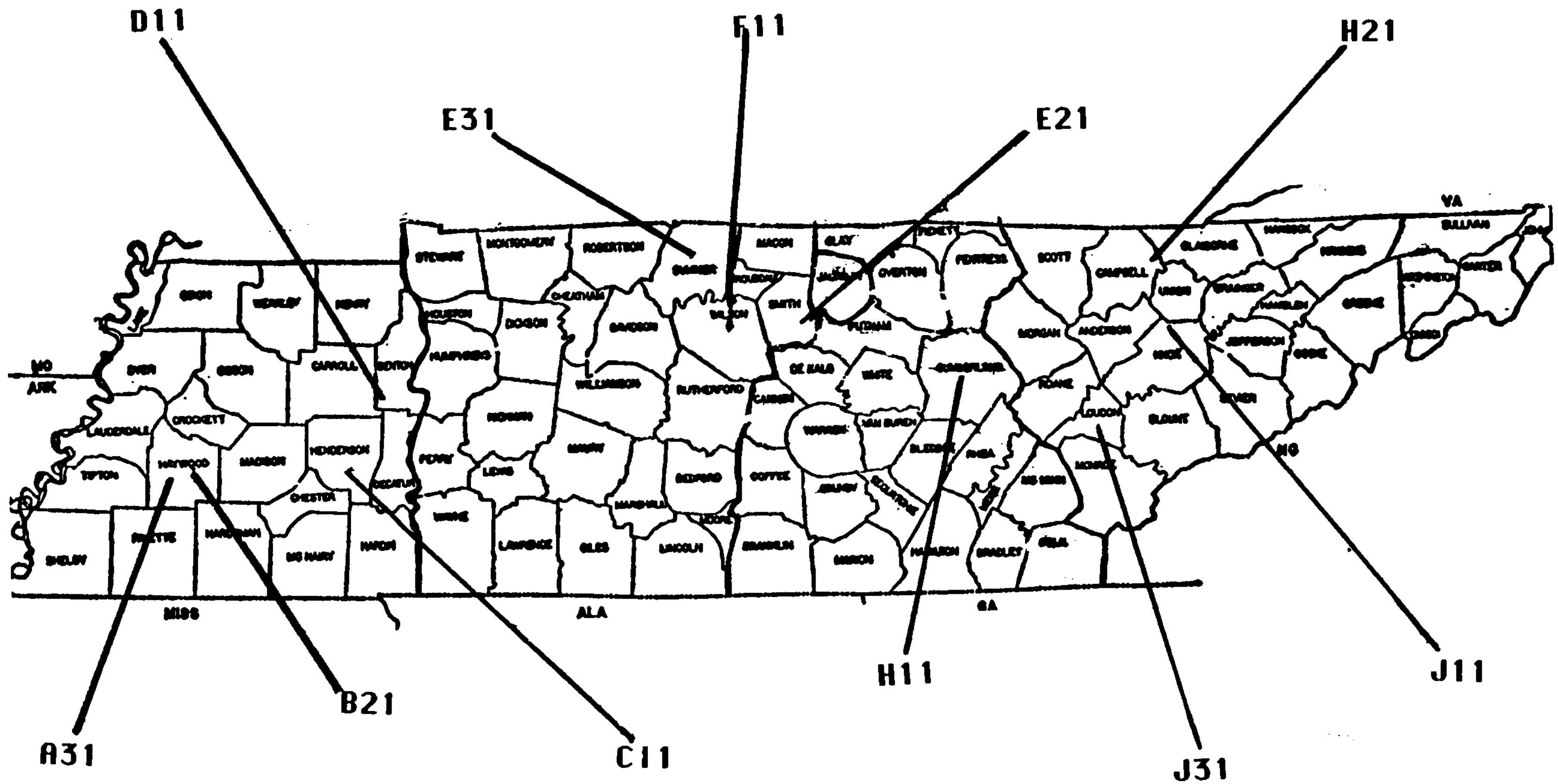

Figure III - 2. Map of Tennessee Showing the Approximate Location of Samples.

CHAPTER IV

REPEATED LOAD TESTING PROGRAM

1. INDEX PROPERTIES OF THE SOIL SAMPLES.

Standard tests were performed to obtain the index properties of the soils for classification purposes and also to form a data base for correlation of the properties to the repeated or resilience test results. The test procedures used are listed in Table IV - 1 and the results presented in Table IV - 2. The unconfined tests were conducted on the same specimens used for resilient modulus tests. It was observed that the soils exhibited two main groups of low and high plasticity index.

Table IV - 1. AASHTO and ASTM Specifications for Various Index Properties Tests

Test	Specification	
	AASHTO	ASTM
Atterberg Limits:		
Liqiud Limit (LL)	T89	D423
Plastic Limit (PL)	T90	D424
Grain Size Analysis:		
Hydrometer Analysis	T88	D4222
Mechanical Sieve Analysis		
Specific Gravity of Solids	T100	C854
Standard Proctor Test:		
Maximum Dry Density	T99	D698
Opt. Moisture Content	T99	D698
Unconfined Compression Test	T208	D2166

A plot of the plasticity indices versus liquid limits generally used for classification purposes is shown in Figure IV - 1. No significant differences between

Table IV - 2. Standard Laboratory Test Results.

Soil Classification			Location County	Clay Content (%)	Passing #200 Sieve (%)	Atterberg Limits			SG of Solids	Proctor Test Data		Unconfined Compression Test data (ps.)	
SCS	USCS	AASHTO				LL	PL	PI		Max. Dry Density (lb/ft^3)	Opt M•C• (%)	Avg. Max. Strength (psi)	Avg. Min. Strength (psi)
A31	CL	A-4	Haywood	17.0	95.0	30.5	22.1	8.4	2.66	103.5	18.0	63.6	28.3
B21	CL	A-6	Haywood	18.0	100.0	38.8	23.3	15.5	2.65	102.0	20.6	66.8	37.8
C11	SM	---	Henderson	17.0	20.0	20.7	19.0	1.7	2.60	111.7	14.7	31.6	5.5
D11	ML	A-4	Benton	18.0	80.0	36.2	34.1	2.1	2.66	83.7	30.0	31.1	13.1
E21	ML	A-4	Smith	35.0	68.0	37.1	27.0	10.0	2.67	94.6	23.1	40.9	40.2
E31	CL	A-7-6	Sumner	36.0	93.0	42.1	22.0	20.1	2.76	96.8	25.0	69.9	60.1
F11	CL	A-4	Wilson	16.0	78.0	29.5	20.1	9.4	2.67	109.0	17.4	48.7	39.2
H11	CL	A-4	Cumberland	20.0	73.0	28.5	19.2	9.3	2.73	110.5	15.5	62.4	30.5
H21	SM-CL	---	Campbell	16.0	36.0	21.0	14.1	6.9	2.65	114.7	13.3	45.8	26.8
J11	MH	A-7-5	Knox	28.7	80.0	68.5	39.2	29.3	2.71	80.2	37.5	27.3	27.3
J31	MH	A-7-5	Loudon	55.0	80.0	69.5	42.6	26.9	2.73	88.3	31.8	49.6	48.4

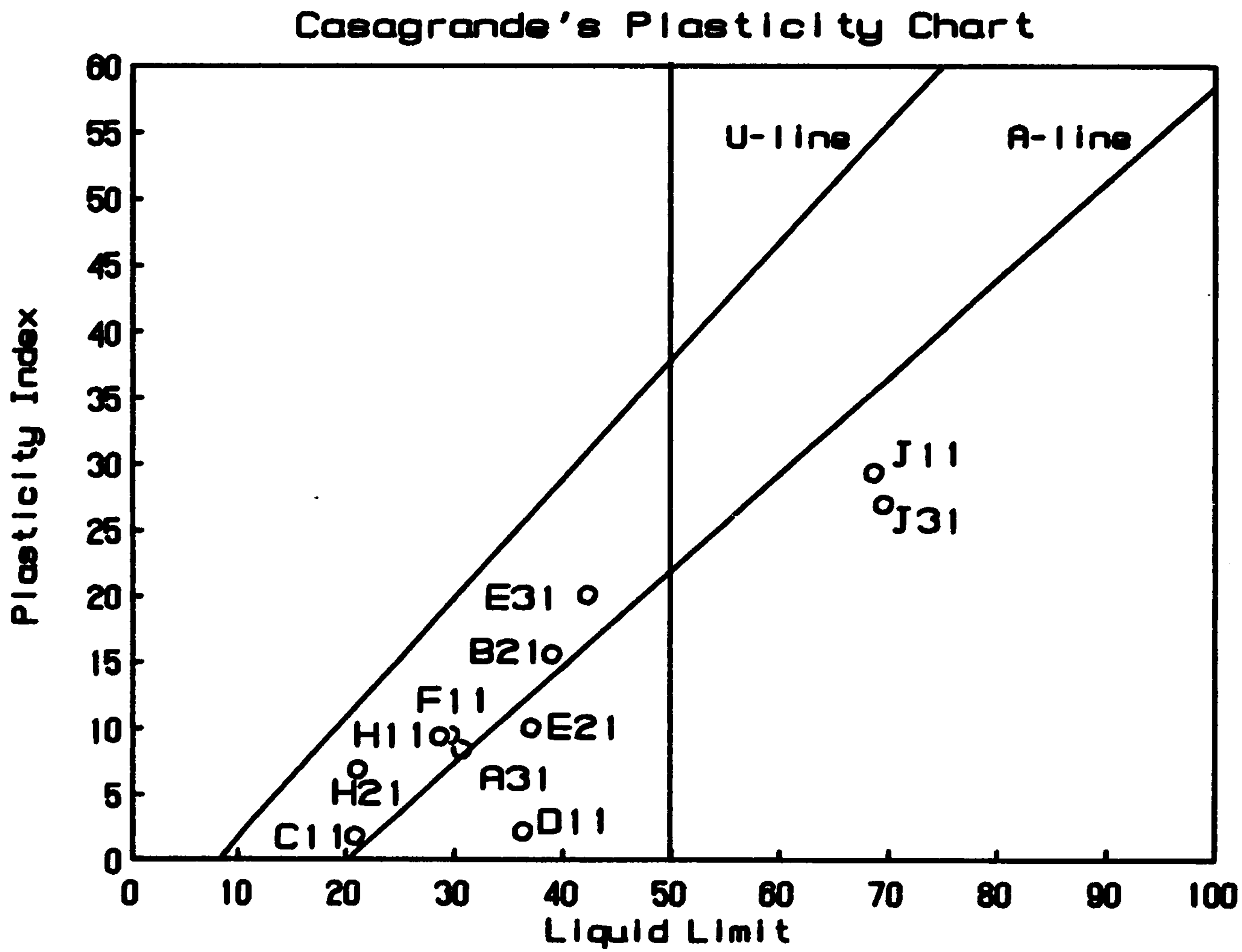

Figure IV - 1. Plasticity Index Versus Liquid Limit on Casagrande's Plasticity Chart.

maximum and residual strengths were noted. The grain size distribution plots of the soil samples are shown in Appendix B2. Each soil was classified according to the main engineering soil classification systems: (1) the Unified Soil Classification System (USCS) and, (2) the American Association of State Highway and Transportation Officials (AASHTO). The USCS and AASHTO classification systems used primarily for engineering purposes are based on grain size distribution and the Atterberg limits of the soils. The A31, B21 and similar designations used thus far for differentiating the soils are agricultural classifications based on physiographic regions of the state (Springer and Elder, 1980). Table IV - 2 contains the three classification results of the selected soils.

2. REQUIREMENTS FOR TEST SPECIMENS

The most important aspect in preparation of the laboratory specimens for resilience testing was obtaining specimens that are representative of the field conditions. Caution was exercised in the preparation, handling, and storage of the test specimens. The moisture content and dry density of the test specimens were based on the requirements of Tennessee Department of Transportation Standard Specification 207.04 (TNDOT, 1981). The specification requires that the subgrade in a pavement system be placed at the optimum moisture content as determined from the Standard Proctor test in accordance with AASHTO T99 or ASTM D698 test method. Therefore, each specimen was compacted at the optimum moisture content and maximum dry density for the soil type. Table B1 - 1 in the appendix shows the actual moisture content and dry density of the specimens tested. It should be noted that no attempt was made to study the effects of moisture content on the resilient modulus of the soils. Such a study would have required resilient testing of each soil at several moisture contents and was not within the scope of this investigation.. Any deviation from the Standard Proctor optimum moisture and maximum density was due to difficulty in reproducing the exact moisture content and dry density in the compacted specimens.

Specimens of 2-inches in diameter and 4-inches in height were used as in the first phase of the Tennessee study (Johnson, 1986). The size was chosen because of the ease and speed of preparation, the small amount of material required, uniformity obtained, and adequacy relative to maximum soil particle size consideration (Thompson and Robnett, 1976). This specimen size represents the minimum size that can be expected to represent the larger mass of material in the pavement (Barksdale et al., 1975).

Standard molds associated with kneading compaction methods such as AASHTO T99 or the Harvard Miniature method may not be of the correct dimensions for direct use in resilience testing (AASHTO, 1982). It should be noted that the selected specimen size is the same as that in the Illinois study (Johnson, 1986), and was chosen to fit available equipment. Trial-and-error adjustments were performed to determine the number of layers and tamps per layer to reproduce the Proctor Test densities.

3. COMPACTION EQUIPMENT

The resilient properties of compacted clay is found to be dependent on the type of remolding action used. As discussed previously, a compaction process that causes shearing deformation in a clay soil having a degree of saturation greater than 80% results in a dispersed (or parallel) clay structure (Barksdale et al., 1975). Clays with a dispersed structure demonstrate more deformation than the same soil with a flocculated (random) structure tested under the same conditions. It was assumed that the field compaction of the soils occurs at moisture contents greater than 80% of the saturation moisture contents that the in-service moisture contents remain greater than 80% of the saturation value. Therefore, a disperse structure was desired in the laboratory specimens.

The dispersed clay structure resulting from field compaction by sheep's foot roller was simulated in the laboratory by kneading-type compaction. A kneading compactor which was designed for the preparation of four inch diameter by six inch long soil and asphalt specimens, was modified for two inch diameter specimen preparation. The compactor was fitted with a sixty degree wedge shaped compaction foot as shown in Figure IV - 2 (Johnson, 1986). The compactor had a turntable base which affords mechanical rotation of the specimen as it is compacted to ensure that uniform pressure and thus equal density is obtained in every part of the specimen, and assures that uniform kneading action takes place.

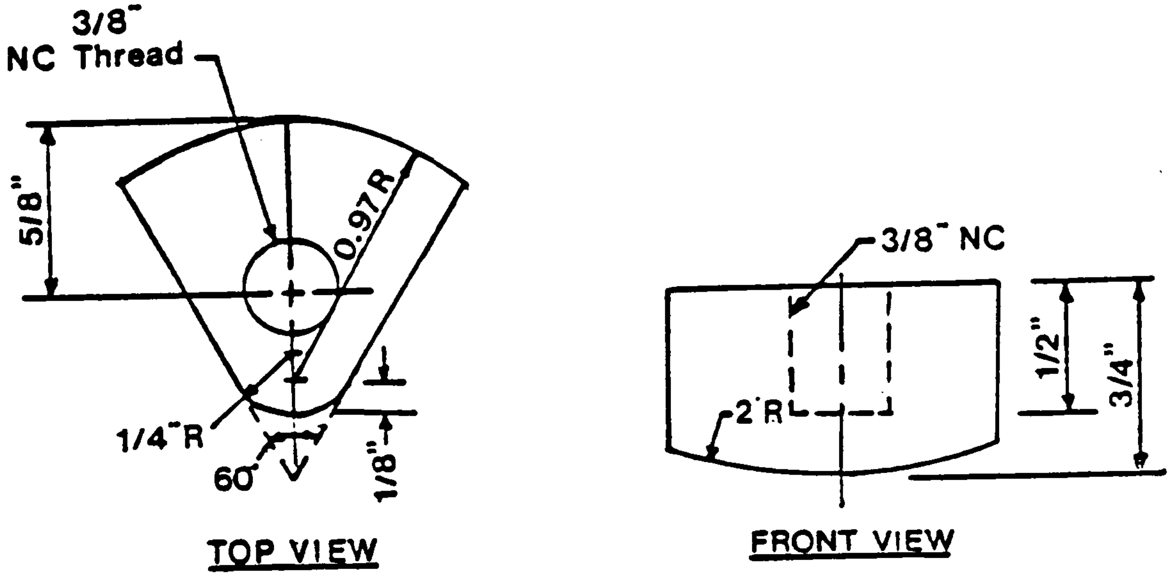

Figure IV - 2. Schematic Diagram of the Kneading Compactor Foot (After Johnson, 1986).

4. PREPARATION OF TEST SPECIMENS

A quantity of a soil type was thoroughly broken up in such a manner as to avoid reducing the natural size of individual particles. An adequate amount of the pulverized soil was sieved through a No. 4 sieve. The coarse material retained on the the sieve was discarded. About 500 grams of the pulverized soil was needed to prepare one test specimen for resilience testing. Moisture content of the prepared soil was determined by oven-drying. Care was taken to avoid any moisture loss from the remaining pulverized soil by placing the soil in sealed plastic bags. After obtaining the moisture content, the weight of water required to increase the moisture content of the pulverized soil to the optimum as determined from the Standard Proctor test was calculated. The required water was added in small quantities to the soil and mixed thoroughly after each addition. The mixture was quickly placed in plastic bags and a complete seal ensured by using two or more plastic bags. The soil was then placed in a moist cure room with a relative humidity of 100% and a constant temperature of 77 degrees. The conditions in the room ensured a uniform distribution of the water in the specimen.

A compaction method developed by Johnson (1986) was adopted for the test specimen preparation. The method essentially involved a trial-and-error adjustments in the weight of soil per layer, the number of compacted layers, or the number of tamps per layer (or both) to produce specimens of the required densities. The specimens were compacted in four layers of approximately 125 grams of soil per layer using 16 tamps of the compaction foot per layer. The top layer received additional 16 tamps to ensure a more uniform density of all four layers. The orientation of the compaction foot for the first , second, third and fourth tamps were offset ninety degrees from the previous layer to help provide uniform compaction (Johnson, 1986). At each layer interface, the surface was scarified before the next layer of soil was added to insure proper bonding between the layers. An important observation made during the compaction process was that an air pressure of 80-85 psi produced specimens of densities identical to that obtained from the Standard Proctor tests.

Each specimen was then carefully trimmed and the length of the specimen was measured with a vernier caliper and recorded. The diameter of the specimen was recorded as 1.975 inches which is the inside diameter of the space in the mold after inserting the rubber membrane. The weight of the specimen was also recorded. These measurements were used for the determination of the wet and dry densities of the specimens and also later during the reslience testing.

The Tennessee Department of Transportation Specification 207.04 requires that the compacted subgrade have a dry density of not less than 100% the maximum dry density obtained from a Standard Proctor test (TNDOT, 1981). Specimens for resilience testing which did not meet this requirement within 2-3% were discarded. The specimens meeting the requirements were wrapped in two or more plastic bags and sealed to insure no moisture loss or gain. The specimens were then placed in the moist cure room. A minimum curing period of seven days was used in the study. This curing period minimized any effects "thixotropic" strength gain might have on the determination of the resilient modulus (Robnett and Thompson, 1973). Thixotropy simply refers to strength gain with time at a constant soil composition.

5. REPEATED LOAD TESTING EQUIPMENT

The repeated load testing essentially involved application of a repeated axial deviator stress of a fixed magnitude, specified duration, and frequency to the carefully prepared and conditioned cylindrical soil specimen. The test simulated the physical conditions and possible states of stress of subgrade materials under flexible pavements subjected to moving wheels loads.

The equipment was set up in the first phase of the study (Johnson, 1986). A Research Engineering Model RE-SS-2400 load frame was used to apply the cyclic loading. A pneumatic actuator mounted on top of the loading frame supplies the cyclic load to the specimen. A modified Exact Electronic Waveform generator electronically controls the shape, size, and frequency of the applied load pulse. The "amplitude" and "DC offset" controls on the waveform generator govern the magnitude of the load pulse to be applied on the specimen. An Interface load cell rated at a capacity of ± 1000 lb is mounted within the loading ram, and a spring-loaded linear variable differential transducer (LVDT) with a measuring range of ± 1 inch was attached using a bracket to the loading ram. The LVDT measures the axial deformation of the specimen during the resilience testing. The geometry of the triaxial cell requires that the LVDT be placed at about two inches to the right of the loading shaft. The effect of this offset was not thought to be significant due to the rigidity of the mounting bracket and the slow loading rate (Johnson, 1986).

Voltage signals from the load cell and the LVDT corresponding to the axially and the axial deformation of the specimen were displayed on digital transducer readouts. The signal from the load cell was boosted using a DC bridge amplifier before it was digitally displayed. No attempt was made to measure radial deformation of the specimen during the resilience testing. An X-Y recorder was used to record the axial load and deformation, producing the hysteretic load-displacement loops during the loading and unloading of the specimen.

A Watanabe A4-size X-Y recorder WX 1000, with a maximum pen speed of 500 millimeters per second was used. The width of the line drawn by a new pen was about 0.3 millimeters . The amplitude of the pen's oscillation in response to input signals could be switched through 11 steps of 0.5, 1, 5, 10, 20, 100, 500, and 5000 mV/cm that is, a measuring range of 0.5 mV/cm to 5 V/cm. The calibration procedure, resulted in a unit measurement of the load cell of 50 lb/V and for the LVDT was 0.2 in/V. The use of the X-Y recorder allowed the resilient response to be recorded at several gain settings for each deviator stress. By switching the amplitude of the pen's oscillation through different gains at a particular stress level, magnifications or reductions of the same loops were obtained. The resilient moduli calculated from the different loops were found to be approximately the same, but, the larger loops provided greater precision.

6. REPEATED LOAD TESTING AND DATA REDUCTION

After the curing period, a specimen was ready for the resilient testing. The specimen was left in the rubber membrane to prevent excessive moisture loss during testing. A good surface of contact was ensured by again trimming and measuring the specimen to ascertain that the top and bottom surfaces, and the length were uniform. By using a thin film of vaseline at the base plate of the mold during the specimen preparation a uniform surface was already ensured. Porous stones were placed at the top and bottom of the specimen which was then placed in the loading frame.

The AASHTO test requirements specifies that for cohesive soils the specimen should be tested with a maximum deviator stress of 1 psi with a confining pressure of 6 psi, 3 psi and, 0 psi for a total of 600 applications. The procedure is to be repeated for deviator stresses of 2 psi, 4 psi, 8 psi and, 10 psi. The total number of load application should be around 3000. Prior to testing, the specimens are conditioned by applying 100 cycles at the stress levels of 2 psi, 4 psi, 6 psi, 8 psi and, 10 psi. Specimen conditioning before testing adds 1000 more load application for a total of 4000 load applications. All test in this investigation were conducted with zero confining stress for the following reasons (Thompson and Robnett, 1976):

1. Simplicity and ease of testing
2. It can be shown (finite element, elastic theory, etc) that the magnitude of of the confining pressure that exists in the upper regions of the subgrade of a typical flexible highway is very low, normally less than 5 psi
3. Results obtained during the Illinois laboratory studies indicated that small magnitudes of confining pressure up to lateral pressure of 5 psi had no significant effect on the resilient behavior of the fine-grained soils examined (Thompson and Robnett, 1976)

After the specimen was placed in the triaxial cell, the loading frame, porous stones, and the specimen were properly aligned. The graph paper was properly aligned on the X-Y recorder, and testing was accomplished at each stress level by applying the required load and switching the X-Y recorder to the measure mode. Different loops were obtained at the same stress by turning the voltage gain controls of the X and the Y panels on different voltage levels one or both at a time. In all, about four different loops were obtained at the each stress level. The gain settings and specimen length were recorded adjacent to the load deflection loops. The cyclic load was turned off after testing at each stress level to prevent any further loading of the specimen. The length of the specimen was measured, the function generator adjusted for the next stress level, the pen of the X-Y recorder set on a clear part of the paper, and the procedure repeated.

The AASHTO test method suggests testing at deviator stresses of 2 psi, 4 psi, 6 psi, 8 psi and, 10 psi (AASHTO, 1982). In order to evaluate the resilient modulus versus deviator stress curve more closely, the Tennessee study was conducted at nominal stress levels of 2 psi, 3 psi, 4 psi, 5 psi, 6 psi, 7 psi, 8 psi, 10 psi, 15 psi, 20 psi and, 25 psi.

A schematic diagram of how the resilient modulus was obtained and calculated in the testing program is shown in Figure IV - 3. A listing of the computer program used in the calculation of the resilient modulus is found in Appendix A. The computer program works by entering the specimen length, the x- and y-gains from the X - Y recorder, and the angle between the line through the ends of the loop and the horizontal. The equation used is of the following forms and explained in Figure IV - 3:

$$Er = \sigma_d / \varepsilon_T$$

$$E_r = \frac{\text{vertical}}{\text{horizontal}} = \frac{[\tan\theta\;][\text{ygain (volts)}][\text{loadfactor 1 (lb/volts)}] \,/\, [\text{area } (i^2)]}{[\text{xgain (volts)}][\text{dispfactor (in/volts)}] \,/\, [\text{length (in)}]}$$

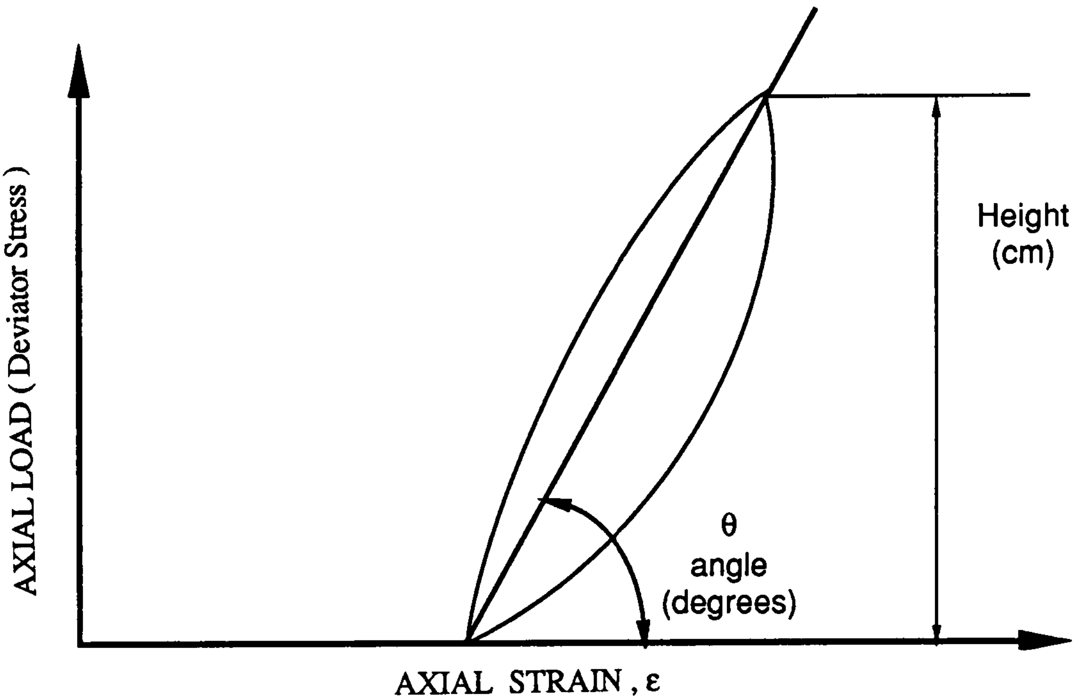

Figure IV - 3. Schematic Diagram Depicting the X-Y Plotter Determined Resilient Modulus.

where θ = angle between the line through the ends of the loop and the horizontal in degrees as in Figure IV - 3

ygain = reading of the y-gain on the X-Y plotter for a loop in volts/cm

loadfactor = load factor for the pneumatic loading in lb/volts

area = nominal area of the specimen ends in square inches

xgain = reading of the x-gain on the X-Y plotter for a loop in volts/cm

dispfactor = deflection factor for the LVDT from calibration in in/volts

height = vertical length of the loop in centimeters as in Figure IV - 3

length = length of the specimen at a stress level in inches

Due to differences in the response of various soils, it was not always possible to read data at the specific levels of deviator stress. However, sufficient data points were obtained to determine the resilient modulus over the entire range of expected deviator stress.

7. REPEATED LOAD TESTING RESULTS

The resilient behavior of each soil was determined at various levels of axial deviator stress. At each incremental stress level, the stress applications were enough to develop distinct deflection output recorded on the X-Y recorder but not enough to introduce significant "number of load application" effects on the resilient property of the soil. Two specimens of each soil type were tested in the program. An arithmetic plot of resilient modulus in ksi versus deviator stress in psi was used to illustrate the resilient response. A typical plot of the response for soil type A31 is shown in Figure IV - 4. Similar plots for the rest of the soils are contained in Appendix B1. The "stress - softening" behavior of the soils were exhibited by the decrease in the resilient moduli with increasing deviator stress.

After the test, the specimen was tested in unconfined compression in accordance with AASHTO and ASTM specifications as listed in Table IV - 1.

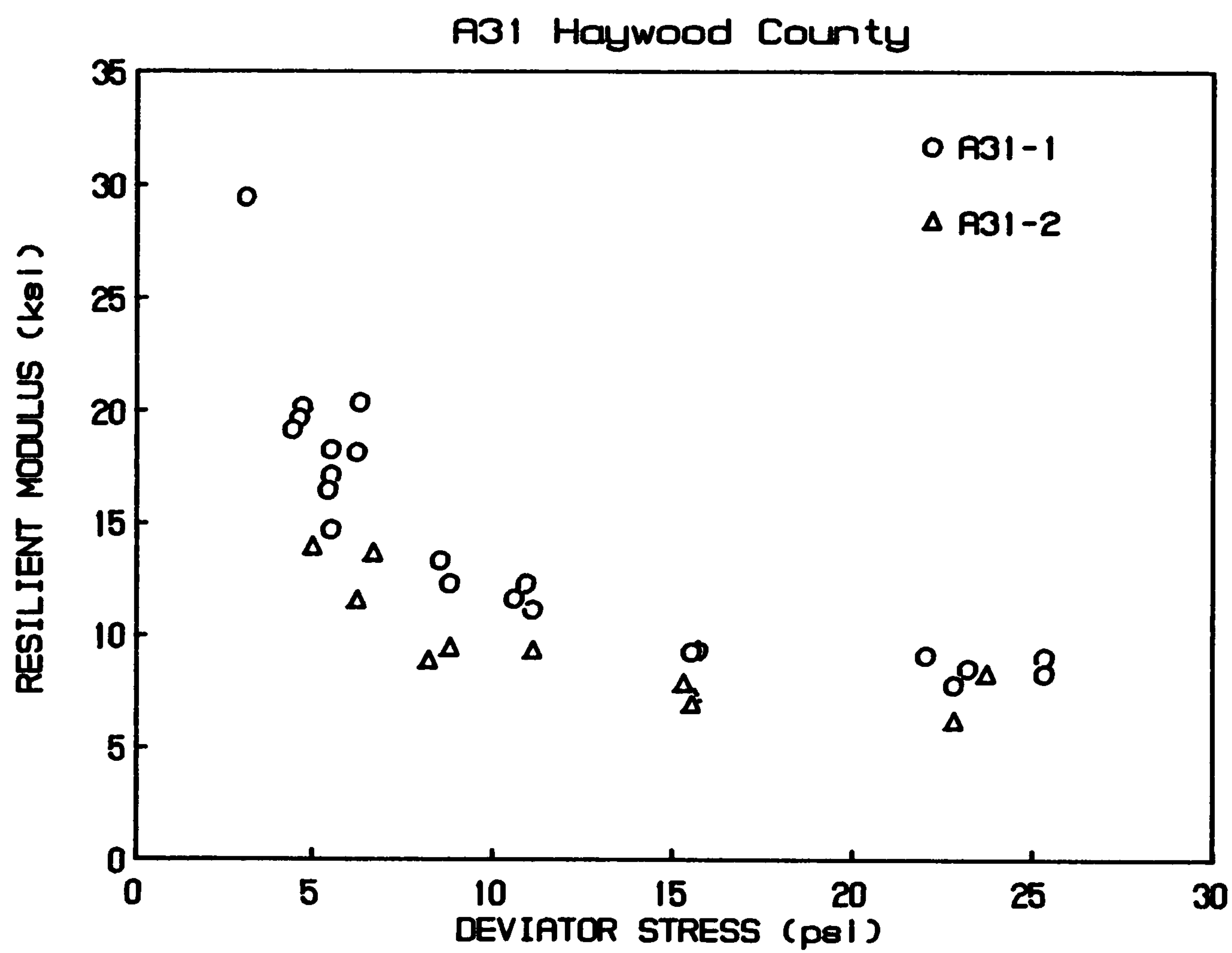

Figure IV -4. Resilient Modulus Versus Deviator Stress for Soil Type A31.

CHAPTER V

EVALUATION AND MODELING OF RESULTS

The primary objective of this study was to correlate the results of the resilience response data to that of standard index properties, and investigate the relationship between resilient modulus and the initial tangent modulus obtained from unconfined compression tests. The initial modulus is relatively easy to obtain from the unconfined test data, and should be related in some manner to the resilient modulus determined from the more complex repeated load test. A consistent method for determining the initial modulus is obtained if it is assumed that the stress-strain response of the unconfined compression test can be represented by a hyperbola. The hyperbolic model in its original form was used to represent the nonlinear stress versus displacement behavior of direct shear results and used in the analysis of a retaining wall (Clough and Duncan, 1971).

The hyperbolic relationship between stress and strain is of the form:

$$\sigma = \varepsilon / (\mathbf{a} + \mathbf{b}\varepsilon)$$

where: σ = the axial stress

ε = the axial strain

$\mathbf{a}, \mathbf{b}$ = empirical coefficients determined experimentally

A schematic unconfined compression stress versus strain curve with the initial tangent modulus is shown in Figure V - 1. By plotting the lab data in the transformed axes ε/σ versus ε, the linearized parameters $\mathbf{a}$ and $\mathbf{b}$ are obtained as shown schematically in Figure V - 2. Deviations from linearity indicate the degree to which the stress-strain data deviates from a hyperbolic relationship. The reciprocal of the coefficient $\mathbf{a}$ corresponds to the initial slope of the stress curve shown in Figure V - 1.

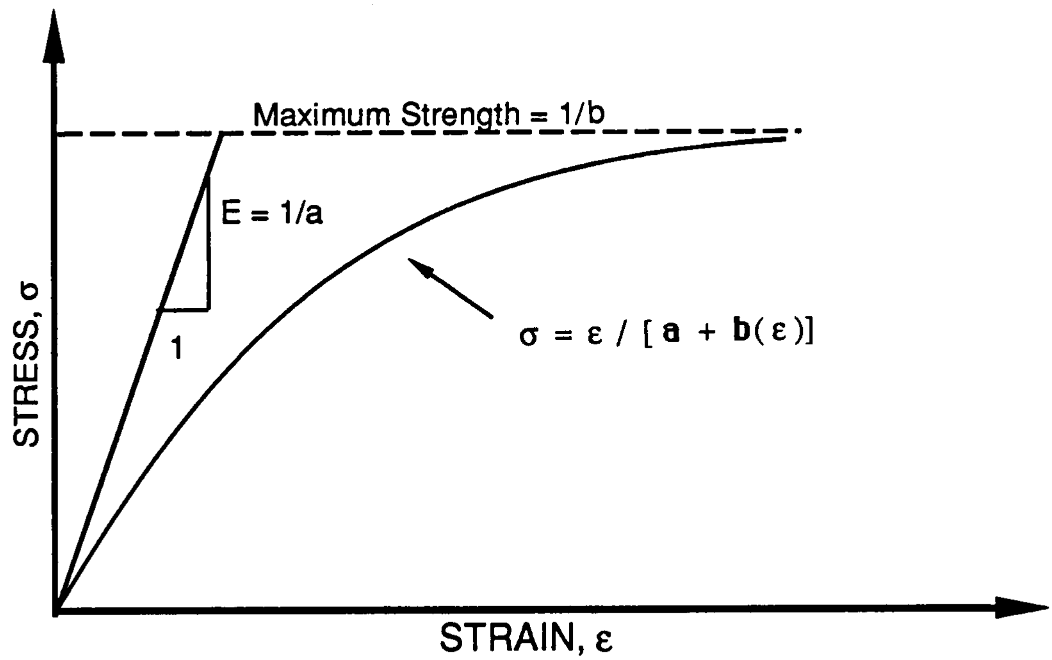

Figure V - 1. Schematic Diagram Depicting the Unconfined Compression Test Curve.

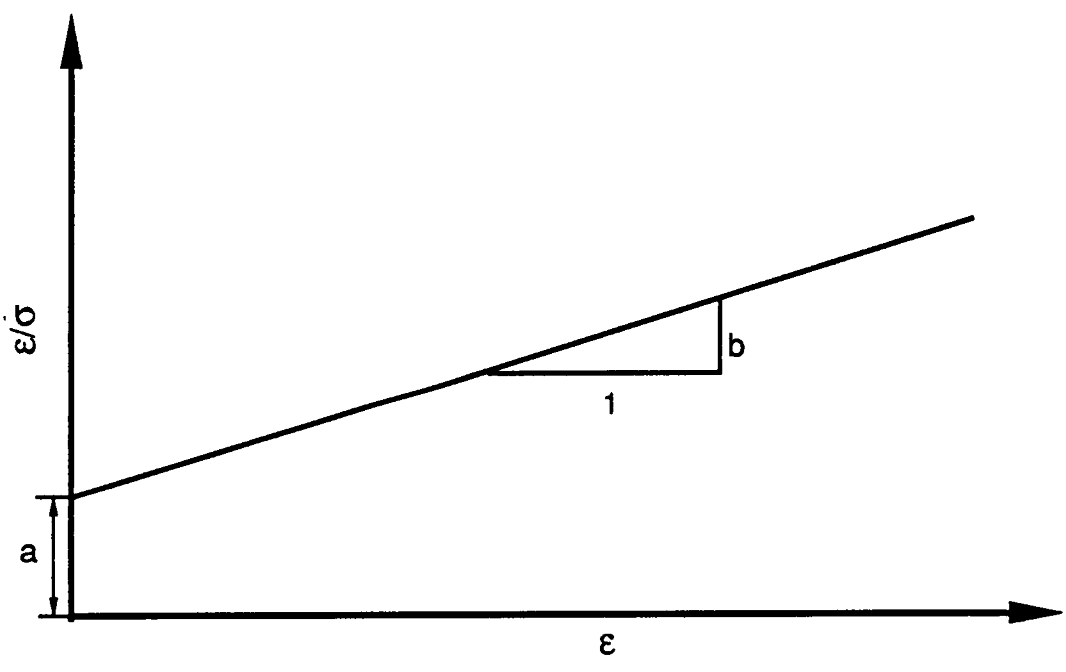

Figure V - 2. Transformed Axes for Determination of Hyperbolic Model Parameters.

The reciprocal of the coefficient **b** is the asymptote approached by the curve at large strains or the maximum strength as shown in Figure V - 1. Mathematically, the relationships are explained as follows:

$$1/\mathbf{a} = E_t$$

$$1/\mathbf{b} = \sigma_{ult}$$

Where: E_t = the initial tangent stiffness modulus

σ_{ult} = the ultimate strength

Typical results in the transformed axes for the unconfined compression test data for soil type A31 are shown in Figure V - 3. The transformed axes plots of all the tested specimens are shown in Appendix C2, and the data listed in Appendix E2. The linear relations were obtained by using only strains up to 0.04 in/in. The data at values of strain greater than 0.04 in/in were discarded due to deviations from linearity. This decision was made, to simplify the parameter determination process, and justified since it is the initial response that is of interest.

A typical back prediction of the stress-strain curve using the hyperbolic parameters is presented in Figure V - 4. The deviation from hyperbolic response at large strains is observed, but the desired initial response is predicted. The numerical values obtained for the **a** and **b** parameters for each of the selected soils are listed in Table V - 1. It should be noted that the reciprocal of **a** corresponding to the initial tangent modulus is also reported. The definitions of the symbols used are found in Table VI - 3 on page 53, and the stress-strain predictions for the remaining soils are shown in Appendix D2.

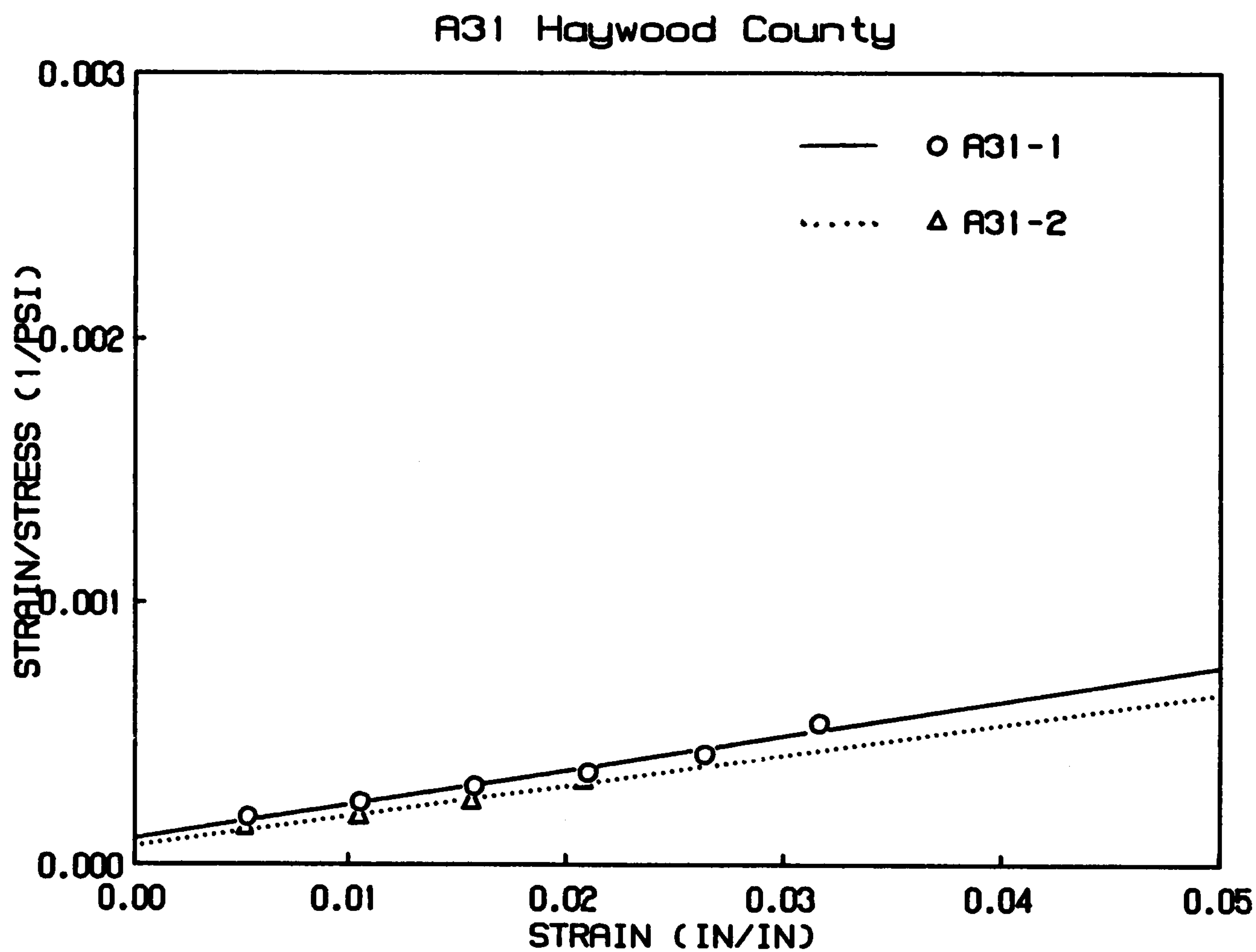

Figure V - 3. Hyperbolic Model Plot for Unconfined Compression Test For Soil Type A31.

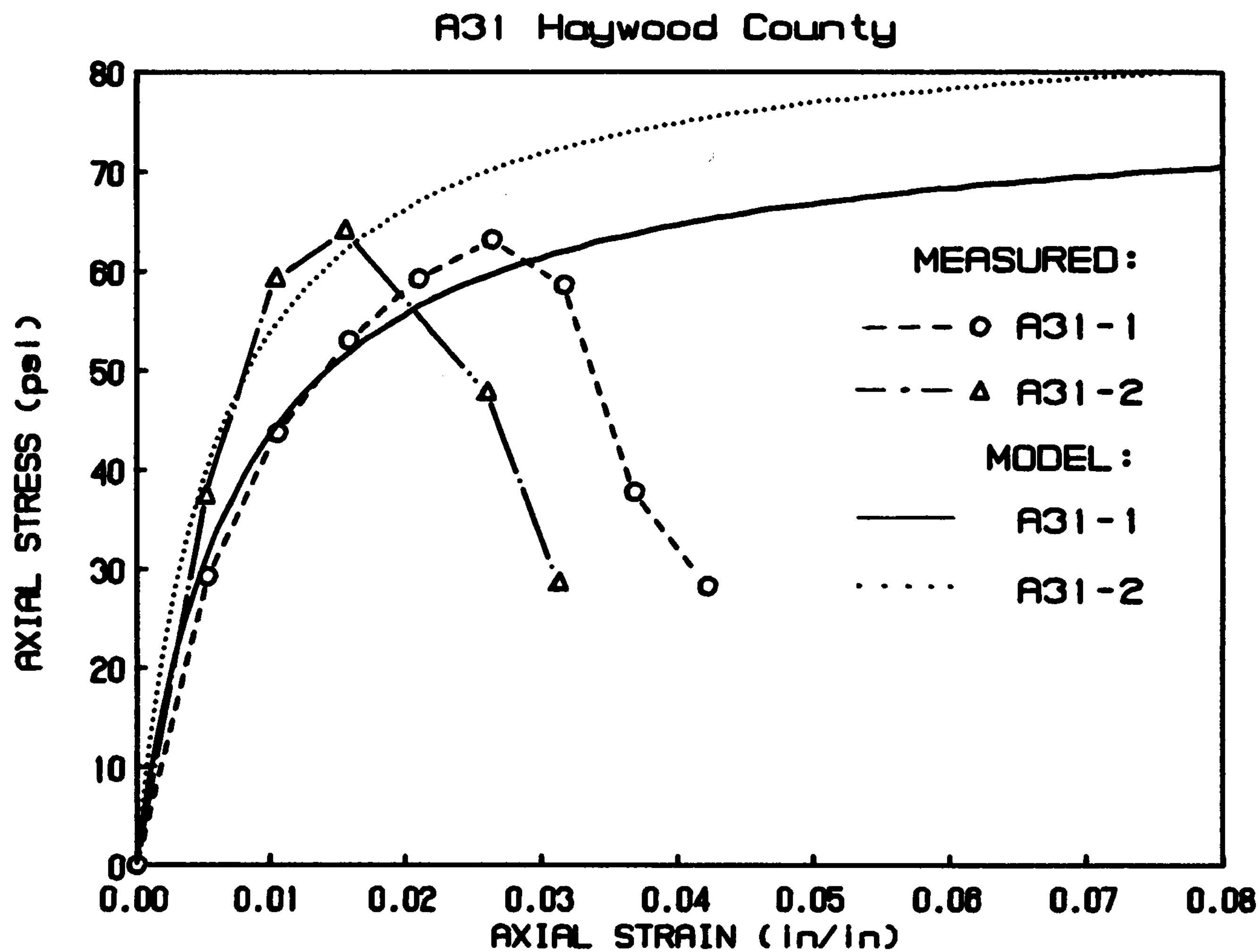

Figure V - 4. Measured and Predicted Stress-Strain Curves for Soil Type A31 Unconfined Compression Test Results.

Table V - 1. Index Properties and Hyperbolic Model Parameters for the Unconfined Compression Test Specimens.

Specimen	γ (lb/ft^3)	S. (%)	q_{max} (psi)	q_{res} (psi)	Hyperbolic Model Parameters		
					a (psi)	b (psi)	1/a (1/psi)
A31-1	105.0	70.7	63.3	28.1	0.0001	0.01295	10000.0
A31-2	106.0	72.6	63.9	28.1	0.00007	0.01160	14286.0
B21-1	100.3	80.5	68.8	37.7	0.00011	0.01300	9091.0
B21-2	102.1	78.6	64.8	37.9	0.00016	0.01180	6250.0
C11-1	113.1	81.2	30.9	6.3	0.00008	0.02780	12500.0
C11-2	112.7	84.5	32.3	4.7	0.00008	0.02780	12500.0
D11-1	83.3	86.7	28.7	14.2	0.00068	0.03160	1470.0
D11-2	83.2	83.4	33.5	12.0	0.00068	0.03160	1470.0
E21-1	97.2	84.8	67.7	55.5	0.00010	0.01120	10000.0
E21-2	98.6	79.8	72.1	64.7	0.00013	0.01280	7692.0
E31-1	98.9	92.8	45.6	44.8	0.00012	0.02080	8333.0
E31-2	96.8	87.5	36.2	35.6	0.00019	0.02500	5263.0
F11-1	105.7	80.0	53.5	39.9	0.00016	0.01520	6250.0
F11-2	106.4	80.8	44.0	38.6	0.00012	0.02020	8333.0
H11-1	109.9	77.3	62.6	32.1	0.00019	0.01220	5263.0
H11-2	109.9	83.0	62.3	28.8	0.00023	0.01020	4348.0
H21-1	114.2	81.8	39.7	26.6	0.00062	0.01240	1613.0
H21-2	115.2	83.9	51.9	27.0	0.00025	0.01360	4000.0
J11-1	82.9	97.2	27.3	22.9	0.00019	0.03360	5263.0
J11-2	81.4	93.7	27.3	22.9	0.00019	0.03360	5263.0
J31-1	89.5	92.9	46.0	45.0	0.00014	0.01720	7143.0
J31-2	86.3	91.9	53.0	51.8	0.00019	0.01920	5263.0

The resilient modulus versus deviator stress can also be represented by a hyperbola:

$$E_r = [\,\mathbf{a}' + \mathbf{b}'(\sigma_d)\,] \,/\, \sigma_d \quad : \text{for } \sigma_d > 0$$

where E_r = the resilient modulus

σ_d = the deviator stress

$\mathbf{a}', \mathbf{b}'$ = empirical coefficients determined experimently

The modified hyperbolic equation for the resilient modulus versus deviator stress is a direct inverse of that for the unconfined compression test mentioned earlier. The inverse relation of the two equations is obvious since the E_r and σ_d curve decreases with increasing $\sigma_{d,}$ while the σ and ε curve increases with increasing ε up to the maximum strength value. A schematic diagram of resilient modulus versus deviator stress curve for cohesive soils is represented in Figure V - 5. By plotting the data in the transformed axes $\sigma_d \times E_r$ versus σ_d, the parameters $\mathbf{a}'$ and $\mathbf{b}'$ are obtained as shown in Figure V - 6, where $\mathbf{a}'$ is the initial slope of E_r versus σ_d response and $\mathbf{b}'$ is E_{rmin}. The hyperbolic model from the repeated load testing data for soil type A31 is shown in Figure V - 7. The transformed axes plots of all the tested specimens are shown in Appendix C1, and the data listed in Appendix E1. The values of the minimum resilient modulus corresponding to the minimum on a resilient modulus deviator stress curve, the break point resilient modulus read at 6 psi deviator stress, and the hyperbolic parameters from the resilience testing data are listed in Table V - 2. The definitions of the symbols used are also found in Table VI - 3 on page 53.

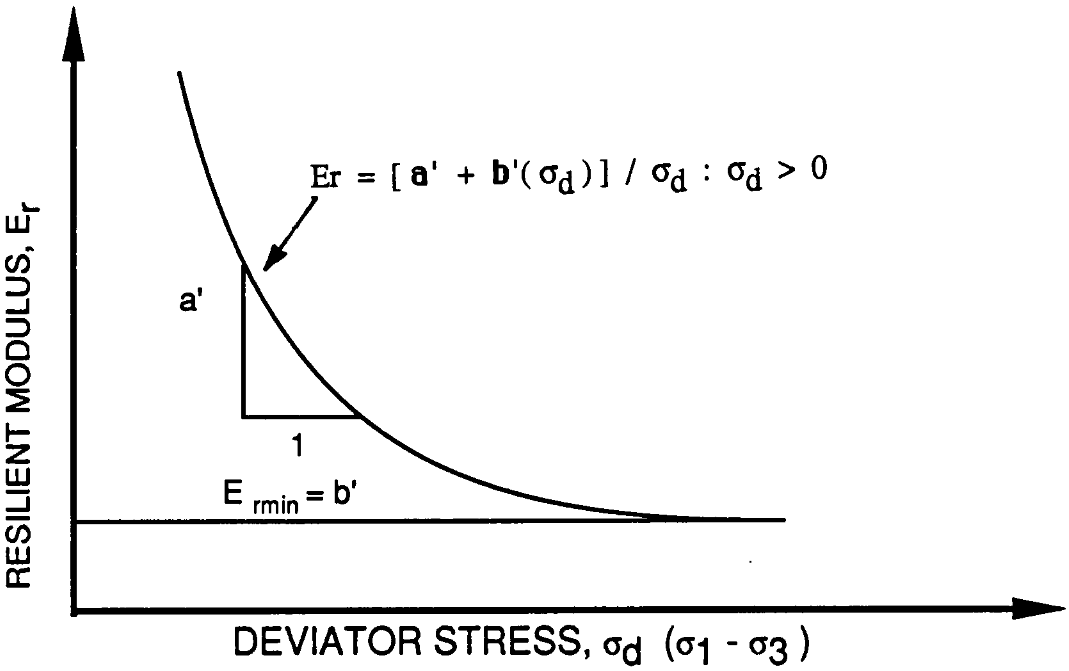

Figure V - 5. Schematic Diagram Depicting the Resilient Modulus Versus Deviator Stress Curve for Repeated Load Testing.

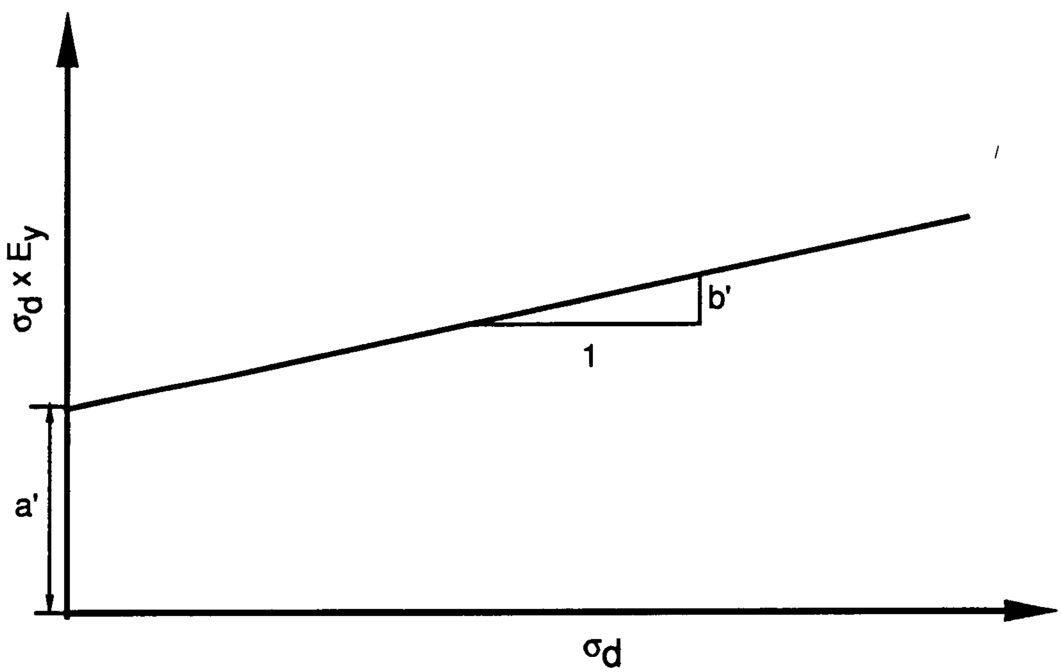

Figure V - 6. Transformed Axes for Determination of Hyperbolic Model for Repeated load Test.

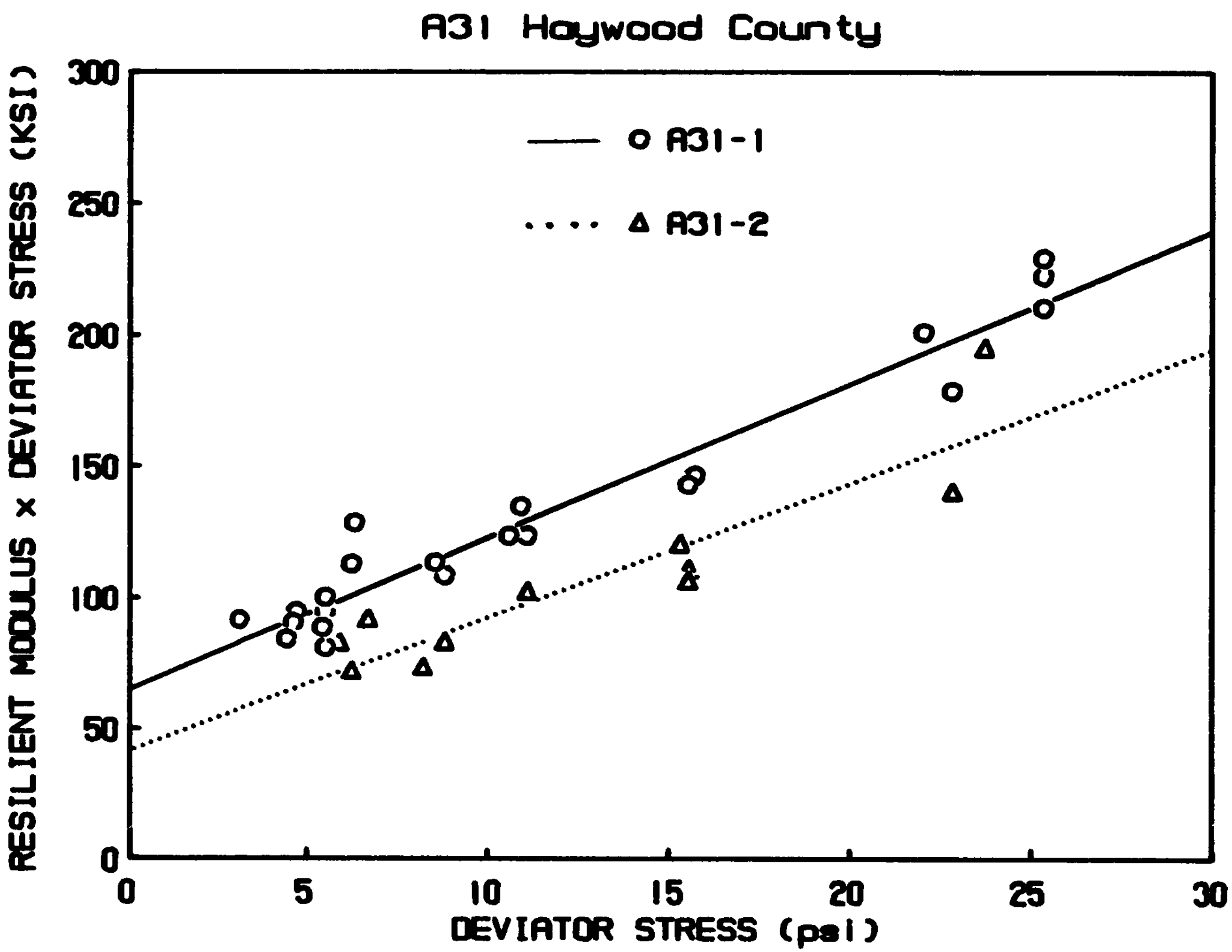

Figure V - 7. Hyperbolic Model Plot for Soil Type A31.

Table V - 2. Minimum and Breakpoint Resilient Modulus and Hyperbolic Model Parameters from Repeated Load Test Specimens.

Specimen	E_{rmin} (ksi)	E_{ri} (ksi)	Hyperbolic Model Parameters	
			a'	b'
A31-1	10.0	15.0	64.29	5.84
A31-2	7.0	11.0	41.52	5.10
B21-1	11.5	14.0	29.23	10.17
B21-2	10.0	15.0	44.25	6.96
C11-1	10.5	11.5	6.10	11.65
C11-2	11.5	12.0	6.66	10.61
D11-1	2.0	2.0	3.74	2.11
D11-2	2.0	2.0	4.58	2.08
E21-1	14.0	18.0	52.06	10.26
E21-2	13.0	15.0	69.88	7.02
E31-1	5.0	8.0	25.14	3.06
E31-2	5.0	10.0	52.44	2.03
F11-1	5.0	6.0	18.84	4.02
F11-2	5.0	6.0	12.38	4.37
H11-1	5.0	7.5	20.06	4.58
H11-2	6.5	10.0	39.04	4.82
H21-1	6.0	8.0	15.49	5.48
H21-2	6.5	8.0	2.03	6.13
J11-1	6.5	12.0	55.60	2.99
J11-2	11.5	13.0	55.20	4.43
J31-1	14.0	17.0	64.82	9.68
J31-2	12.5	16.5	62.04	8.34

CHAPTER VI

PREDICTIONS OF RESILIENT MODULUS

The primary goal of this study was to obtain design equations which accurately predict the resilient modulus as a function of deviator stress. The parameters obtained from the hyperbolic models and index tests were analyzed using the STATGRAPHICS (Statistical Graphics System) computer program to evaluate the data for any correlations. The STATGRAPHICS is a unique software package integrating a wide variety of statistical functions. These functions provide many modeling techniques that relate a dependent variable to one or more independent variables.

The STATGRAPHICS program contains many statistical functional utilities. However, only the Data Management and the Regression Analysis capabilities were used in this study. The Data Management section facilitates the creation, storage, and manipulation of the data stored in variables. The Regression Analysis provides a variety of multivariate modeling procedures. In its common usage, it expresses the dependent variable as a function of the independent variables based on the strength of the relationships among them. The Regression Analysis section contains six procedures, which are summarized in Table VI -1 (Statisitical Graphics Corporation, 1986).

The Stepwise Variable Selection procedure was used in this study. It allows either a forward or backward selection procedure to control the entry of variables into the model. Variables are entered or removed with the primary aim of obtaining a model with a small set of significant variables. The forward procedure starts with no variable in the model and ~~and~~ then adds one at a time based on the importance or significance of the new variable to the model. The program at this stage checks to see that the previously selected variables are significant; any insignficant variable is discarded in the model at that point. The backward procedure begins with a model containing all the variables and removes them one at a time based on their insignificance to the model. In backward selection, the program allows the re-entry of a variable into the model if it is later found it would add significance to the fit. The backward procedure was used in this analysis.

Table VI - 1. Summary of Various Procedures in the Regression Analysis Section of STATGRAPHICS (After Statistical Graphics Corporation, 1986).

Procedure	Number of Variables	Data Type	Description
Simple Regression	2	Numbers	Performs an ordinary least squares regression using one independent variabe. Estimates linear or selected nonlinear models.
Interactive Outlier Rejection	2	Numbers	Allows you to selectively exclude outlier points from a simple linear regression plot.
Multiple Regression	2 or more	Numbers	Performs ordinary linear least squares regression using several independent variables.
Stepwise Variable Selection	2 or more	Numbers	Performs backward or forward stepwise multiple regression.
Ridge Regression	2 or more	Numbers	Performs a ridge regression on standardized variables and plots results.
Nonlinear Regression	2 or more	Numbers	Produces least squares estimates of parameters in a nonlinear regression model.

Tabulated output of the Regression Analysis is given, indicating the constant, coefficients and the statistical parameters of the model. The statistical parameters essentially explain the significance of a variable to the model. Table V1 - 2 gives a simple description and explanation of the statistical parameters of importance to the study.

Table VI - 2. Simple Definition and Description of Statistical Parameters (after Statistical Graphics Corporation, 1986).

Parameter	Definition and Description
R - squared	It is called the Coefficient of Determination and indicates the percentage of variation explained by the model.
Adjusted R - squared	It is the Adjusted Coefficient of Determination and may decrease if insignificant variables are in the model. The Adjusted R - squared depicts or give the level of correlation of the model. A value of 1.0 indicates the best and highest correlation.
Standard Error of Estimation	It is equal to the square root of the mean squared error and measures the unexplained variability in the dependent variable.
t - value	It is calculated by dividing the coefficient of determination by the Standard Error of Estimation.
Significance Level	It explains the t - value for each coefficient, and gives the probability that a larger absolute t - value would occur if there were no marginal contribution from that variable. A significance Level of 0.0 for a variable indicates the model is highly dependent on that variable.

The parameters obtained from the hyperbolic modeling and the index properties all listed in Tables IV - 2, V - 1 and V - 2 were used to form the data base for the statistical correlation analyzes. Based on the goal of obtaining means to predict the design resilient modulus and curves for a given soil using simpler test methods, E_{ri}, **a**' and **b**' were each assigned a dependent variable status as indicated by E_{ri}*, **a**'*, **b**'*. The breakpoint modulus E_{ri} was selected because this indicator of resilient modulus is often used in pavement design procedures (Thompson and Robnett, 1976).

Parameters **a**' and **b**' were selected as dependent variables in developing the proposed hyperbolic model for the resilient modulus-deviator stress relationship. The modified hyperbolic equation for the resilience data is of the form:

$$E_r = [\, a'^* + b'^* (\sigma_d)] \;/\; \sigma_d$$

where Er = resilient modulus

σ_d = deviator stress

dependent variable a'^* = initial slope of Er versus σ_d

dependent variable b'^* = minimum resilient modulus E_{rmin}

Each dependent variable was then predicted using the rest of the data base. The independent variables are specifically b, 1/a, q_{max}, q_{res}, cc, LL, PL, PI, F, γ and, S are described and summarized in Table VI - 3. The data as entered in the STATGRAPHICS program are listed in Appendix A2. It should be noted that aa designates a', bb is b', inva is $1/a$, histr is q_{max}, ult is q_{res}, clay is cc, mxdens is γ, sat is S and finer is F. The breakpoint resilient modulus E_{ri}* was predicted first and the results of the STATGRAPHICS statistiscal parameters are listed in Appendix A2. The adjusted R-squared and the R-squared for the model were 0.76 and 0.83 respectively. The model was highly dependent on the plasiticity index, with a significance level of 0.0008, followed by the percent passing the No. 200 sieve and the maximum unconfined compressive strength. The other variables of significance forming the model are the initial tangent modulus, dry unit weight and the degree of saturation. It should be noted that a significance level of 0.0 depicts the highest dependence in a backward substitution method. The final equation for obtaining the predicted break point modulus is as follows:

Table VI - 3. Description of Variables for STATGRAPHICS Analysis.

Variable	Description
a'	The ordinate intercept value for the hyperbolic model of the resilience testing data.
a*	The predicted intercept value for the hyperbolic model of the resilience testing data using STATGRAPHICS.
b'	The slope of the regression line for the hyperbolic model of the resilience testing data.
b*	The predicted slope of the regression line for the hyperbolic model of the resilience testing using STATGRAPHICS.
E_{rmin}	The minimum resilient modulus for each specimen's resilient modulus versus deviator stress curve.
E_{ri}	The break point resilient modulus for each specimen's resilient modulus versus deviator stress curve taken at 6 psi deviator stress.
E_{ri}*	The predicted break point resilient modulus using STATGRAPHICS.
a	The ordinate intercept value for the hyperbolic model of the unconfined compression test data.
1/a	The reciprocal of the intercept value as defined above.
b	The slope of the regression line for the hyperbolic model of the unconfined compression test data.
q_{max}	The maximum unconfined compressive strength of a specimen.
finer	Percent passing #200 sieve
cc	The clay content of a soil sample obtained from grain size distribution analysis.
LL	The liquid limit of a soil sample obtained from the Atterberg Limits tests.
PL	The plastic limit of a soil sample obtained from the Atterberg Limits tests.
PI	Plasticity index of a soil sample; PI = LL - PL.
γ	The dry unit weight of a test specimen.
S	The degree of saturation of a test specimen.

$$E_{ri}^* = 45.8 + 0.00052(1/a) + 0.188(q_{max}) + 0.454(PI) - 0.216(\gamma) - 0.25(S) - 0.15(F)$$

where

E_{ri}^* = predicted break point resilient modulus (ksi)

$1/a$ = initial tangent modulus from unconfined compression tests (psi)

q_{max} = maximum unconfined compressive strength (psi)

PI = plasticity index

γ = dry unit weight

S = degree of saturation (%)

F = passing #200 sieve (%)

Using the equation above, the break point resilient modulus corresponding to 6 psi deviator stress was calculated and compared with the measured values. The measured and predicted values as well as their percent difference are listed in Table VI - 4. Although the percent difference had a range of -50% through 2.1%, it should be noted that the majority of the differences was below ±30% which indicates a relatively satisfactory correlation. It was observed that where a higher difference occurs for a soil specimen, for example H11, the other specimen of the same sample gave a difference equal to or less than 30%, with the exception of D11. The high adjusted R-squared indicates a good level of correlation in the model which yields the low level of percent differences. Thus within the limits of experimental errror, the results were reliable. A plot of the measured and the predicted E_{ri}^* values shown in Figure VI - 1 depicts the the variations in the percent error.

Table VI - 4. Measured E_{ri} and Predicted Values E_{ri} *

Specimen	Measured E_{ri} (ksi)	Predicted E_{ri}* (ksi)	Difference (%)
A31-1	15.0	12.1	19.3
A31-2	11.0	13.8	-25.5
B21-1	14.0	13.7	2.1
B21-2	15.0	11.6	22.7
C11-1	11.5	11.1	3.5
C11-2	12.0	10.6	11.7
D11-1	2.0	1.2	40.0
D11-2	2.0	3.0	-50.0
E21-1	18.0	15.8	12.2
E21-2	15.0	16.4	-9.3
E31-1	8.0	9.3	-16.3
E31-2	10.0	7.7	23.0
F11-1	6.0	8.8	-46.7
F11-2	6.0	7.8	-30.0
H11-1	7.5	10.4	-38.7
H11-2	10.0	8.6	14.0
H21-1	8.0	6.7	16.3
H21-2	8.0	9.5	18.8
J11-1	12.0	12.7	5.8
J11-2	13.0	13.9	-6.9
J31-1	17.0	15.8	7.1
J31-2	16.5	17.1	-3.6

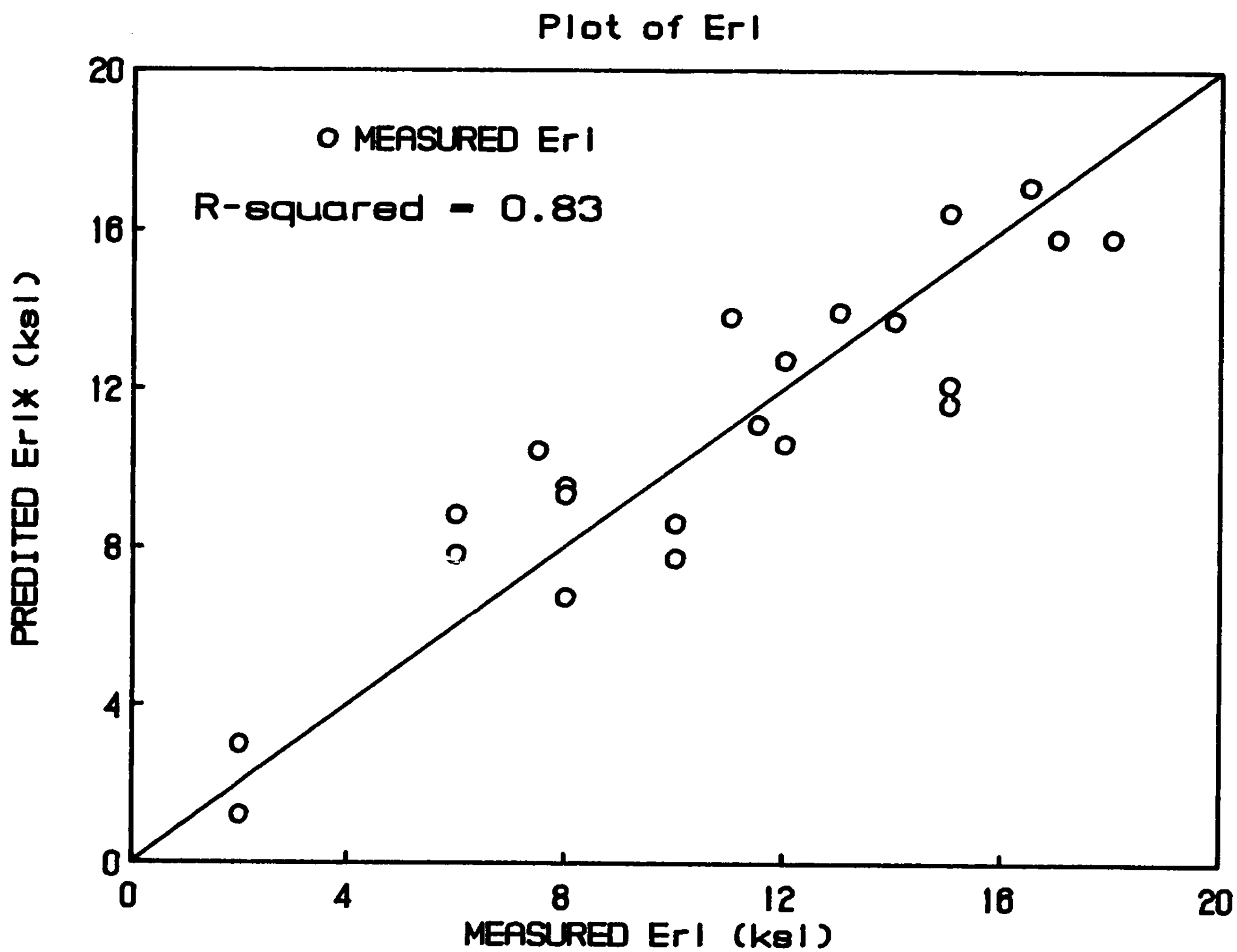

Figure VI - 1. A Plot of Predicted E_{ri}* Versus Measured E_{ri}.

The repeated loading testing hyperbolic parameters **a'*** were next predicted using the independent variables. The adjusted R - squared and the R -squared for the correlation were 0.73 and 0.81 respectively. The statistical parameters from the prediction of a'* are listed in Appendix A2. The model was found to highly dependent on the plasticity index with a significance level of 0.0022, and followed by the degree of saturation with 0.0113. The equation obtained for the predicted **a'*** parameters is as follows:

$$a'^* = 318.2 + 0.337(q_{max}) + 0.73(cc) + 2.26(PI) - 0.915(\gamma) - 2.79(S) - 0.304(F)$$

where
a'^* = predicted initial slope of the E_r versus σ_d (ksi)
q_{max} = maximum unconfined compressive strength (psi)
cc = clay content (%)
PI = plasticity index
γ = dry unit weight (ib/ft^3)
S = degree of saturation (%)
F = passing #200 sieve size (%)

The percent difference between the measured **a'** and predicted **a'*** are listed in Table VI - 5. The percent difference was higher than expected in almost all the specimen, however, parameter **a'** corresponds to the initial slope of the E_r versus σ_d response and a poor correlation may not significantly affect the overall model. Figure VI - 2 shows a plot of the the measured and the predicted values.

Finally, the resilience or repeated loading test hyperbolic **b'*** parameters were predicted. The adjusted R -squared and the R - squared values for the correlation were 0.66 and 0.73 respectively. The statistical parameters from the prediction of **b'*** are listed in Appendix A2. The model was found to be highly dependent on the percent grain size

Table VI - 5. Measured a' and Predicted Values of a'*.

Specimen	Measured a' (ksi)	Predicted a'* (ksi)	Difference (%)
A31-1	64.3	48.6	24.4
A31-2	41.5	42.6	-2.7
B21-1	29.2	42.6	-45.9
B21-2	44.3	44.9	-1.4
C11-1	6.1	8.6	-41.0
C11-2	6.7	0.2	97.0
D11-1	3.7	3.2	13.5
D11-2	4.6	14.1	-206.5
E21-1	52.1	42.8	17.9
E21-2	69.9	57.0	18.5
E31-1	25.1	27.4	-13.7
E31-2	52.4	41.0	21.8
F11-1	18.8	25.4	-35.1
F11-2	12.4	19.3	-55.6
H11-1	20.1	36.2	-80.0
H11-2	39.0	20.4	47.7
H21-1	15.5	15.1	2.5
H21-2	2.0	12.4	-520.0
J11- 1	55.6	43.0	22.7
J11-2	55.2	54.2	1.8
J31-1	64.8	69.1	-6.6
J31-2	62.0	77.3	-24.7

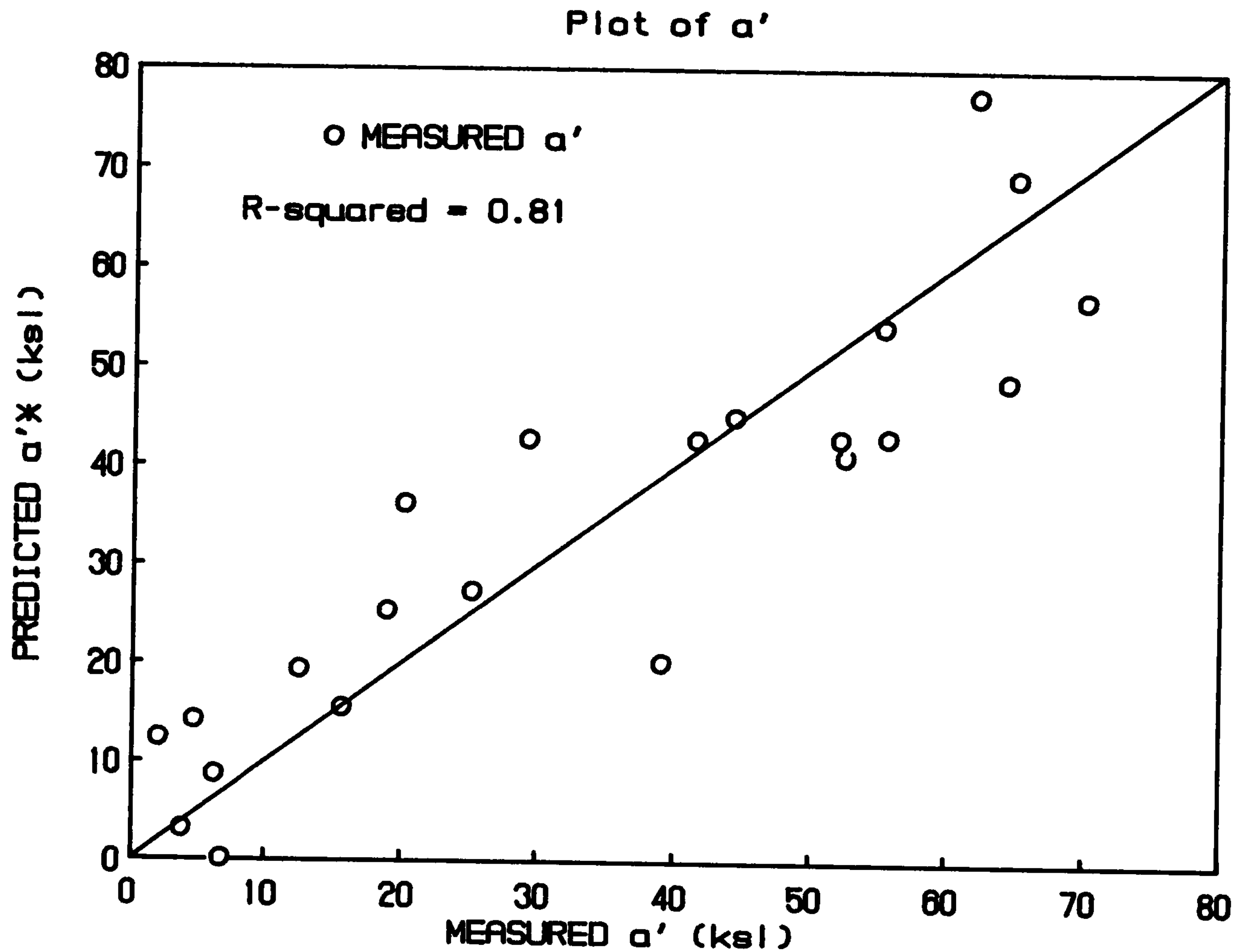

Figure VI - 2. A Plot of Predicted a'* Versus Measured a'.

passing the No. 200 sieve size with a significance level of 0.0002, and followed by the initial tangent modulus and the maximum uncofined compressive strength both with a level of 0.0034. Values of the measured **b'** and the predicted **b'*** are listed in Table VI - 6 and a plot is shown in Figure VI - 3.

The equation for the predicted values of **b'*** is as follows:

$$b'^* = 2.01 + 0.00039(1/a) + 0.104(qmax) + 0.091(LL) - 0.10(F)$$

where
b'^* = predicted minimum resilient modulus (ksi)
$1/a$ = initial tangent modulus from unconfined compressive test (psi)
q_{max} = maximum unconfined compressive strength (psi)
LL = liquid limit (%)
F = passing #200 sieve (%)

It was observed that most of the percent differences were under $\pm$30% and even where a higher difference was observed for a specimen, the other specimen of the same soil type had a lower percent difference. It should be noted that while E_{ri}, **a'** and **b'** were obtained from the resilience or repeated load test data, E_{ri}*, **a'*** and **b'*** were predicted strictly with data from index tests data and unconfined compression.

Table VI - 6. Measured b' and Predicted Values of b'*

Specimen	Measured b' (ksi)	Predicted b* (ksi)	Difference (%)
A31-1	5.8	5.8	0
A31-2	5.1	7.5	-47.0
B21-1	10.2	6.3	38.2
B21-2	7.0	4.7	32.8
C11-1	11.7	10.0	14.5
C11-2	10.6	10.1	4.7
D11-1	2.1	0.9	57.1
D11-2	2.1	1.4	33.3
E21-1	10.3	9.5	7.8
E21-2	7.0	9.1	-30.0
E31-1	3.1	4.5	-45.2
E31-2	2.0	2.4	-20.0
F11-1	4.0	4.9	-22.5
F11-2	4.4	4.7	-17.5
H11-1	4.6	5.9	-28.3
H11-2	4.8	5.5	- 14.6
H21-1	5.5	5.1	7.3
H21-2	6.1	7.3	-19.7
J11-1	3.0	5.1	70.0
J11-2	4.4	5.1	-13.7
J31-1	9.7	7.9	18.6
J31-2	5.1	7.9	4.8

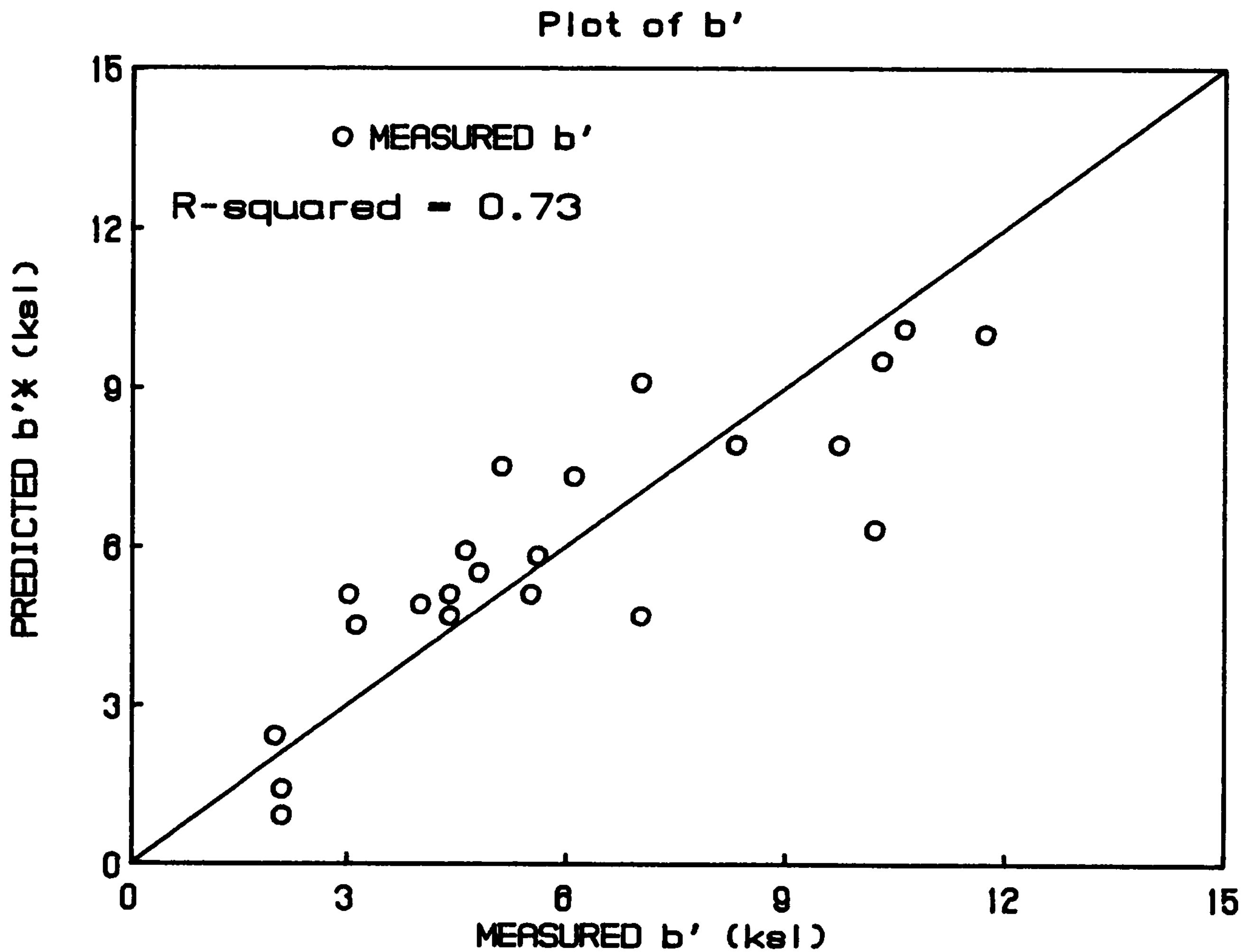

Figure VI - 3. A Plot of Predicted b'* Versus Measured b'.

In summary E_r can be approximated as:

$$E_r = \{ \mathbf{a}'^{*}(PI,\ S,\ \gamma,\ cc,\ F,\ q_{max}) + [\mathbf{b}'^{*}(F,\ 1/a,\ q_{max},\ LL)](\sigma_d)\} \ /\ \sigma_d$$

Where E_r = predicted resilient modulus (ksi)

σ_d = deviator stress (psi)

PI = plasticity index

S = degree of satuaration (%)

γ = dry unit weight

cc = clay content (%)

F = passing #200 sieve (%)

q_{max} = maximum unconfined compressive strength (psi)

1/a = initial tangent modulus from unconfined compression test (psi)

LL = liquid limit (%

$$\mathbf{a}'^{*} = 318.2 + 0.337(qmax) + 0.73(cc) + 2.26(PI) - 0.915(\gamma) - 2.79(S) - 0.304(F)$$

$$\mathbf{b}'^{*} = 2.01 + 0.00039(1/a) + 0.104(qmax) + 0.091(LL) - 0.10(F)$$

The curves of the measured E_r versus σ_d and the predicted E_r* verus σ_d were compared for all the tested specimens. A typical plot for soil type A31 is shown in Figure VI - 3. The other plots of such curves are found in Appendix D1. A satisfactory agreement was found between the measured and the predicted curves for most specimens. It can be deduced that the variations in the values of the **a**'* parameters for the same soil type had little effect on the predicted curves. However, variations in the values of **b**'* for the same soil type affected the outcome of the curves.

Simple regression analysis was conducted on the measured and predicted values of E_{ri}, **a**', **b**', and E_{ri}*, **a**'*, **b**'* respectively. The purpose of the analysis was to examine closely the linear fit of the predicted values on the measured values. Satisfactory correlation coefficients of 0.84 to 0.91 were obtained, where a correlation of 1.00 indicates the best fit. The low probability levels obtained also indicated a good fit since a probability level of 0.0 yields the best fit. The 95% confidence level and the prediction limits for each measured and predicted plot as well as the statistical parameters for their correlation are found in Appendix A2.

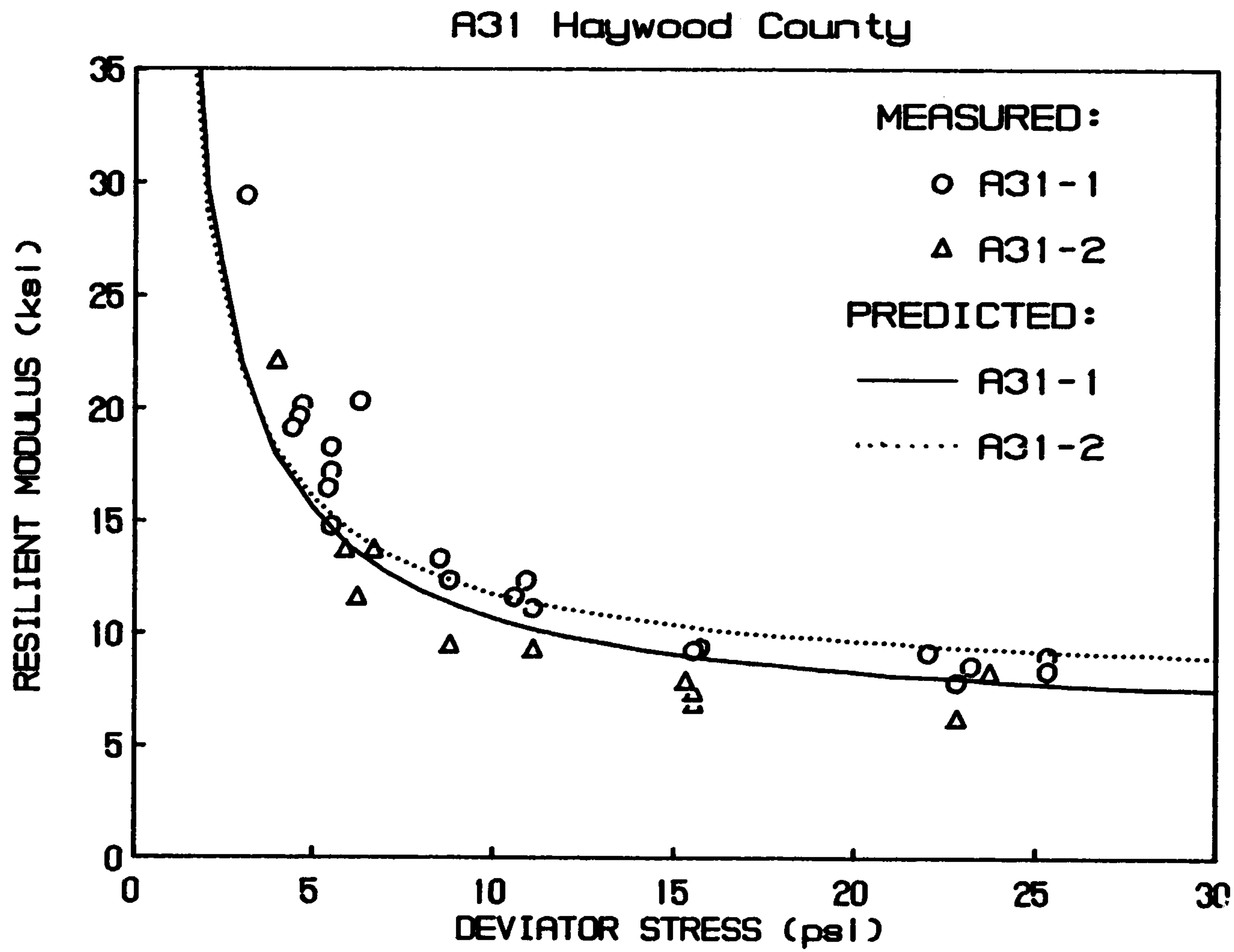

Figure VI - 4. Measured and Predicted Curves of Resilient Modulus Versus Deviator Stress for Soil Type A31.

CHAPTER VII

CONCLUSION

1. SUMMARY

The main objective of this investigation was to determine the resilient modulus of subgrade soils in the state of Tennessee, and develop a model for predicting the modulus on the basis of simple lab tests. A review of previous research on resilient modulus was conducted, and based on the study of the average daily traffic (ADT) on prevalent soils, priority soils were selected for laboratory testing.

Standard laboratory tests were conducted to determine the index properties of each soil type. From the grain size distribution analyses, it was deduced that all the selected soil samples were fine-grained. Test specimens for repeated load testing were prepared in accordance to the Tennessee Department of Transportation (TNDOT) specifications and the requirement of the American Association of State Highway and Transportation Officials (AASHTO) test method T274 - 82. Two specimens of each of the soil types were used for the resilience testing.

The data aquisition for the resilience testing was accomplished by using an X - Y plotter to display the output from the load cell and and the LVDT. The plotter gave loops of the applied stress and the axial displacement of the test specimen. The magnitude of the applied stress was equal to the deviator stress ($\sigma_1 - \sigma_3$) since no confining, or chamber pressure, was used in the triaxial setup. To characterize the resilient response of the soils, a plot of the resilient modulus versus the deviator stress for each specimen was obtained. The well-known trend of decreasing resilient modulus with increasing deviator stress for fine-grained soils was observed. This verified the initial deduction about the fine-grained nature of the soils. Effects of factors affecting resilient modulus such as dry density and degree of saturation were not investigated in this study.

Modified hyperbolic equations were used to model the non-linear resilient modulus versus deviator stress response. Using the hyperbolic parameters from the resilience testing as the dependent variables, and the index properties and stiffness from unconfined compression tests as the independent variables, regression equations were obtained for back-predicting the measured curves. The break point resilient modulus, selected at 6 psi deviator stress, was also predicted for each of specimen tested. The correlation was accomplished by using the statistical computer program STATGRAPHICS.

The coefficient of determination, R-squared was 0.81 and 0.73 for the two dependent variables in the proposed resilient modulus model. The model for the breakpoint modulus E_{ri} yielded an R-squared of 0.83. In view of the inherent variability in the resilient modulus testing, and uncertainties related to characterization of soil, the proposed model can be assumed to be satisfactory.

2. RECOMMENDATIONS

The following recommendations are based on the outcome of the laboratory testing and correlation procedure.

1. Extreme caution should be used in the laboratory determination of the index properties of the soil samples since the regression equations are highly dependent on their outcome.
2. Hyperbolic modeling is appropriate if the results obtained from the repeated load tests follow hyperbolae. Sensitive equipment must be used in the testing program, and care taken to read the data in the lower stress range, that is 1 - 4 psi. An X - Y plotter is an appropriate method to record repeated load data and may be more reliable than computer data aquisition systems.
3. Extensive laboratory testing should be conducted to study the effects of factors such as the degree of saturation and density affecting the resilient modulus, how they pertain to the soils in Tennessee and how such

variation would affect the modeling so far obtained.

4. The hyperbolic model analyses of the data from the unconfined compression tests should be evaluated to a maximum strain of 0.05 in/in. Tests conducted in this study indicate that beyond this strain value the specimen softens to a point where the modeling may be unrepresentative of the soil. It is also difficult to obtain the hyperbolic parameters with a curved transformed plot.

5. Investigate the effect of the repeated load on the unconfined strength of the soil. In this investigation, the unconfined strength was determined from the same specimens used in the resilient modulus testing to reduce specimen error. However, the conditioning and the repeated loading may affect the unconfined response, and these effects should be investigated.

6. Additional testing to provide a larger data base may improve the correlation coefficients. The testing of other soil types, may permit the extension of the proposed model.

REFERENCES

REFERENCES

1. American Association of State Highway and Transportation Officials, "Standard Specifications for Transportation Materials and Methods of Sampling and Testing, AASHTO, Washington, D. C. July 1982, 13th Edition, 1182 pp.

2. American Society of Testing And Materials, "New Standard for Resilient Modulus of Untreated Soils -- Third Draft," ASTM D 18.09.06, February 25, 1985, 21 pp.

3. American Society of Testing and Materials, "Soil and Rock; Building Stones ,"Annual Book of ASTM Standards, ASTM, Phildeldelphia, Pennsylvania , 1984, Vol. 04.08, 830 pp.

4. Asphalt Institute, "Asphalt Overlays and Pavement Rehabilitation,"Manual Serias No. 17, Nov. 1969.

5. Asphalt Institute, Thickness Design: Asphalt Pavements for Highways and Streets. Manual No. 1, College Park, Md., Sept. 1981.

6. Bandyopadhay, S. S. and J. A. Frantzen, "Investigation of Moisture Variation in Subgrade Modulus by Cross-Correlation Method," Transportation Research Record, No. 945, Transportation Research Board, 1983, pp 10-15.

7. Barksdale, R. D., et al., "Test Procedures for Chararacterizing Dynamic Stress- Srain Properties of Pavement Materials," Special Report 162, Transportation Research Board, National Research Council, 1975, Washington , D. C., 40 pp.

8. Canadian Good Roads Association, "Field Performance Studies of Flexible Pavements in Canada," Proceedings, Second International Conference on the Structural Design of Asphalt Pavements, Ann Arbor, Michigan, 1967.

9. Clough, G. W. and J. M. Duncan, "Finite Analyses of Retaaining Wall Behavior" Journal of the Soil Mechanics and foundation Division, Proceeding of ASCE, Vol. 97, No. SM12 December 1971.

10. Cole D. M., L. H. Irwin and T. C. Johnson, "Effect of Freezing and Thawing on Resilient Modulus of a Granular Soil Exhibiting Nonlinear Behavior," Transportation Research Record, No. 809, National Academy of Sciences Washington D. C. 1981.

11. Cole, D. M., G. Durrell and G. Chamberlain, "Repeated Load Triaxial Testing of Frozen and Thawed Soils," Geotechnical Testing Journal, Vol. 8. No. 4. Dec. 1985, pp. 166-170.

12. Costa Filho, L. de M., "Measurement of Axial Strains in Triaxial Tests on London Clay," Geotechnical Testing Journal, GTJODJ, Vol. 8, No. 1, March 1985. pp. 3-13.

13. Department of the Army, "Laboratory Soil Testing," Engineer Manual, No. 1110-2-1906, Washington D. C. Nov. 1970.

14. Drumm, E. C. and A. B. Moore, "Pavement Design using Rapid Method of Collecting and Analyzing Deflection Data Phase II - Design Procedure Development" Draft Final Report, University of Tennessee, Knoxville, 1987.

15. Gonzalo R. and M. W. Witczak "Comprehensive Evaluation of Laboratory Resilient Modulus Results for Granular Materials" Transportation Research Records, No. 810, National Academy of Sciences, Washington D. C., 1981, pp. 23-33.

16. Heuklelom W. and A. J. G. Klomp "Dynamic Testing as a Means of Controlling Pavement During and After Construction" Proceedings of the First International Conference on Structural Design of Asphalt Pavement, University of Michigan, 1962.

17. Hicks, R. G., and C. L. Monismith, "Factors Influencing the Resilient Response Granular Materials" Highway Research Record, No. 345, Highway Research Board, Washington, D. C., 1971, pp. 14-31.

18. Highter, W. H. and A. B. Moore, "Pavement Design using Rapid Methods of Collecting and Analyzing Deflection Data Phase II - Design Procedure development, Progress Report I and Interim Design 1984

Procedure," Civil Engineering Department, The University of Tennessee, 984, Knoxville, Tennessee, 150 pp.

19. Hsu, Shih-Ying and Ted S. Vinson., "Determination of Resilient Properties of Unbounded Materials With Repeated Load Triaxial and Diametrical Test Systems," Oregon Department of Transportation, Salem; Oregon State University, Corvallis, Oregon, 1981.

20. Johnson, D. J., "The Resilient Moduli of Subgrade Soil in the East Tennessee Area," Thesis presented for the Master of Science Degree, The University of Tennessee, Knoxville, 1986, 124 pp.

21. May R. W. and M. W. Witczak "Effective Granular Modulus to Model Pavement Responses" Transportation Research Records, No. 810, National Academy of Sciences, Washington D. C., 1981, pp. 1-9.

22. Moossazadeh J. M., W. Witczak, "Prediction of Subgrade Moduli for Soil That Exhibit Nonlinear Behavior," Traansportation Research Records, No. 810, National Academy of Sciences, Washington D. C., 1981.

23. Pumphrey Jr., N. D., R. W. Lentz, "Deformation Analysis of Florida Highway Subgrade Sand Subjected to Repeated Load Triaxial Test," Transportation Research Record, No. 1089, National Research Council, Washington D. C., 1986, pp. 49-56.

24. Robnett, Q. L. and Thompson, M. R., "Interim Report - Resilient Properties of Subgrade Soils, Phase I - Developement of Testing Procedures," Illinois Cooperative Highway Research Program No. IHR - 603, University of Illinois, May 1973, Urbana - Champaign, Illinois, 25pp.

25. Robnett Q. C. and M. R. Marshall, Effects of Lime Treatment on the Resilient Behavior of Fine-Grained Soils," Transportation Research Records, No. 560, Transportation Research Board, 1976.

26. Sarby, R. W., N. Kalteziotis., and E. M. Haddad, "Bedding Errors in Triaxial Tests on Granular Media," Geotechnique, Vol. 30, 1980. pp. 302-309.

27. Springer, M. E. and J. A. Elder, "Soils of Tennessee," U. S. Department of Agriculture Soil Conservation Service and the University of Tennessee Agriculural Experiment Station, Knoxville, Tennessee, August 1980, pp. 1-64.

28. Sodernman L. G., Y. D. Kim, V. Milligan "Field and Laboratory Studies of the Modulus of Elasticity of a Clay Till," Highway Research Record, No. 243.

29. Tennessee Department of Transportation Bureau of Highways, "Subgrade Construction and Preparation," Specifications for Road and Bridge Construction, TNDOT Bureau highways, Kingsport, Tennessee, March 1981 Section 207.04, p. 126.

30. Terrel R. L. and I. S. Award "Laboratory Considerations" Proceedings, Association of Asphalt paving Technologists, AAPT Symposium of Technology of Thick Lift Construction, 1972.

31. "The AASHO Road Test, Part 5, Pavement Research," Special Report 61E, Highway Research Board, 1962.

32. "The WASHO Road Test, Part 2, Test Data, Analysis, Findings," Special Report 22, Highway Research Board, 1955.

33. Thompson M. R. and Q. L. Robnett, "Final Report, Resilient Properties of Subgrade Soils," Civil Engineering Studies Transportation Engineering Series No. 14, Illinois Cooperative Highway and Transportation Series No. 160, 1976.

34. Thorton S. I and R. P. Elliot, "Resilient Modulus - What Is It?," Proceedings of the 37th Annual Highway Geology Symposium, Helena, Montana, 1986, pp. 267-282.

35. Yoder, E. J. and M. W. Witczak, Principles of Pavement Design, Second Edition, John Wiley and Sons, Inc., 1975, 711 pp.

APPENDICES

APPENDIX A

APPENDIX A1

COMPUTER PROGRAM FOR REPEATED LOAD TEST DATA REDUCTION

```
10 'data reduction for x-y plotter
20 'ecd 7-9-87, 7-11-87
30 INPUT " enter sample length in inches ";LENGTH
40 INPUT " enter X-gain in mv/cm";XGAIN
42 INPUT " enter Y-gain in mv/cm";YGAIN
50 LOADFACTOR = 50:DISPFACTOR = .2:'50#/volt, 0.2 inch/volt
60 PI=3.141593:AREA = 3.0635
70 INPUT "     enter load reading in cm ";AXIAL
75 INPUT "     enter angle of slope from horz in degrees";THETA
80 STRESS = AXIAL*YGAIN*LOADFACTOR/(AREA*1000):'PRINT "Stress = ";STRESS;" psi "
90 'PRINT : PRINT "  X-gain in mv/cm, Y-gain in mv/cm";XGAIN,YGAIN
100 'PRINT "        sample length = ";LENGTH;" inches, area = ";AREA;"inches^2 "
110 'PRINT "  load reading in cm";AXIAL;" theta = ";THETA;" degrees"
120 THETA = THETA * PI/180
130 SLOPE  = TAN(THETA):'PRINT "   slope = ";SLOPE
140 DISP = AXIAL/SLOPE
150 STRAIN = DISP*XGAIN*DISPFACTOR/(LENGTH*1000)
160 STRAIN = STRAIN/100
170 SIGCOEF= YGAIN*LOADFACTOR/(AREA*1000)
180 EPSCOEF= XGAIN*DISPFACTOR/(LENGTH*1000)
190 ER = SLOPE*SIGCOEF/(EPSCOEF*1000)
200 'PRINT :PRINT "  stress = ";STRESS;" psi,   strain = ";STRAIN;" %,  modulus
= ";ER;" psi ":PRINT :PRINT
201 PRINT :PRINT "  stress = ";STRESS;" psi,       modulus = ";ER;" psi ":PRINT
:PRINT
210 GOTO 40
220 END
```

APPENDIX A2
STATGRAPHICS INPUT AND OUTPUT DATA

STATGRAPHICS Input Data

Row	AA	SAMPLE		BD	ERM	ERI	A	B	INVA	HISTR	ULT	CLAY	LL	PL	PI	MXDENS	SAT	FINES
1	54.29	A31		5.84	10	15	1E-4	0.01295	10000	63.25	28.14	17	30.5	22.1	8.4	105	70.7	95
2	29.23	B21		10.17	11.5	14	1.1E-4	0.013	9091	68.8	37.7	18	38.8	23.3	15.5	100.3	80.5	100
3	44.25	B21		6.96	10	15	1.6E-4	0.0118	6250	64.8	37.87	18	38.8	23.3	15.5	102.1	78.6	100
4	6.1	C11		11.65	10.5	11.5	8E-5	0.0278	12500	30.85	6.33	17	20.7	19	1.7	113.1	81.2	20
5	5.65	C11		10.61	11.5	12	8E-5	0.0278	12500	32.3	4.74	17	20.7	19	1.7	112.7	84.5	20
6	3.74	D11		2.11	2	2	6.8E-4	0.0316	1470	28.71	14.2	18	36.2	34.1	2.1	83.3	86.7	80
7	4.58	D11		2.08	2	2	6.8E-4	0.0316	1470	33.53	12	18	36.2	34.1	2.1	83.2	83.4	80
8	52.06	E21		10.26	14	18	1E-4	0.0112	10000	67.7	55.5	35	37	27	10	97.2	84.8	68
9	69.89	E21		7.02	13	15	1.3E-4	0.0128	7692	72.07	64.68	35	37	27	10	98.6	79.8	68
10	25.14	E31		3.06	5	8	1.2E-4	0.0238	8333	45.55	44.8	36	42.1	22	20.1	98.9	92.3	93
11	52.44	E31		2.03	5	10	1.9E-4	0.025	5263	36.2	35.57	36	42.1	22	20.1	96.8	87.5	93
12	18.84	F11		4.02	5	6	1.6E-4	0.0152	6250	53.48	39.85	16	29.5	20.1	9.4	105.7	80	78
13	12.38	F11		4.37	5	6	1.2E-4	0.0202	8333	43.97	38.6	16	29.5	20.1	9.4	106.4	80.8	78
14	20.06	H11		4.56	5	7.5	1.3E-4	0.0122	5263	62.3	32.14	20	28.5	19.2	9.3	109.9	77.3	73
15	33.04	H11		4.82	6.5	10	2.3E-4	0.0102	4348	62.57	28.78	20	28.5	19.2	9.3	109.9	83	73
16	15.49	H21		5.40	6	8	5.2E-4	0.0124	1613	39.73	26.63	16	21	14.1	6.9	114.2	81.8	36
17	2.03	H21		6.13	6.5	8	2.5E-4	0.0136	4000	51.93	26.96	16	21	14.1	6.9	115.2	83.9	36
18	54.82	J31		9.68	14	17	1.4E-4	0.0173	7143	46	45	55	69.5	42.6	26.9	89.5	92.9	80
19	62.04	J31		8.34	12.5	16.5	1.9E-4	0.0192	5263	53.3	51.83	55	69.5	42.6	26.9	86.3	91.9	80
20	41.52	A31		5.1	7	11	7E-5	0.0116	14286	63.95	28.46	17	30.5	22.1	8.4	106	72.6	95
21	55.5	J11		2.99	6.5	12	1.9E-4	0.0336	5263	27.31	22.9	28.7	68.5	39.2	29.3	82.9	97.2	80
22	55.2	J11		4.43	11.5	13	1.9E-4	0.0336	5263	27.31	22.9	28.7	68.5	39.2	29.3	81.4	93.7	80
23																		
24																		
25																		
26																		
27																		
28																		
Length	22	22	22	22	22	22	23	22	22	22	22	22	22	22	22	22	22	22
Type	N	C	C	N	N	N	N	N	N	N	N	N	N	N	N	N	N	N

STATGRAPHICS Output Data

Stepwise Selection for ERI

Selection: Backward   Maximum steps: 500   F-to-enter: 4.00
Control: Manual   Step: 4   F-to-remove: 4.00

R-squared: .82812   Adjusted: .75937   MSE: 4.93672   d.f.: 15

Variables in Model	Coeff.	F-Remove	Variables Not in Model	P.Corr.	F-Enter
2. INVA	0.00052	11.1292	1. B	.2062	.6220
3. HISTR	0.18836	15.7528	4. CLAY	.1564	.3512
6. PI	0.45434	17.3514	5. LL	.0023	.0001
7. MXDENS	-0.21562	7.1428			
8. SAT	-0.25121	2.0298			
9. FINER	-0.14960	15.5553			

Model fitting results for: ERI

Independent variable	coefficient	std. error	t-value	sig.level
CONSTANT	45.789984	21.581646	2.1217	0.0509
INVA	0.000519	0.000155	3.3360	0.0045
HISTR	0.188364	0.047459	3.9690	0.0012
PI	0.454339	0.109072	4.1655	0.0008
MXDENS	-0.215617	0.080677	-2.6726	0.0174
SAT	-0.251215	0.176328	-1.4247	0.1747
FINER	-0.149601	0.037931	-3.9440	0.0013

R-SQ. (ADJ.) = 0.7594   SE= 2.221874   MAE= 1.605537   DurbWat= 1.896
Previously: 0.6620   1.735869   1.233763   1.088
22 observations fitted, forecast(s) computed for 0 missing val. of dep. var.

Regression results for ERI

Observation Number	Observed Values	Fitted Values
1	15.0000	12.0939
2	14.0000	13.6972
3	15.0000	11.5595
4	11.5000	11.0792
5	12.0000	10.6096
6	2.00000	1.20509
7	2.00000	3.96358
8	18.0000	15.8379
9	15.0000	16.4183
10	8.00000	9.27367
11	10.0000	7.70454
12	6.00000	8.81907
13	6.00000	7.75611
14	7.50000	10.4438
15	10.0000	5.58822
16	3.00000	5.68671
17	8.00000	9.47953
18	17.0000	15.7773
19	16.5000	17.1187
20	11.0000	13.7556
21	12.0000	12.7150
22	13.0000	13.9177

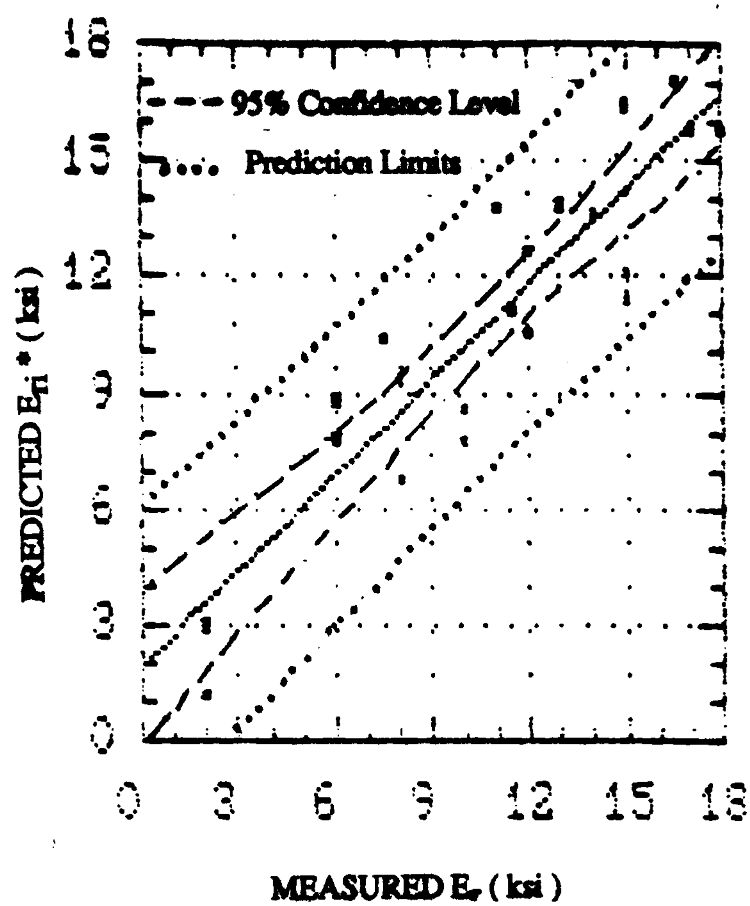

Simple Regression Plot of E_{ri}* Versus E_{ri}

Simple Regression Statistical Parameters for E_{ri}* Versus E_{ri}

Regression Analysis - Linear model: Y = a+bX

Dependent variable: PR   Independent variable: OB

Parameter	Estimate	Standard Error	T Value	Prob. Level
Intercept	1.88056	0.986058	1.90714	0.0709685
Slope	0.825801	0.0845149	9.77107	4.66354E-9

Analysis of Variance

Source	Sum of Squares	Df	Mean Square	F-Ratio	Prob. Level
Model	293.60317	1	293.60317	95.47375	.00000
Error	61.546373	20	3.077319		
Total (Corr.)	355.14955	21			

Correlation Coefficient = 0.909236   R-squared = 82.67 percent
Stnd. Error of Est. = 1.75423

Stepwise Selection for AA

Selection: Backward	Maximum steps: 500	F-to-enter: 4.00
Control: Manual	Step: 6	F-to-remove: 4.00

R-squared: .80913   Adjusted: .73278   MSE: 144.738   d.f.: 15

Variables in Model	Coeff.	F-Remove	Variables Not in Model	P.Corr.	F-Enter
3. HISTR	0.33656	1.1871	1. B	.0964	.1314
4. CLAY	0.73010	3.4806	2. INVA	.1578	.3574
6. PI	2.25902	13.5827	5. LL	.2057	.6133
7. MXDENS	-0.91532	3.8543			
8. SAT	-2.79136	8.3279			
9. FINER	-0.30371	2.0049			

Model fitting results for: AA

Independent variable	coefficient	std. error	t-value	sig.level
CONSTANT	318.206763	114.868975	2.7702	0.0143
HISTR	0.336561	0.308899	1.0895	0.2931
CLAY	0.730098	0.391337	1.8656	0.0818
PI	2.259023	0.612954	3.6855	0.0022
MXDENS	-0.915323	0.466233	-1.9632	0.0684
SAT	-2.791364	0.967274	-2.8858	0.0113
FINER	-0.303705	0.21449	-1.4159	0.1772

R-SQ. (ADJ.) = 0.7328	SE=	12.030694	MAE=	8.085691	DurbWat=	2.192
Previously: 0.0000		0.000000		0.000000		0.000

22 observations fitted, forecast(s) computed for 0 missing val. of dep. var.

Regression results for AA

Observation Number	Observed Values	Fitted Values
1	64.2900	48.5713
2	29.2300	42.6365
3	44.2500	44.9463
4	6.10000	8.58573
5	5.66000	1.22837
6	1.74000	5.20099
7	4.58000	14.1263
8	52.0600	42.8065
9	69.8800	56.9526
10	25.1400	27.4183
11	52.4400	40.9879
12	18.8400	25.3746
13	12.3900	19.3001
14	20.0600	36.2484
15	39.0400	20.4235
16	15.4900	15.0502
17	2.03000	12.3751
18	64.5200	69.0751
19	52.1400	77.2534
20	41.5200	42.5830
21	55.6000	43.0441
22	55.2000	54.1869

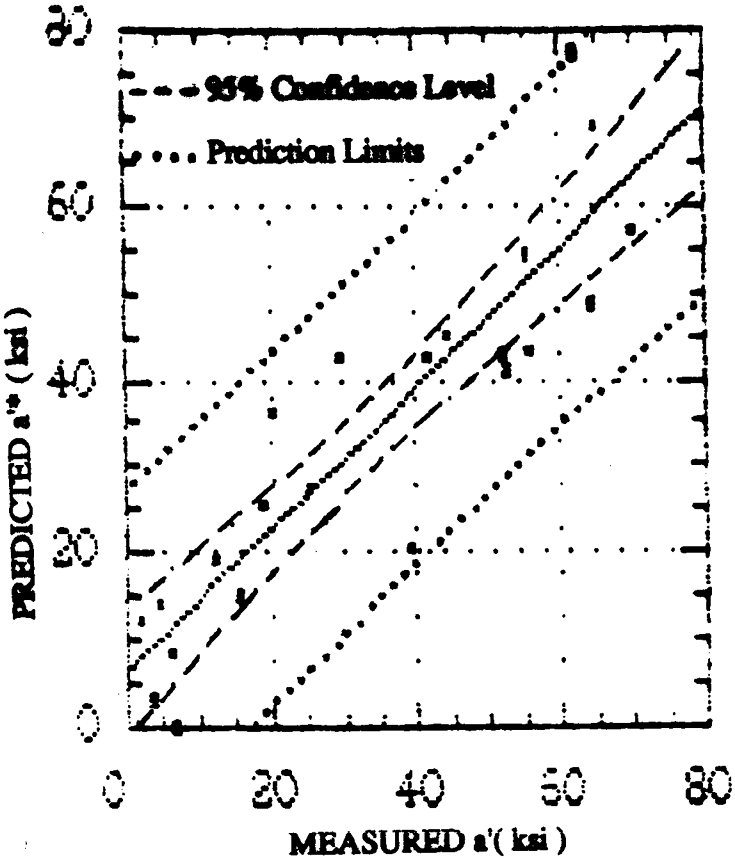

Simple Regression Plot of a'* Versus a'

Simple Regression Statistical Parameters for a'* Versus a'

Regression Analysis - Linear model: Y = a+bX

Dependent variable: PR — Independent variable: OB

Parameter	Estimate	Standard Error	T Value	Prob. Level
Intercept	6.45526	3.58694	1.79965	0.0870207
Slope	0.909504	0.0979097	9.20936	1.24273E-8

Analysis of Variance

Source	Sum of Squares	Df	Mean Square	F-Ratio	Prob. Level
Model	7451.4311	1	7451.4311	84.7938	.00000
Error	1757.5547	20	87.8777		
Total (Corr.)	9208.9858	21			

Correlation Coefficient = 0.899527 R-squared = 80.91 percent
Stnd. Error of Est. = 9.37431

Stepwise Selection for BB

Selection: Backward	Maximum steps: 500	F-to-enter: 4.00
Control: Manual	Step: 5	F-to-remove: 4.00

R-squared: .72640 Adjusted: .66202 MSE: 3.01324 d.f.: 17

Variables in Model	Coeff.	F-Remove	Variables Not in Model	P.Corr.	F-Enter
2. INVA	0.00039	11.5855	1. B	.0133	.0028
3. HISTR	0.10446	11.5701	4. CLAY	.0238	.0091
5. LL	0.09068	9.5933	6. PI	.2299	.8933
9. FINER	-0.09931	22.8734	7. MXDENS	.1371	.3067
			8. SAT	.0790	.1005

Model fitting results for: BB

Independent variable	coefficient	std. error	t-value	sig.level
CONSTANT	2.011634	1.840699	1.0929	0.2897
INVA	0.000388	0.000114	3.4038	0.0034
HISTR	0.104458	0.030709	3.4015	0.0034
LL	0.090681	0.029277	3.0973	0.0065
FINER	-0.099809	0.020869	-4.7826	0.0002

R-SQ. (ADJ.) = 0.6620	SE=	1.735869	MAE=	1.233763	DurbWat=	1.088
Previously: 0.7328		12.030694		8.085691		2.192

22 observations fitted, forecast(s) computed for 0 missing val. of dep. var.

Regression results for BB

Observation Number	Observed Values	Fitted Values
1	5.84000	5.78276
2	10.1700	6.26339
3	6.96000	4.74317
4	11.6500	9.96540
5	10.6100	10.1169
6	2.11000	0.87894
7	2.08000	1.38242
8	10.2600	9.53187
9	7.02000	9.09278
10	3.06000	4.53853
11	2.03000	2.37061
12	4.02000	4.91318
13	4.37000	4.72805
14	4.58000	5.85988
15	4.82000	5.53304
16	5.48000	5.09380
17	6.13000	7.29940
18	9.68000	7.90597
19	8.34000	7.93902
20	5.10000	7.51836
21	2.99000	5.13348
22	4.43000	5.13348

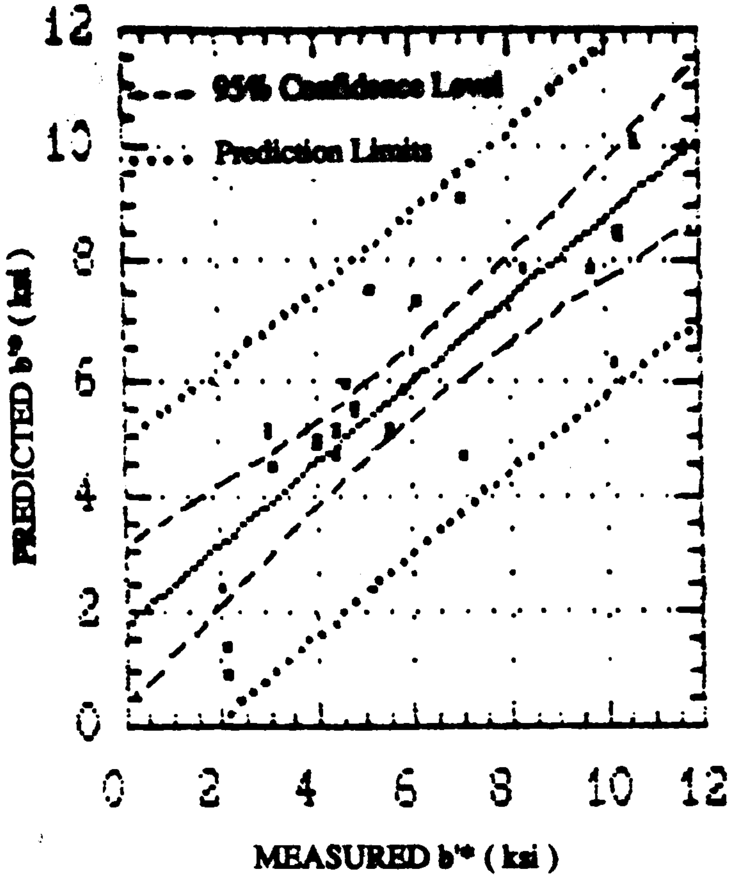

Simple Regression Plot of b'* Versus b'

Simple Regression Statistical Parameters for b'* Versus b'

Regression Analysis - Linear model: Y = a+bX

Dependent variable: PR Independent variable: OB

Parameter	Estimate	Standard Error	T Value	Prob. Level
Intercept	1.73908	0.662236	2.62607	0.0161866
Slope	0.700609	0.0993336	7.05309	7.70635E-7

Analysis of Variance

Source	Sum of Squares	Df	Mean Square	F-Ratio	Prob. Level
Model	92.387342	1	92.387342	49.746080	.00000
Error	37.143567	20	1.857178		
Total (Corr.)	129.53091	21			

Correlation Coefficient = 0.844533 R-squared = 71.32 percent
Stnd. Error of Est. = 1.36278

APPENDIX B

APPENDIX B1

MEASURED RESILIENT MODULUS VERSUS DEVIATOR STRESS

Actual Properties of the Test Specimens

Specimen	Actual Unit Weight (lb/ft^3)	Actual Moisture Content, (%)	Degree of Saturation (%)
A31-1	105.0	15.4	70.7
A31-2	106.0	15.4	72.6
B21-1	100.3	19.7	80.5
B21-2	102.1	18.6	78.6
C11-1	113.1	13.6	81.2
C11-2	112.7	14.3	84.5
D11-1	83.3	30.2	86.7
D11-2	83.2	31.2	83.4
E21-1	97.2	22.1	84.8
E21-2	98.6	20.6	79.8
E31-1	98.9	24.9	92.8
E31-2	96.8	24.7	87.5
F11-1	105.7	17.3	80.0
F11-2	106.4	17.2	80.8
H11-1	109.9	16.7	77.3
H11-2	109.9	16.7	83.0
H21-1	114.2	13.9	81.8
H21-2	115.2	13.9	83.9
J11-1	82.9	37.2	97.2
J11-2	81.4	37.2	93.7
J31-1	89.5	30.8	92.9
J31-2	86.3	32.2	91.9

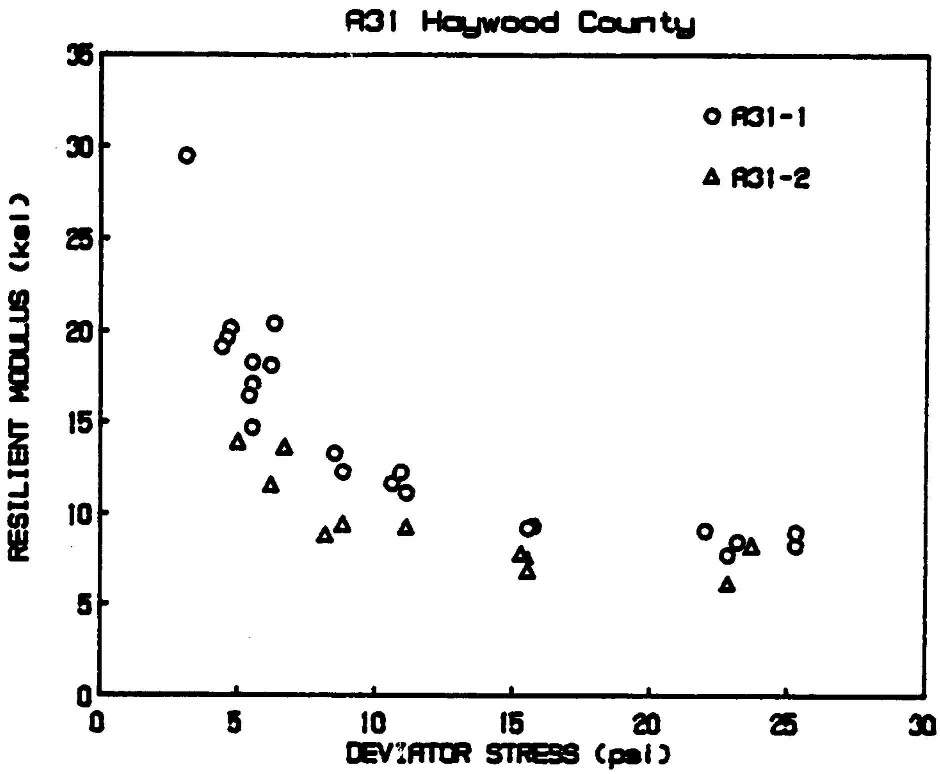
A31 Haywood County
A31-1
A31-2
RESILIENT MODULUS (ksi)
DEVIATOR STRESS (psi)
0
5
10
15
20
25
30
35

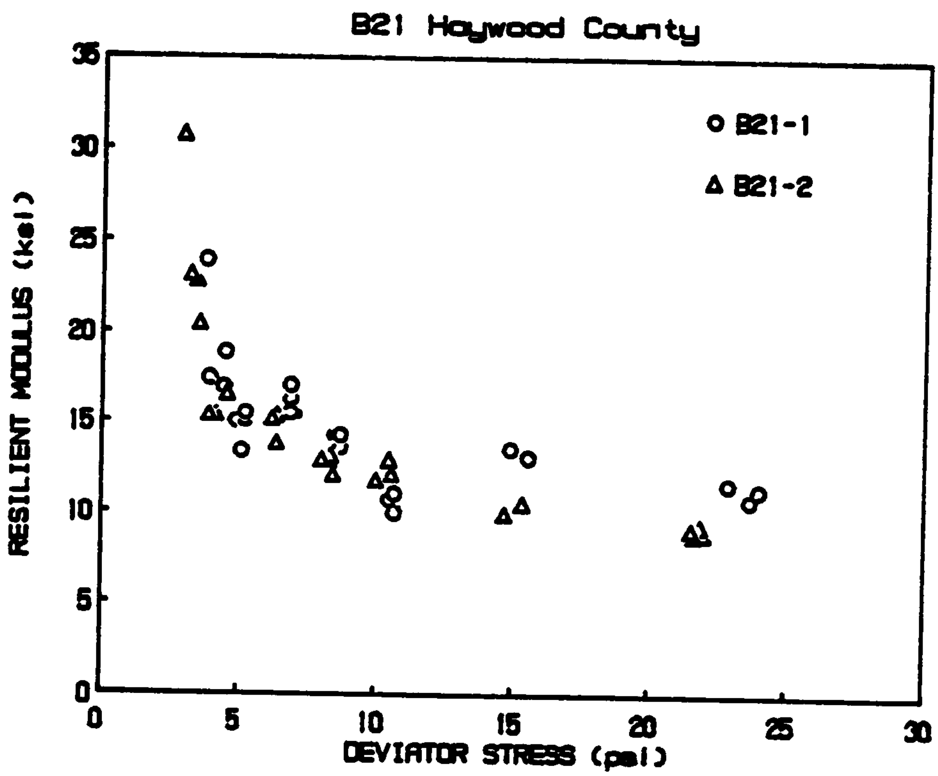
B21 Haywood County
B21-1
B21-2
RESILIENT MODULUS (ksi)
DEVIATOR STRESS (psi)
0
5
10
15
20
25
30
35

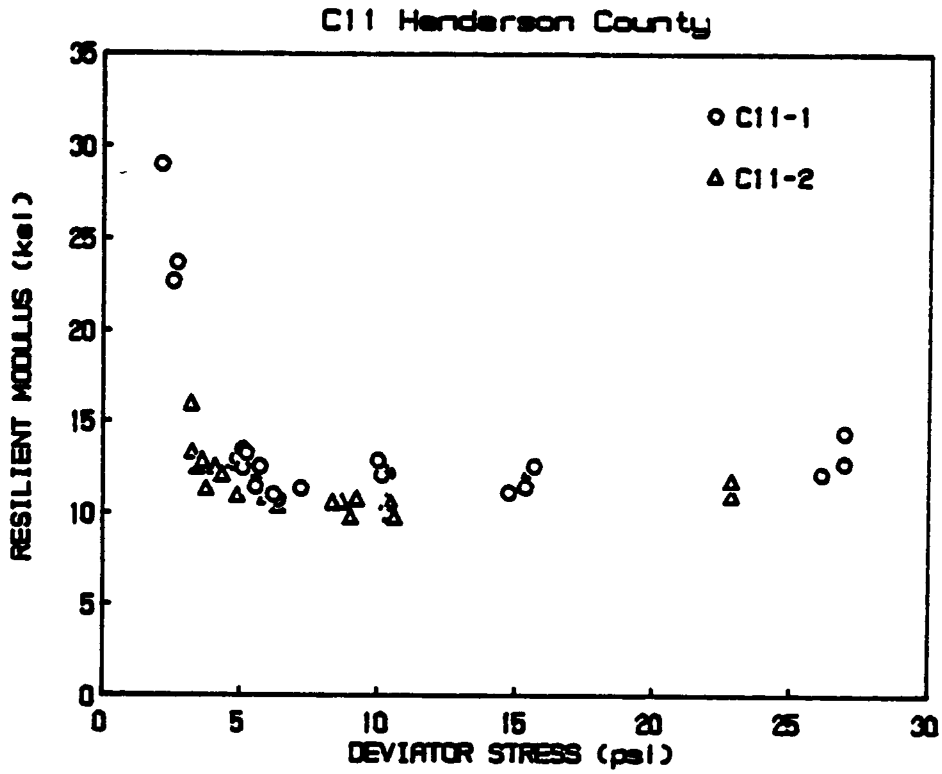
C11 Henderson County
RESILIENT MODULUS (ksi)
DEVIATOR STRESS (psi)
C11-1
C11-2
0
5
10
15
20
25
30
35

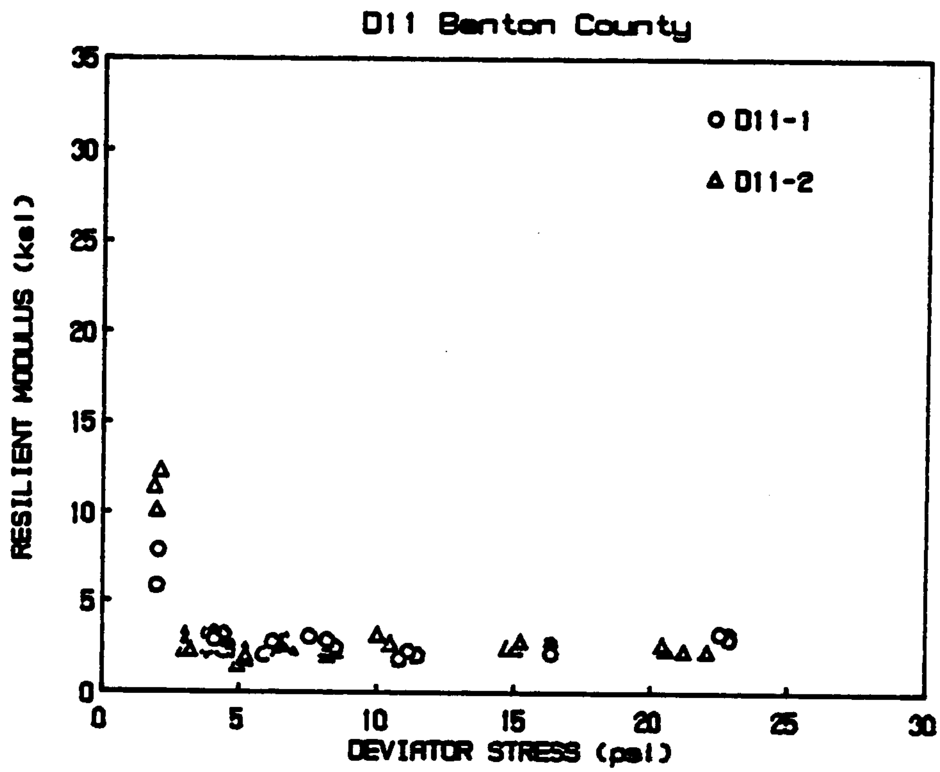
D11 Benton County
RESILIENT MODULUS (ksi)
DEVIATOR STRESS (psi)
D11-1
D11-2
0
5
10
15
20
25
30
35

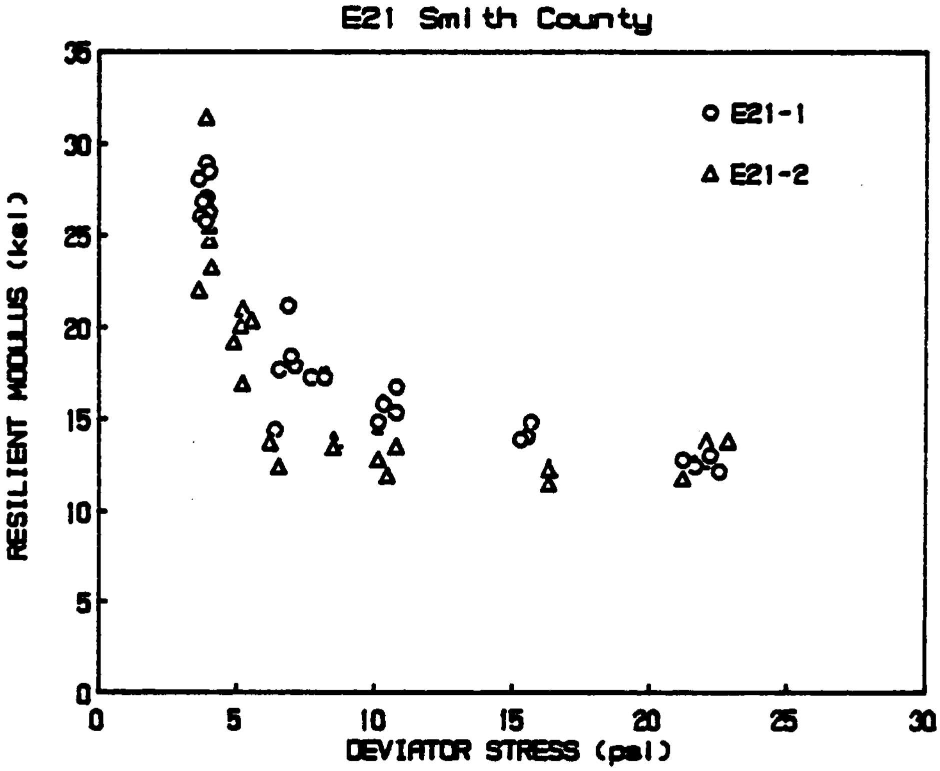

E21 Smith County
E21-1
E21-2
RESILIENT MODULUS (ksi)
DEVIATOR STRESS (psi)
0
5
10
15
20
25
30
35

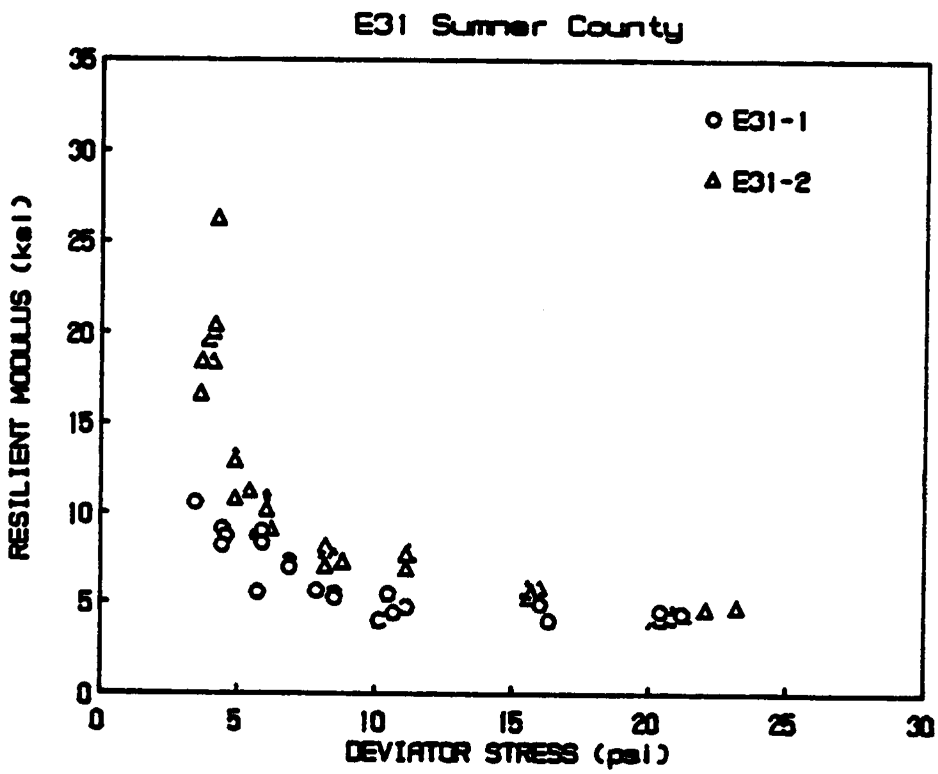

E31 Sumner County
E31-1
E31-2
RESILIENT MODULUS (ksi)
DEVIATOR STRESS (psi)
0
5
10
15
20
25
30
35

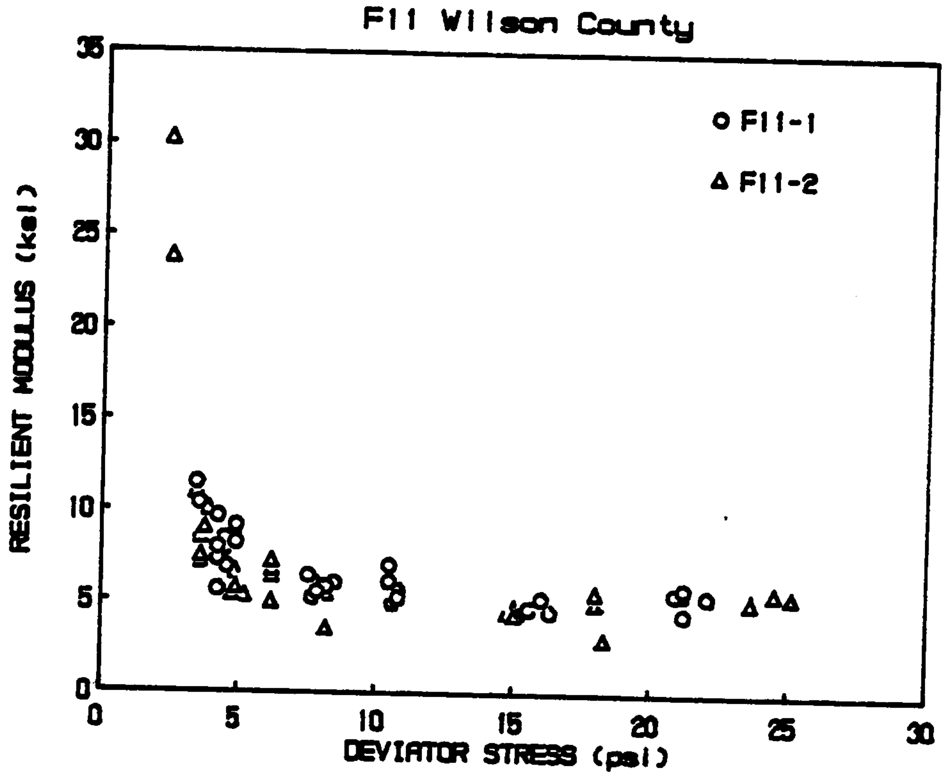
F11 Wilson County
RESILIENT MODULUS (ksi)
DEVIATOR STRESS (psi)
F11-1
F11-2
0
5
10
15
20
25
30
35

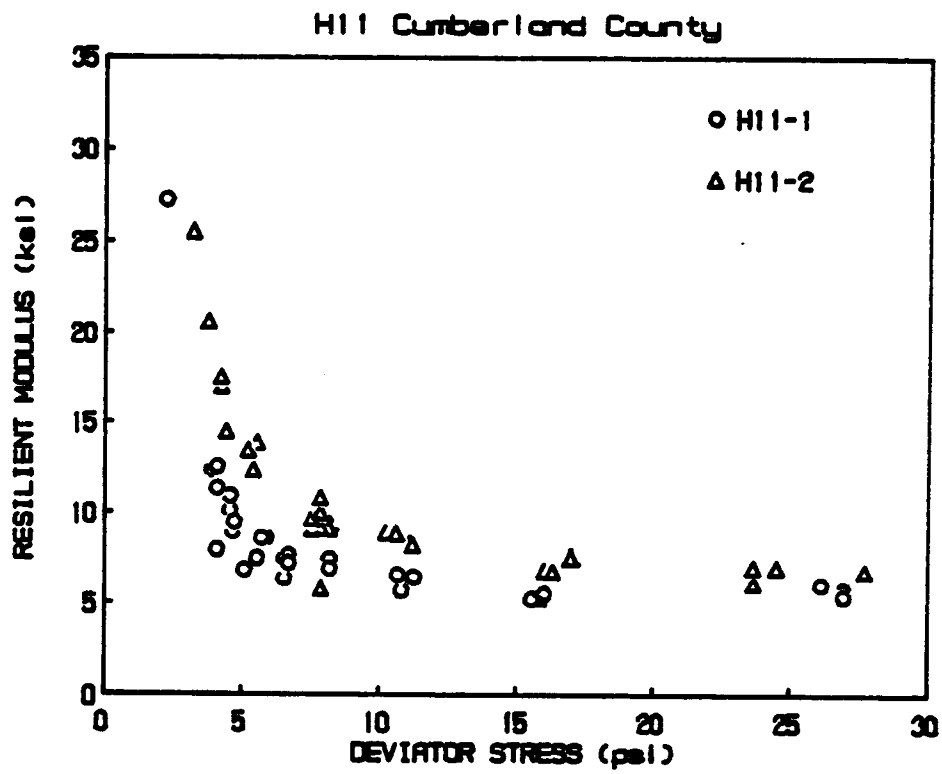
H11 Cumberland County
RESILIENT MODULUS (ksi)
DEVIATOR STRESS (psi)
H11-1
H11-2
0
5
10
15
20
25
30
35

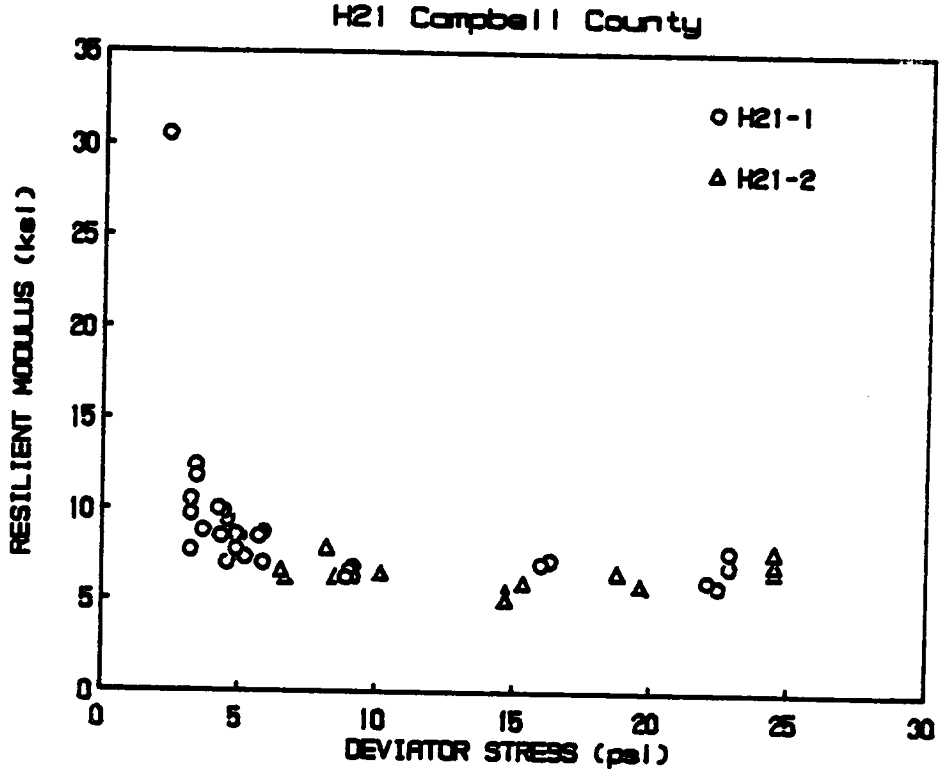
H21 Campbell County
H21-1
H21-2
RESILIENT MODULUS (ksi)
DEVIATOR STRESS (psi)
0
5
10
15
20
25
30
35

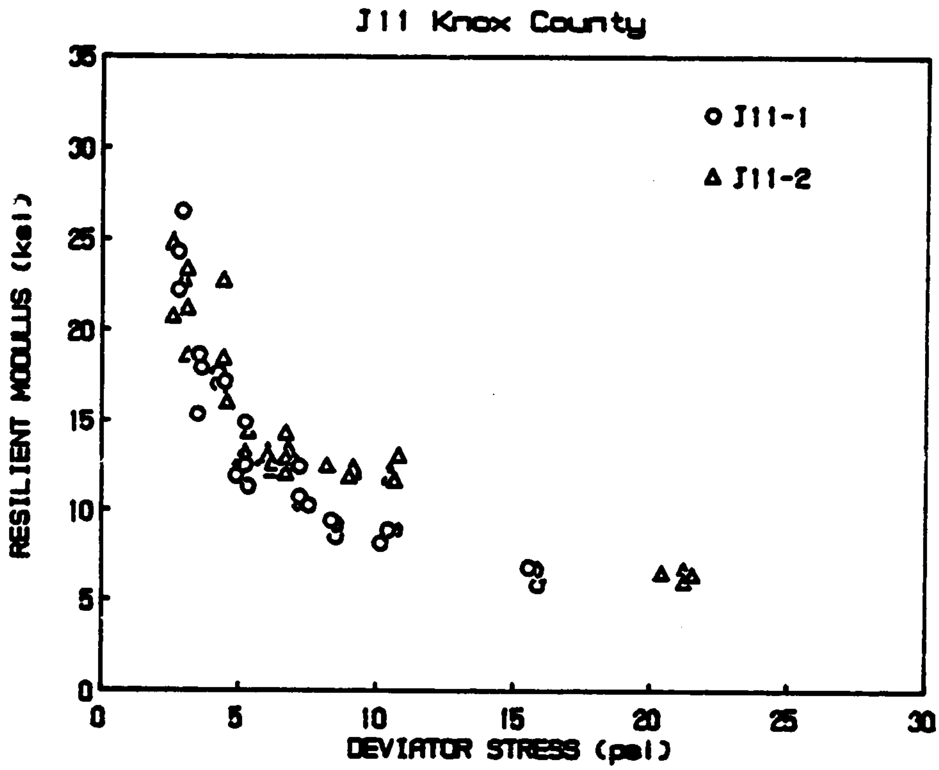
J11 Knox County
J11-1
J11-2
RESILIENT MODULUS (ksi)
DEVIATOR STRESS (psi)
0
5
10
15
20
25
30
35

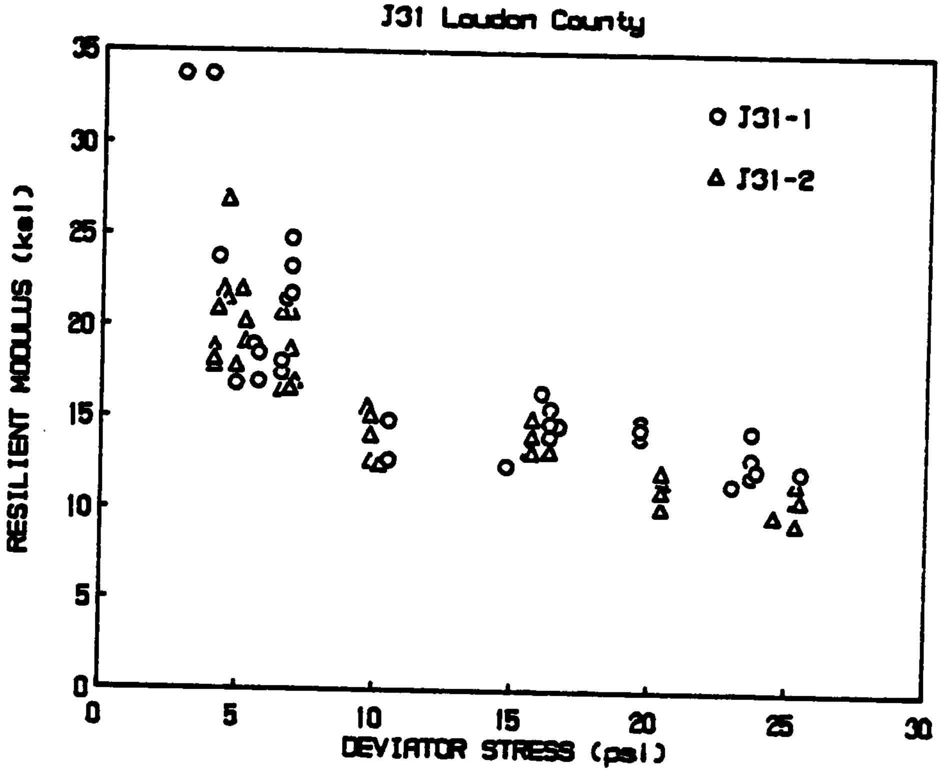
J31 Loudon County
RESILIENT MODULUS (ksi)
DEVIATOR STRESS (psi)
0
5
10
15
20
25
30
35
J31-1
J31-2

APPENDIX B2

GRAIN SIZE DISTRIBUTION

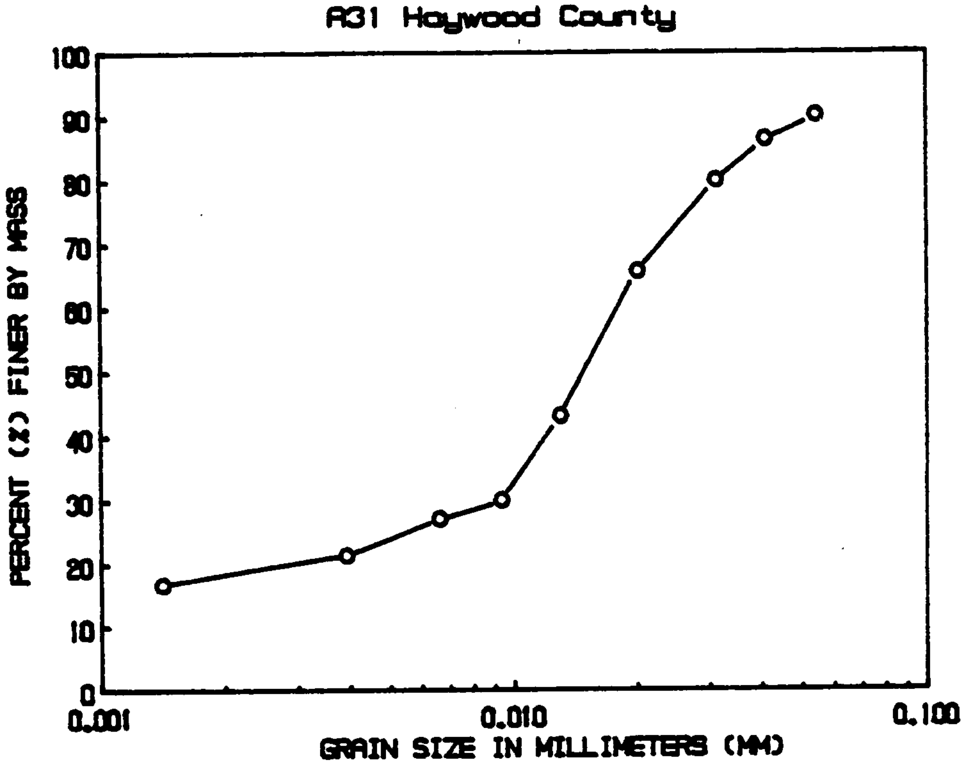

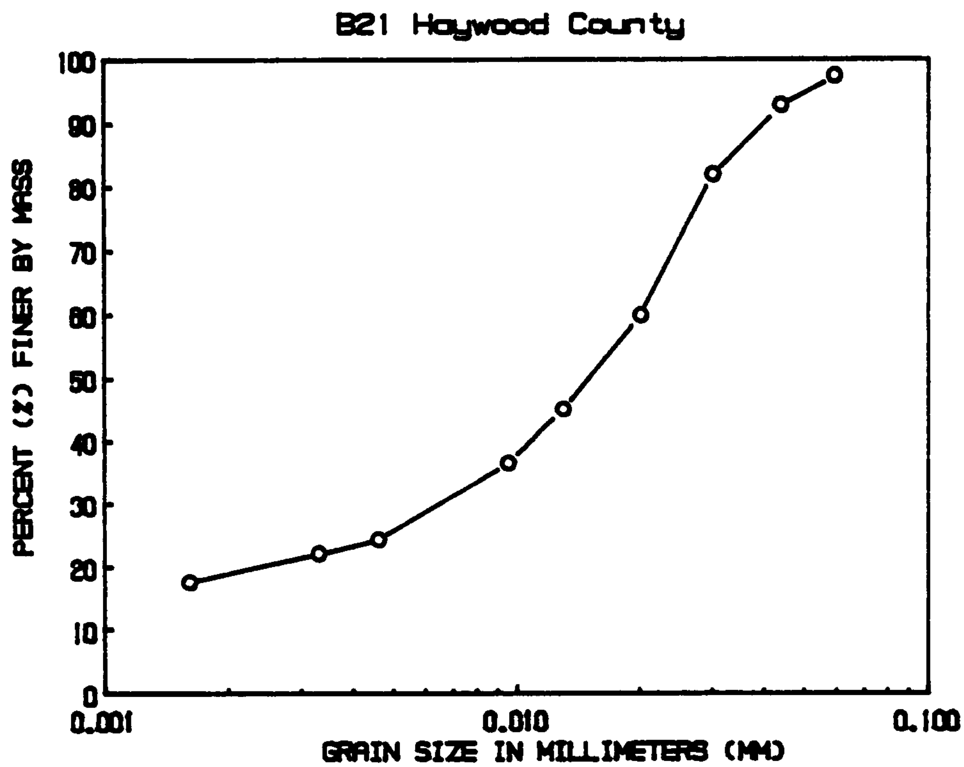

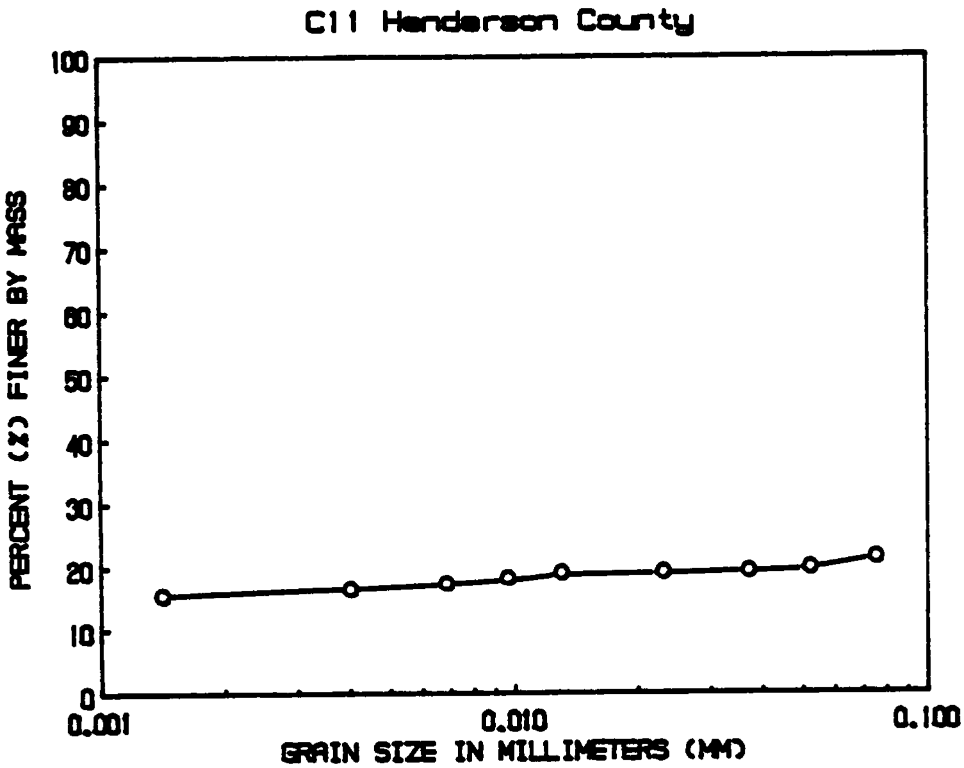
C11 Henderson County
100
90
80
70
60
50
40
30
20
10
0
PERCENT (%) FINER BY MASS
0.001
0.010
0.100
GRAIN SIZE IN MILLIMETERS (MM)

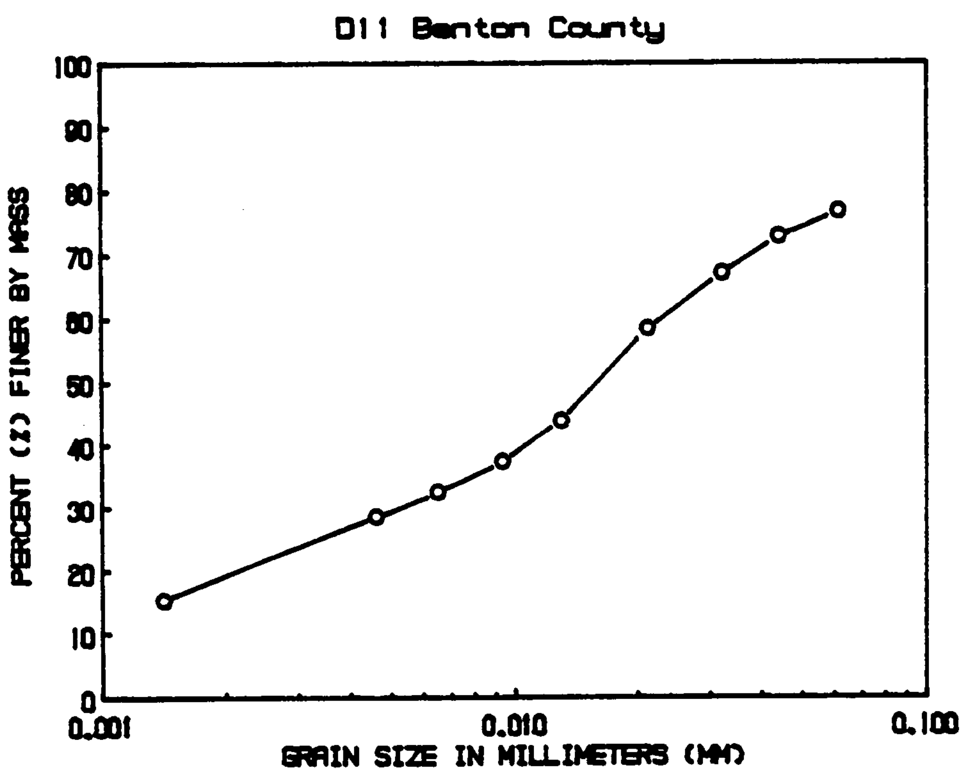
D11 Benton County
100
90
80
70
60
50
40
30
20
10
0
PERCENT (%) FINER BY MASS
0.001
0.010
0.100
GRAIN SIZE IN MILLIMETERS (MM)

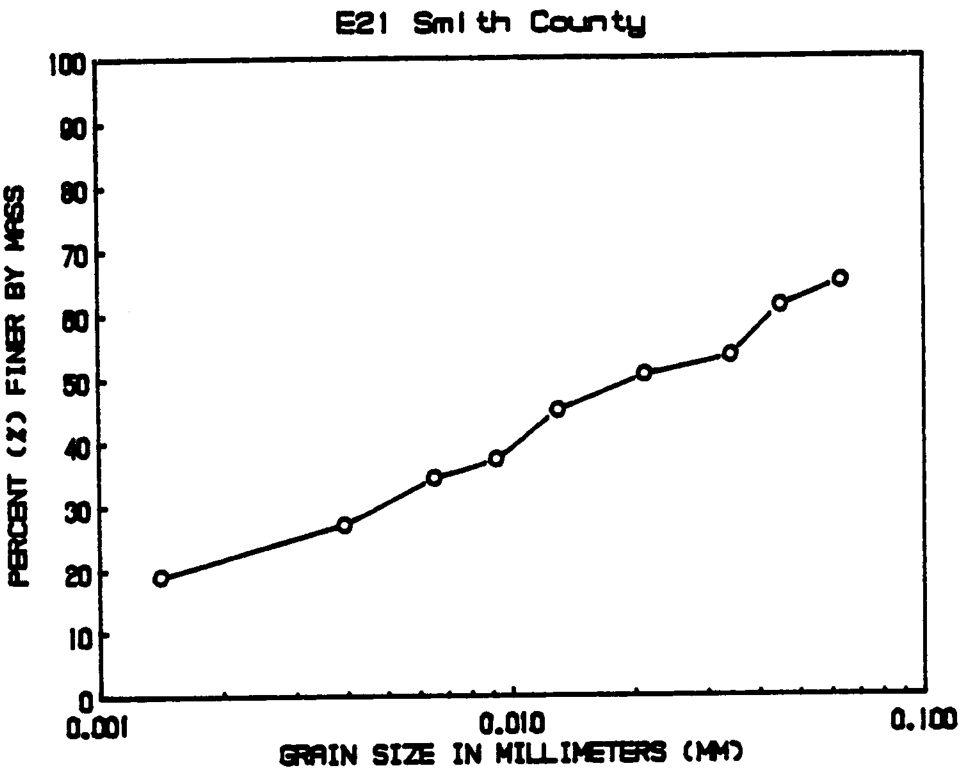
E21 Smith County
PERCENT (%) FINER BY MASS
100
90
80
70
60
50
40
30
20
10
0
0.001
0.010
0.100
GRAIN SIZE IN MILLIMETERS (MM)

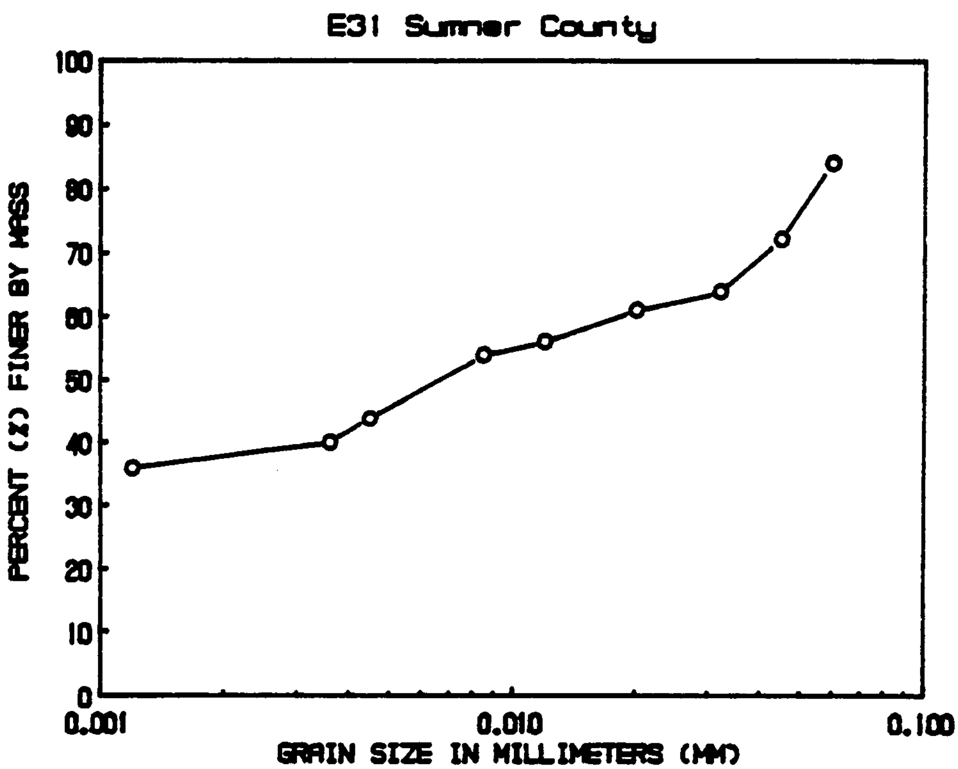
E31 Sumner County
PERCENT (%) FINER BY MASS
100
90
80
70
60
50
40
30
20
10
0
0.001
0.010
0.100
GRAIN SIZE IN MILLIMETERS (MM)

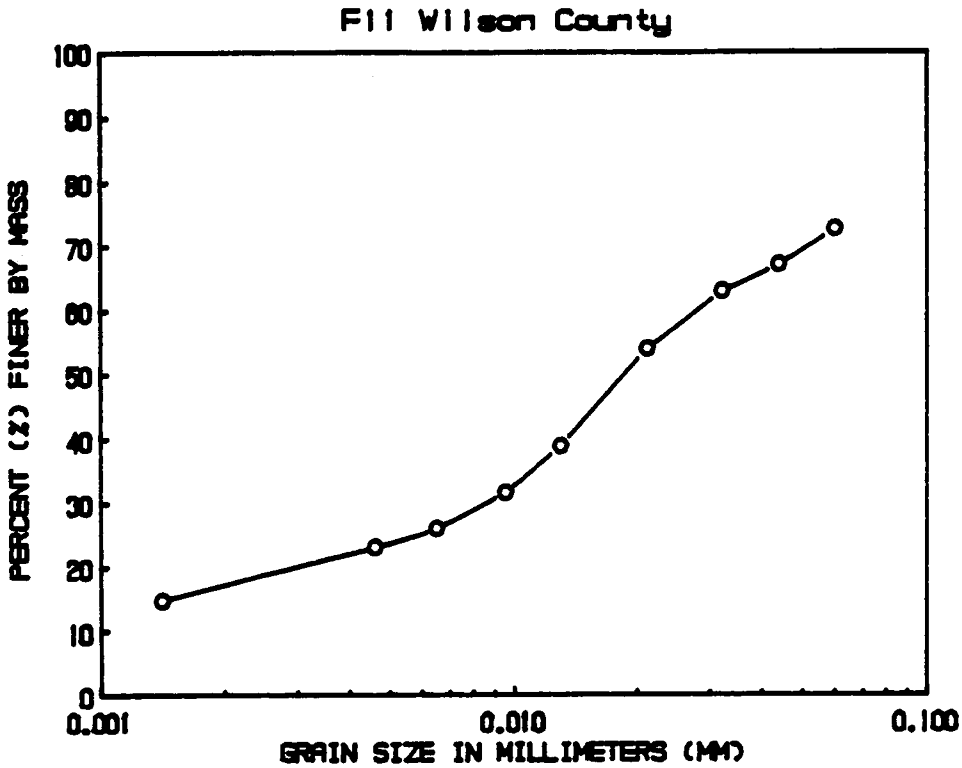

F11 Wilson County
PERCENT (%) FINER BY MASS
0
10
20
30
40
50
60
70
80
90
100
0.001
0.010
0.100
GRAIN SIZE IN MILLIMETERS (MM)

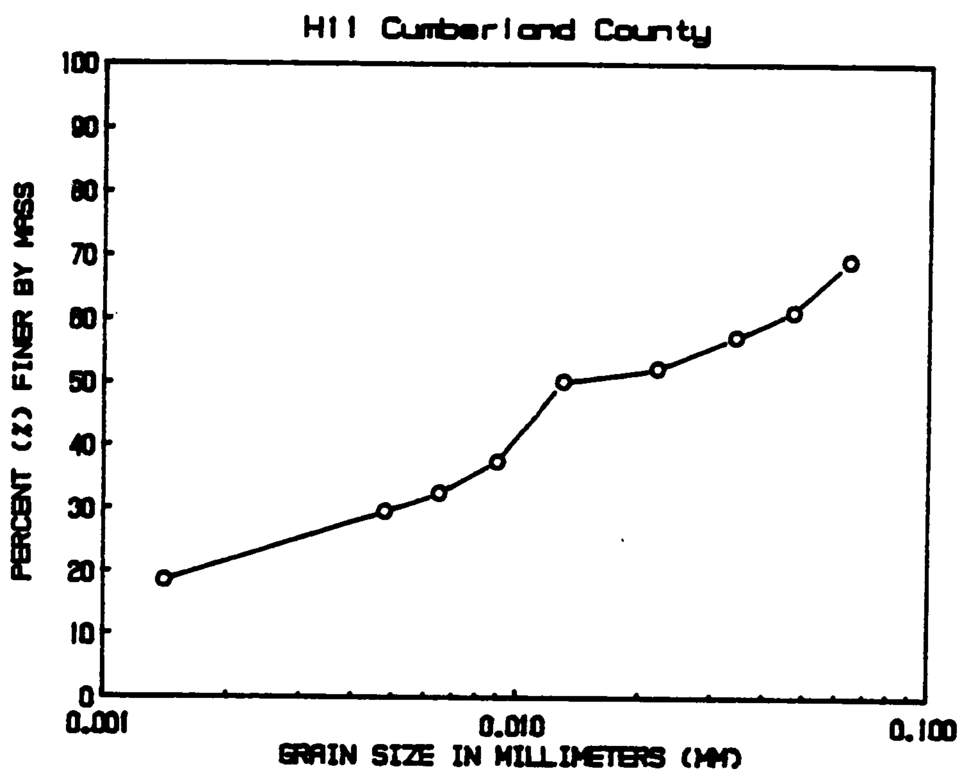

H11 Cumberland County
PERCENT (%) FINER BY MASS
0
10
20
30
40
50
60
70
80
90
100
0.001
0.010
0.100
GRAIN SIZE IN MILLIMETERS (MM)

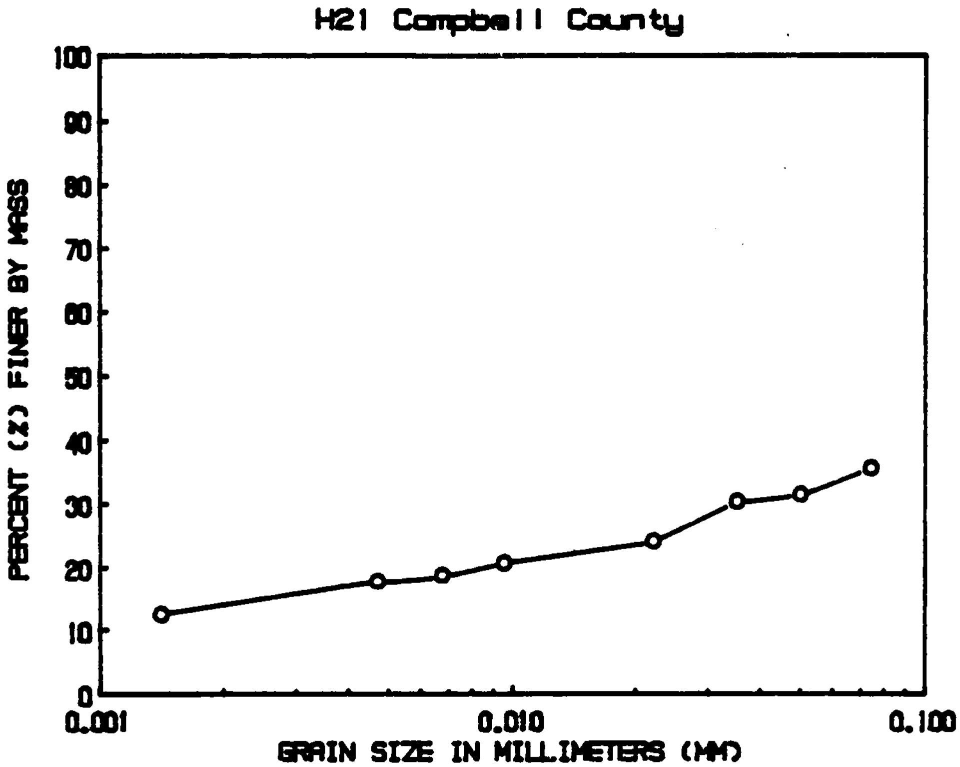
H21 Campbell County
PERCENT (%) FINER BY MASS
100
90
80
70
60
50
40
30
20
10
0
0.001
0.010
0.100
GRAIN SIZE IN MILLIMETERS (MM)

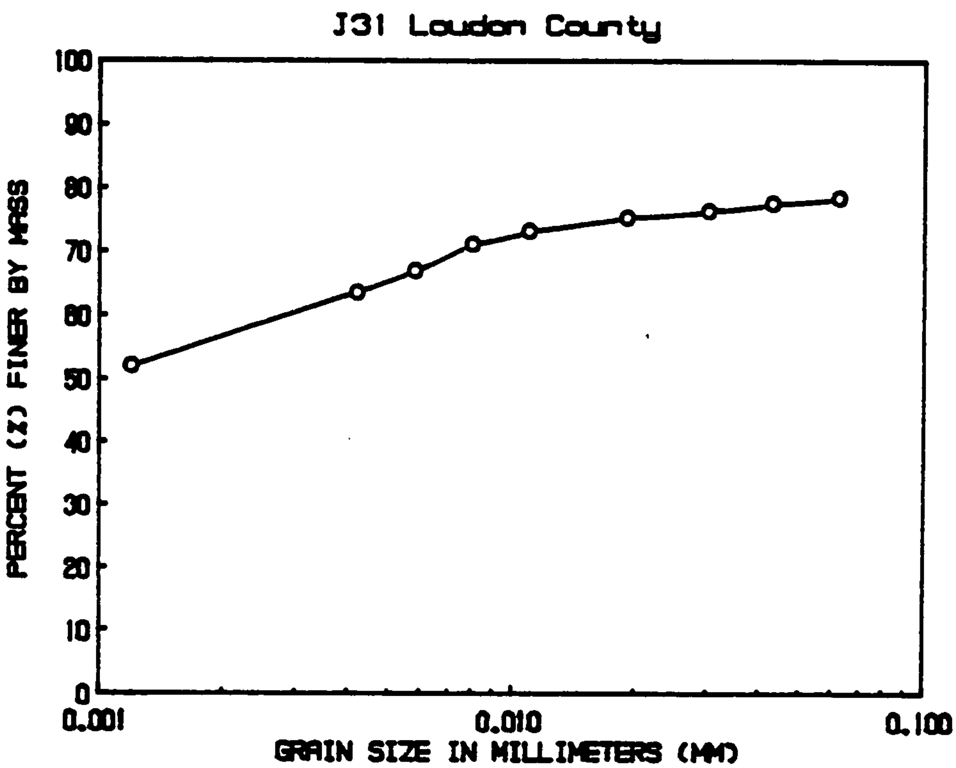
J31 Loudon County
PERCENT (%) FINER BY MASS
100
90
80
70
60
50
40
30
20
10
0
0.001
0.010
0.100
GRAIN SIZE IN MILLIMETERS (MM)

APPENDIX C

APPENDIX C1

HYPERBOLIC MODEL PLOT OF REPEATED LOAD TEST DATA

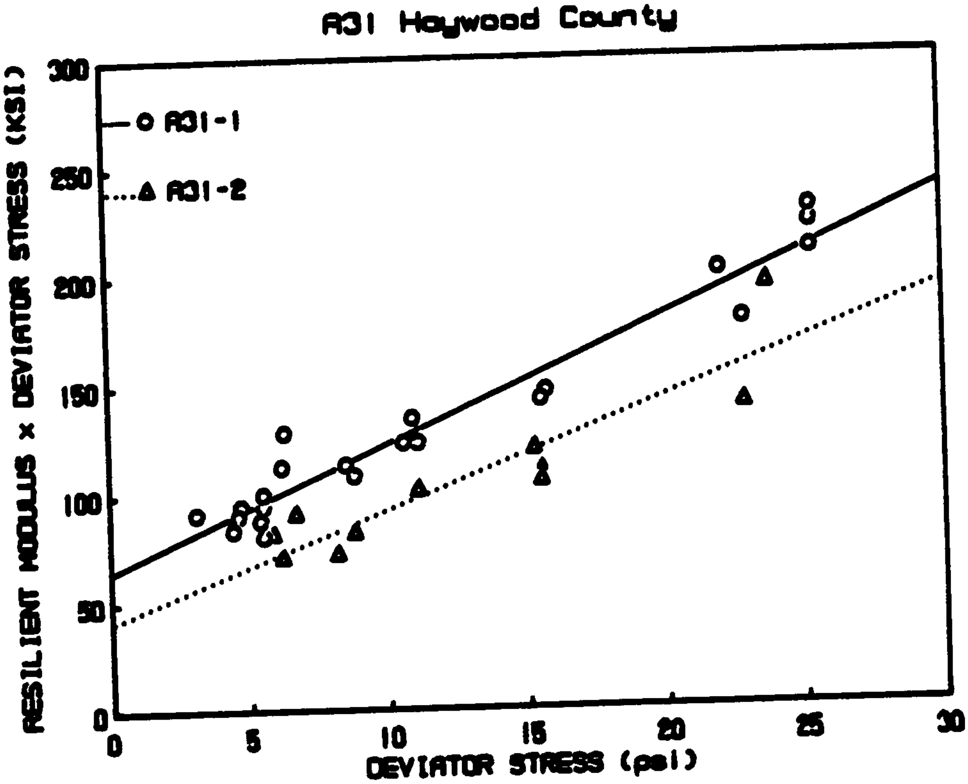

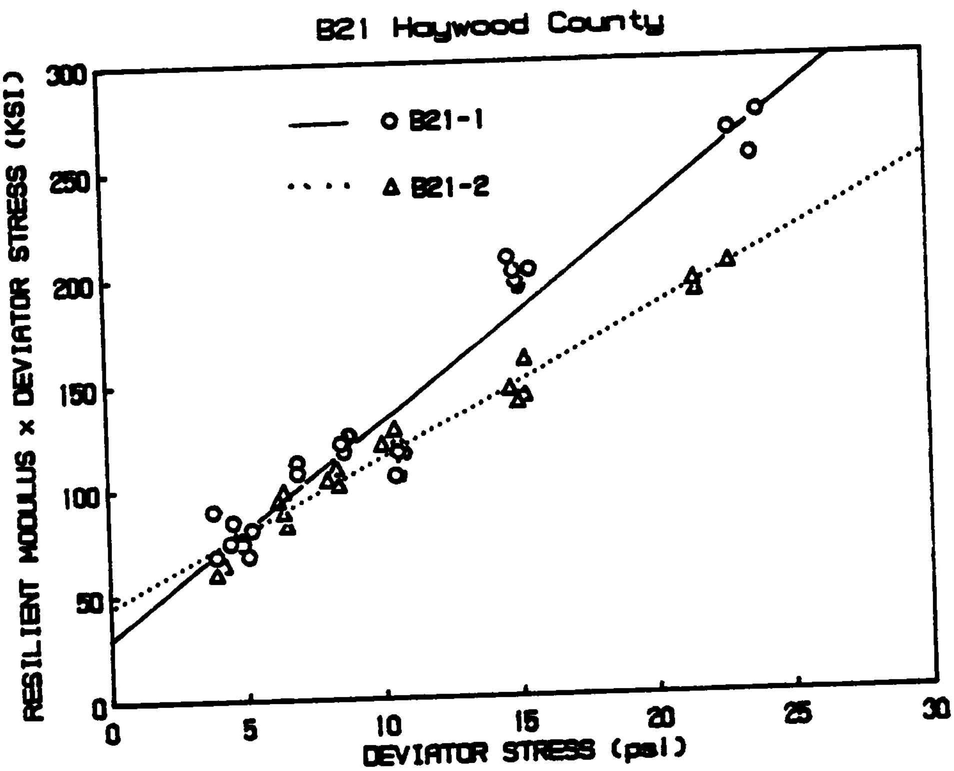

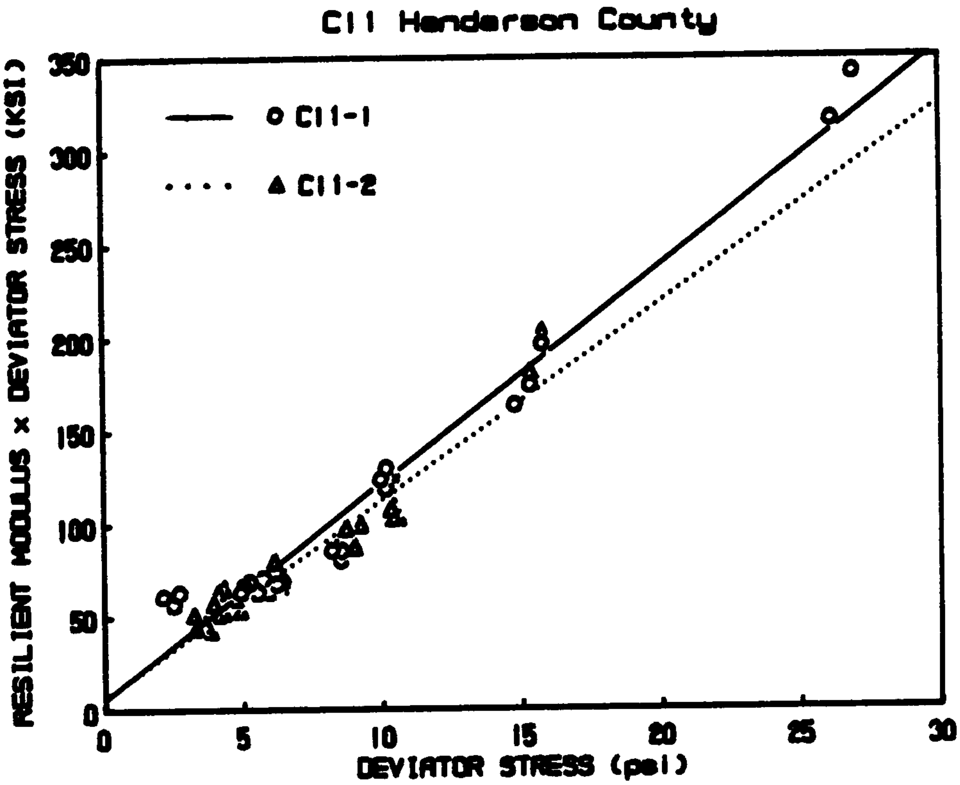
C11 Henderson County
RESILIENT MODULUS x DEVIATOR STRESS (KSI)
DEVIATOR STRESS (psi)
C11-1
C11-2
0
50
100
150
200
250
300
350
0
5
10
15
20
25
30

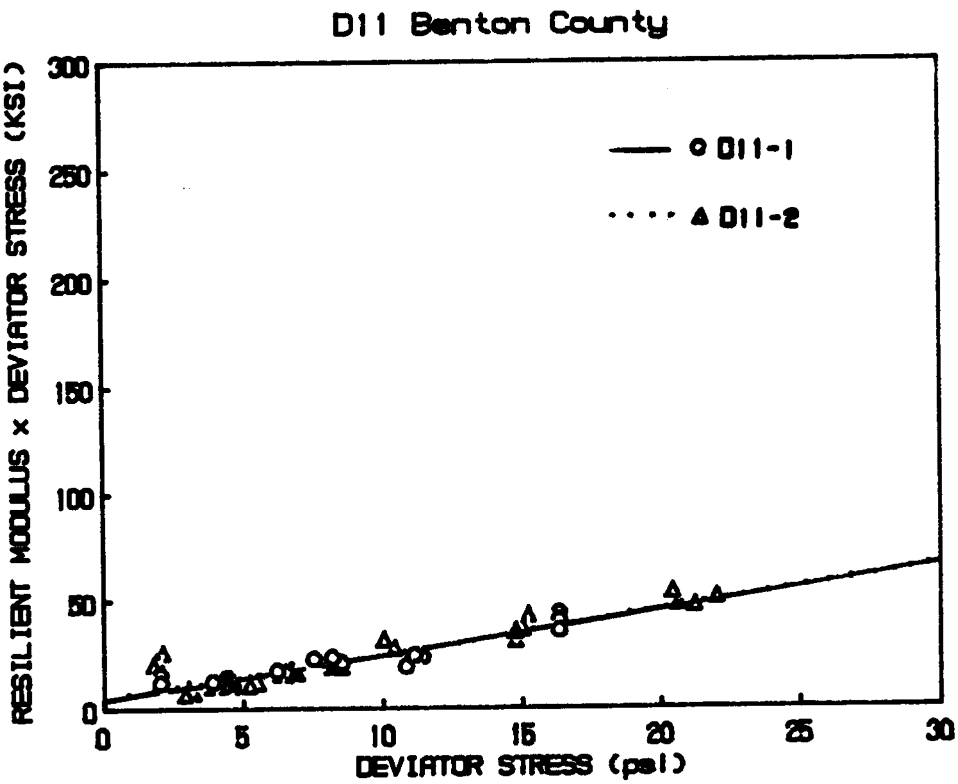
D11 Benton County
RESILIENT MODULUS x DEVIATOR STRESS (KSI)
DEVIATOR STRESS (psi)
D11-1
D11-2
0
50
100
150
200
250
300
0
5
10
15
20
25
30

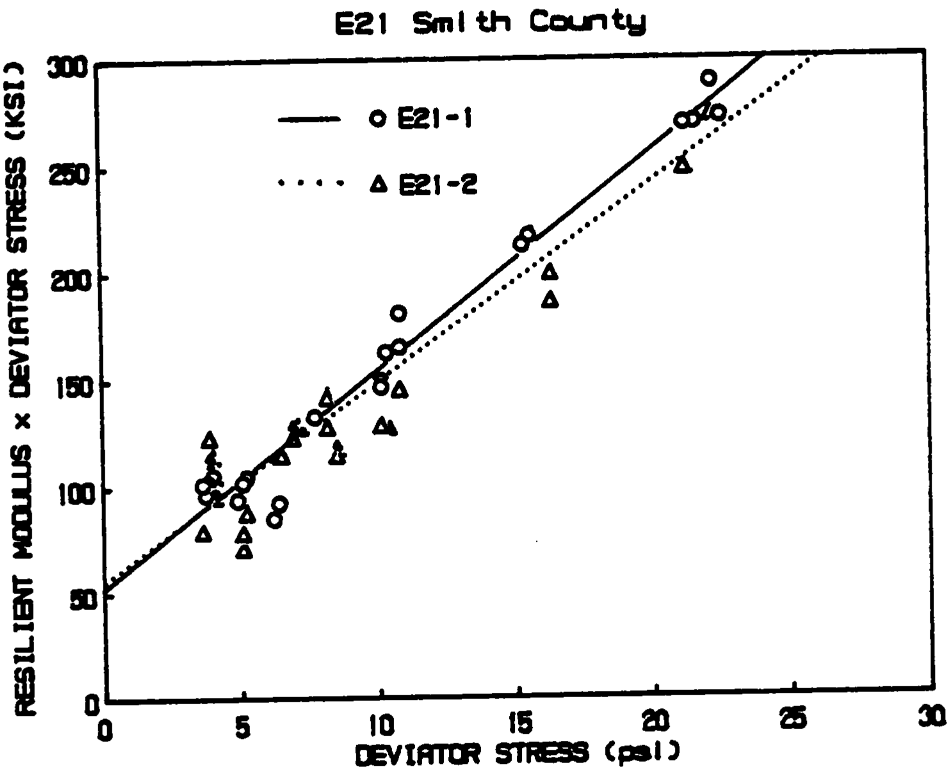

E21 Smith County
E21-1
E21-2
RESILIENT MODULUS x DEVIATOR STRESS (KSI)
DEVIATOR STRESS (psi)
0
50
100
150
200
250
300
0
5
10
15
20
25
30

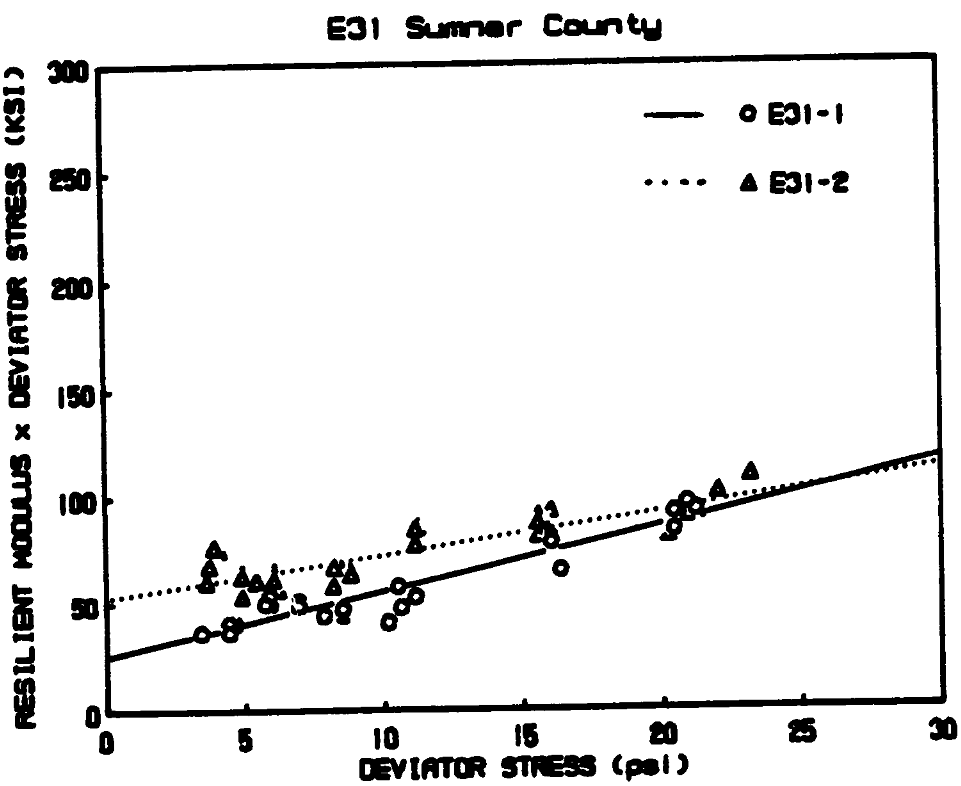

E31 Sumner County
E31-1
E31-2
RESILIENT MODULUS x DEVIATOR STRESS (KSI)
DEVIATOR STRESS (psi)
0
50
100
150
200
250
300
0
5
10
15
20
25
30

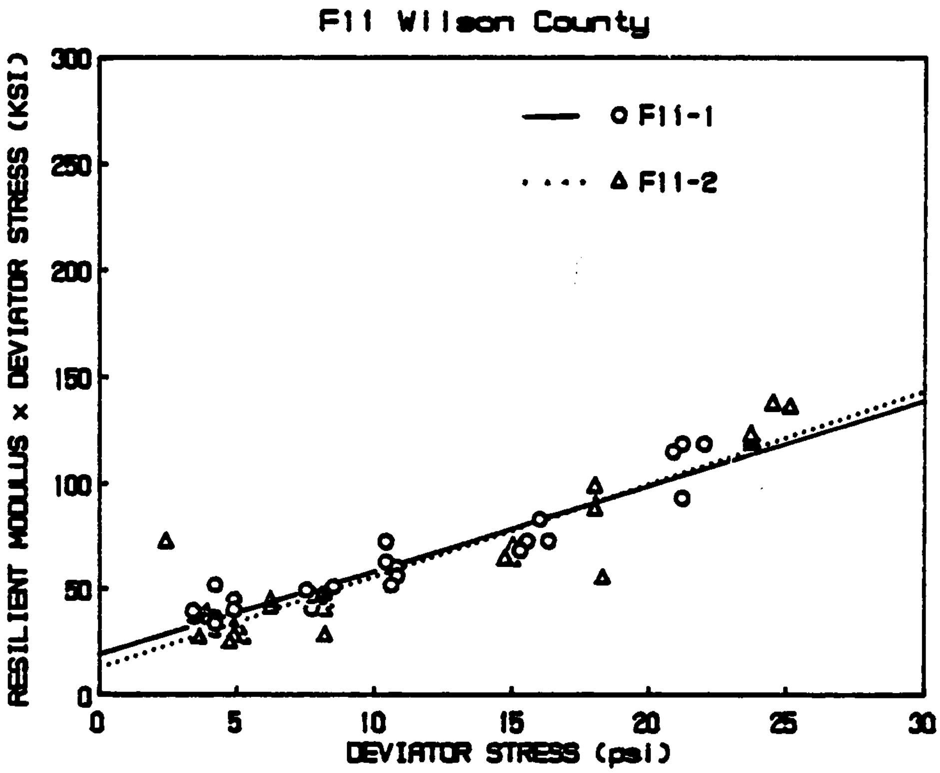
F11 Wilson County
RESILIENT MODULUS x DEVIATOR STRESS (KSI)
DEVIATOR STRESS (psi)
F11-1
F11-2
0
50
100
150
200
250
300
0
5
10
15
20
25
30

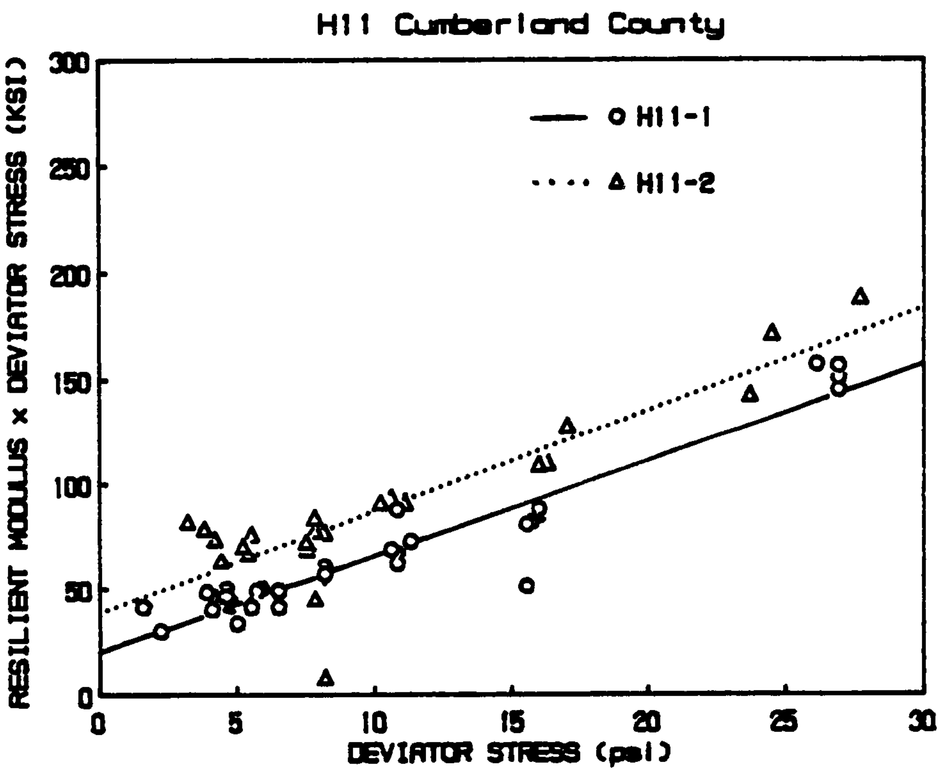
H11 Cumberland County
RESILIENT MODULUS x DEVIATOR STRESS (KSI)
DEVIATOR STRESS (psi)
H11-1
H11-2
0
50
100
150
200
250
300
0
5
10
15
20
25
30

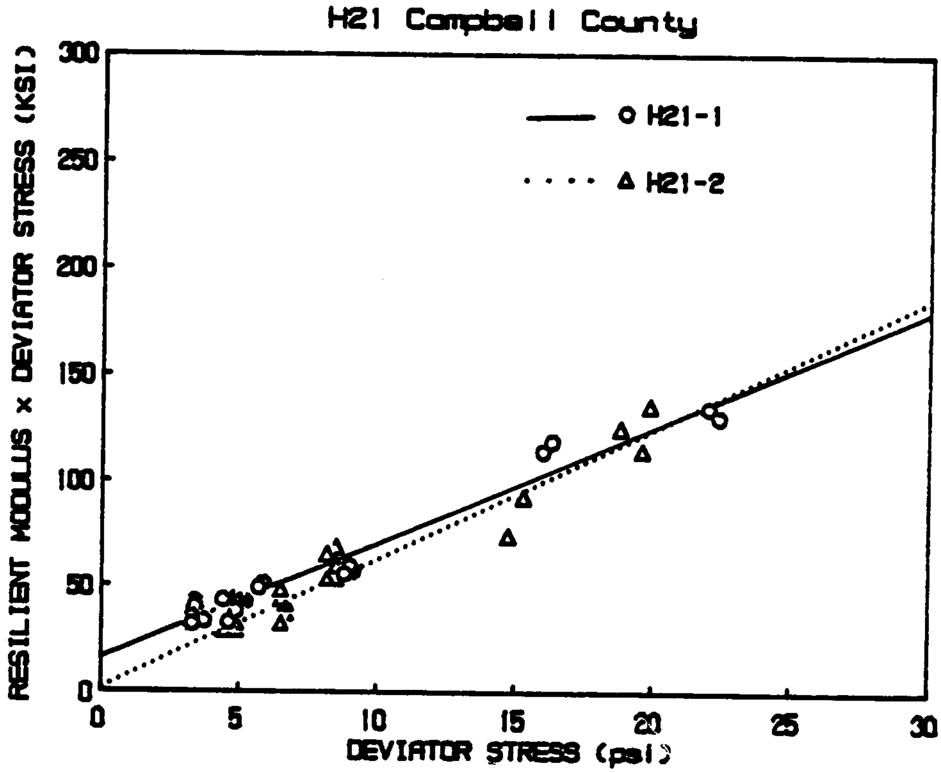

H21 Campbell County
RESILIENT MODULUS x DEVIATOR STRESS (KSI)
DEVIATOR STRESS (psi)
H21-1
H21-2
0
50
100
150
200
250
300
0
5
10
15
20
25
30

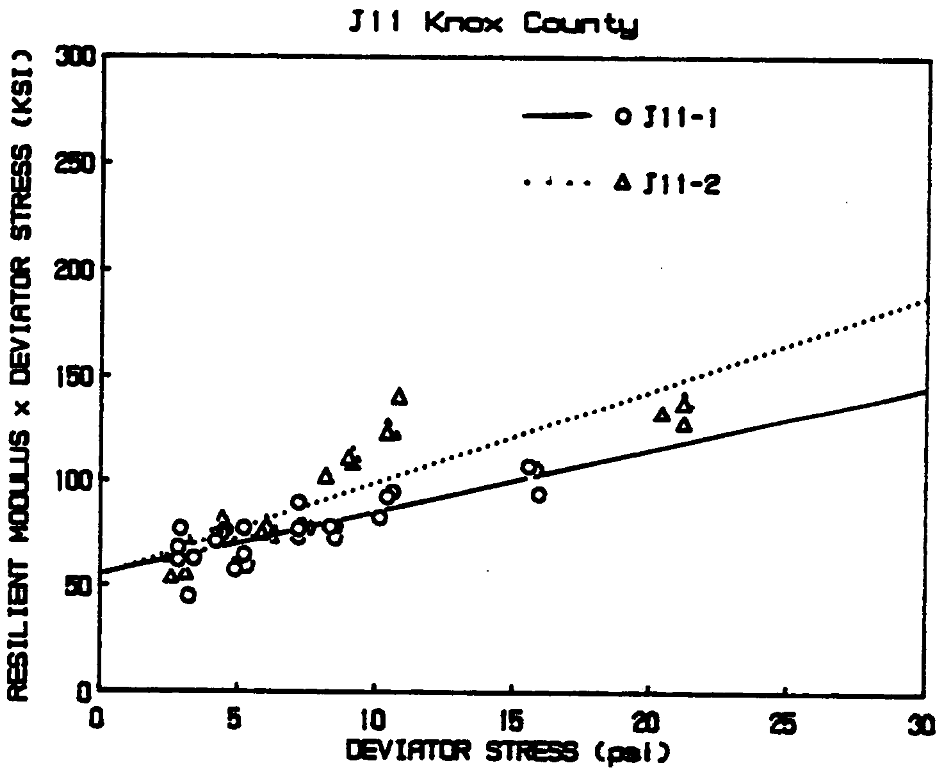

J11 Knox County
RESILIENT MODULUS x DEVIATOR STRESS (KSI)
DEVIATOR STRESS (psi)
J11-1
J11-2
0
50
100
150
200
250
300
0
5
10
15
20
25
30

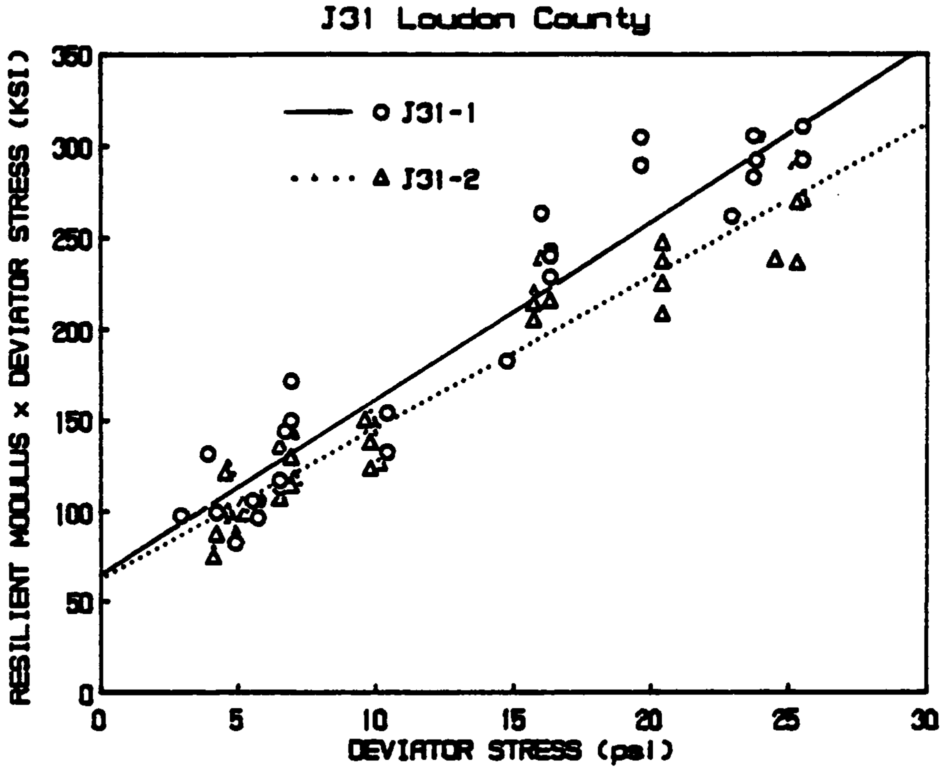

J31 Loudon County
RESILIENT MODULUS x DEVIATOR STRESS (KSI)
DEVIATOR STRESS (psi)
J31-1
J31-2
0
50
100
150
200
250
300
350
0
5
10
15
20
25
30

APPENDIX C2

HYPERBOLIC MODEL PLOT OF UNCONFINED COMPRESSION TEST DATA

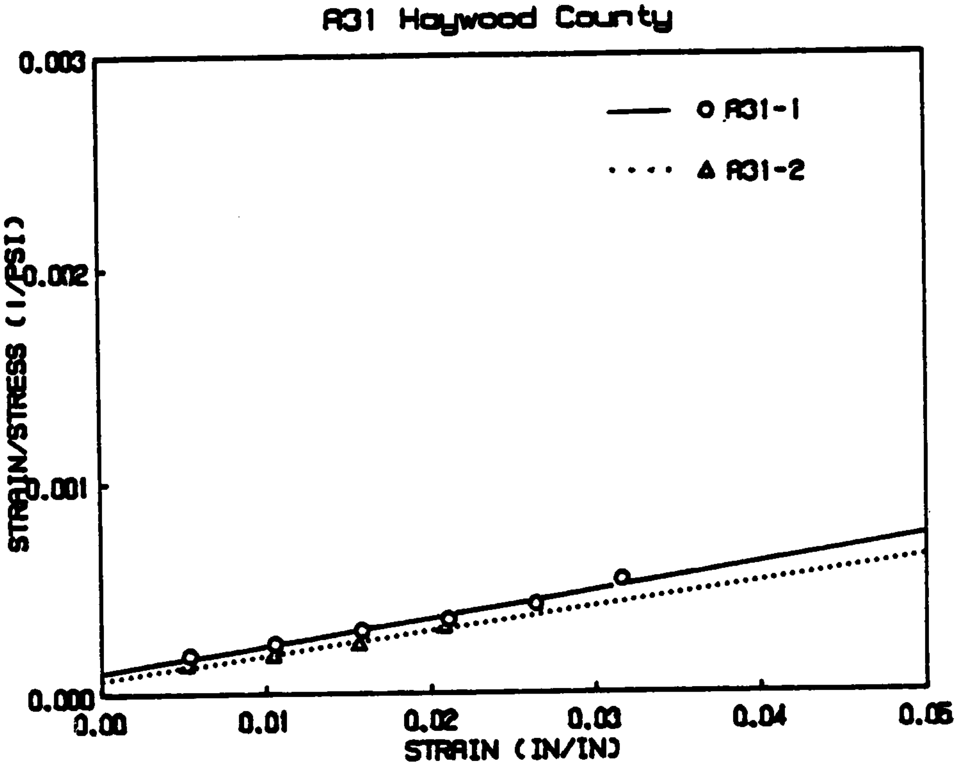

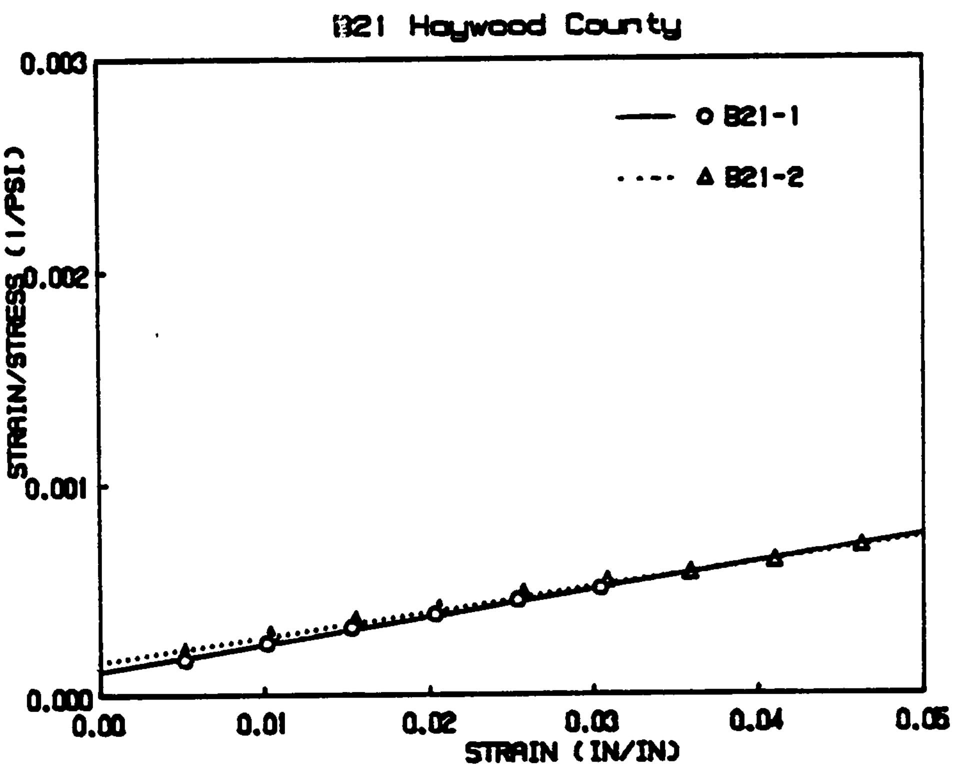

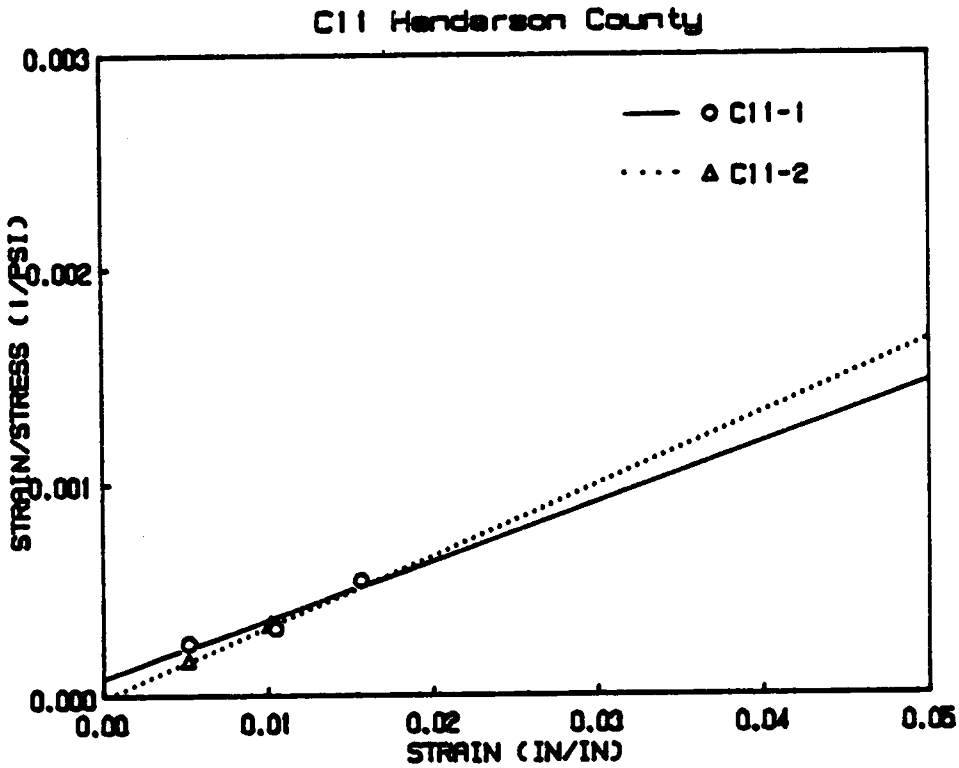
C11 Henderson County
C11-1
C11-2
STRAIN/STRESS (1/PSI)
0.003
0.002
0.001
0.000
0.00
0.01
0.02
0.03
0.04
0.05
STRAIN (IN/IN)

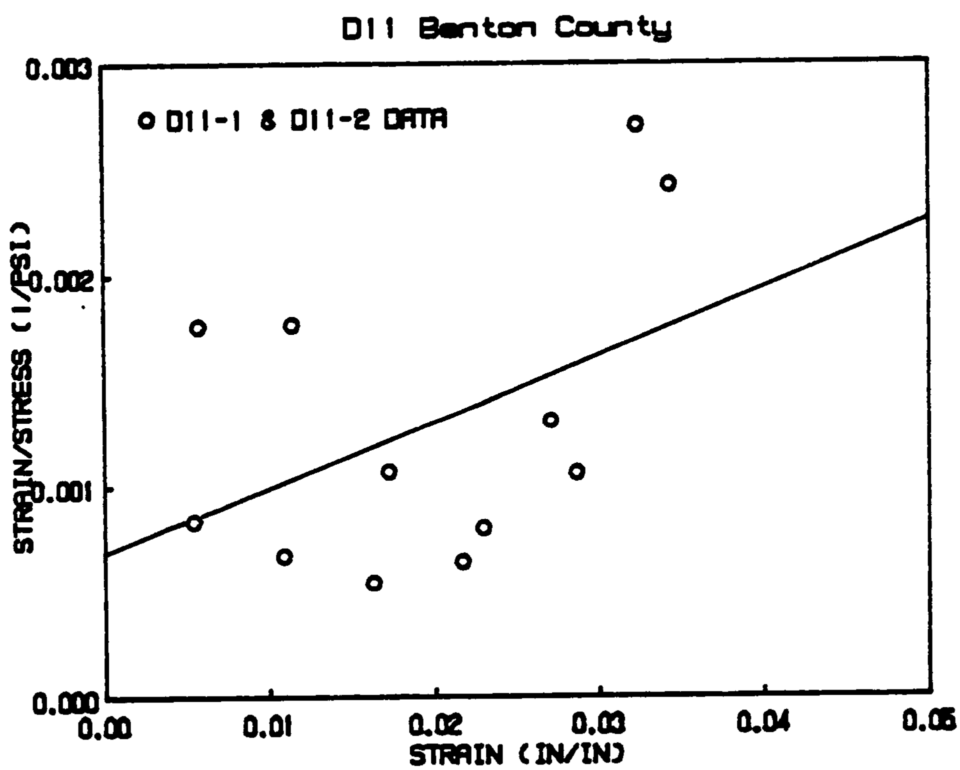
D11 Benton County
D11-1 & D11-2 DATA
STRAIN/STRESS (1/PSI)
0.003
0.002
0.001
0.000
0.00
0.01
0.02
0.03
0.04
0.05
STRAIN (IN/IN)

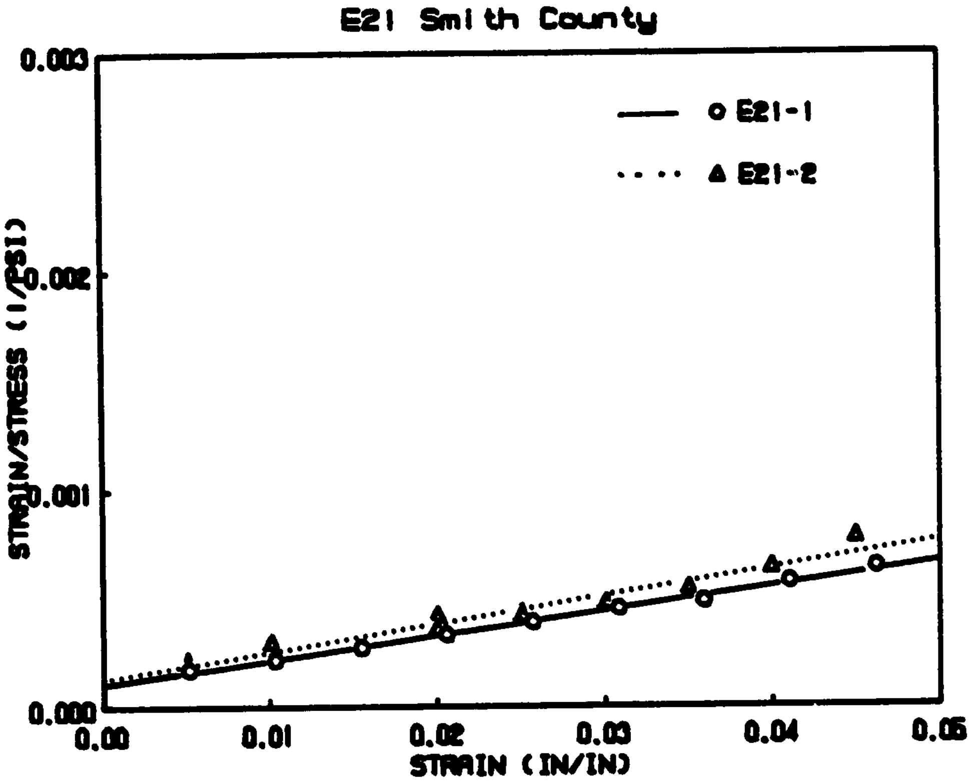
E21 Smith County
E21-1
E21-2
STRAIN/STRESS (1/PSI)
0.003
0.002
0.001
0.000
0.00
0.01
0.02
0.03
0.04
0.05
STRAIN (IN/IN)

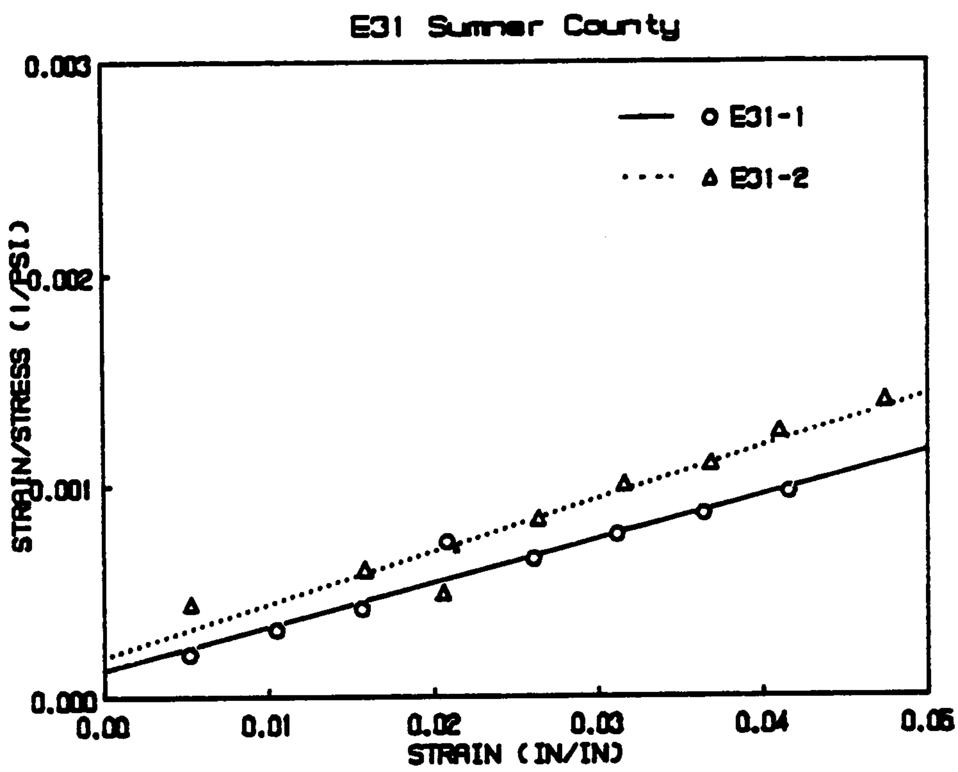
E31 Sumner County
E31-1
E31-2
STRAIN/STRESS (1/PSI)
0.003
0.002
0.001
0.000
0.00
0.01
0.02
0.03
0.04
0.05
STRAIN (IN/IN)

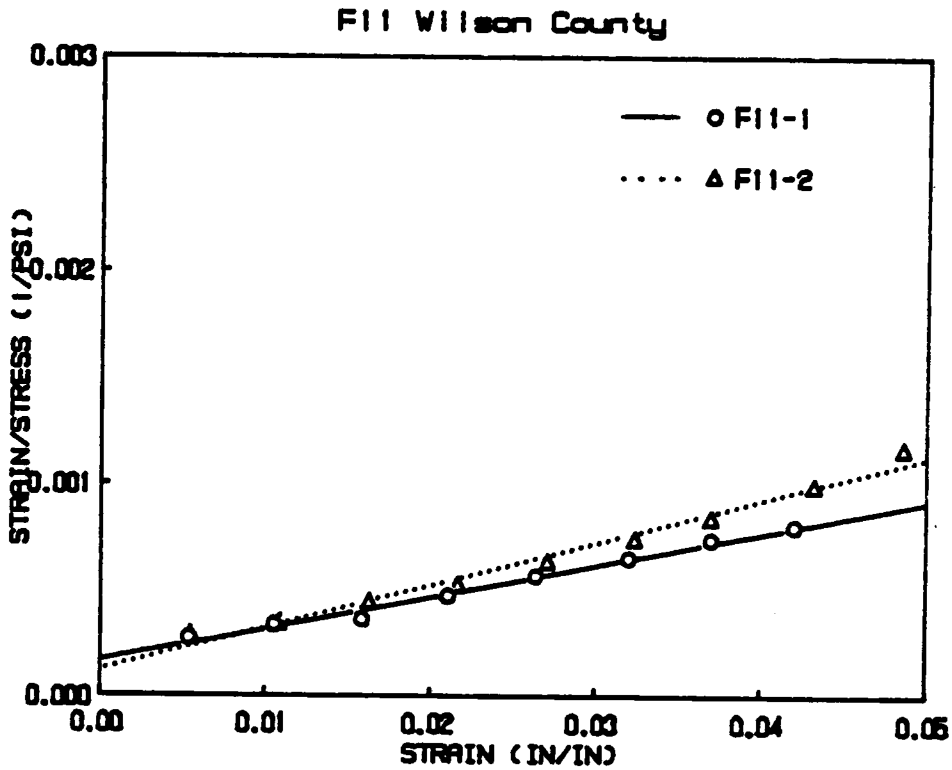
F11 Wilson County
F11-1
F11-2
STRAIN/STRESS (1/PSI)
0.003
0.002
0.001
0.000
0.00
0.01
0.02
0.03
0.04
0.05
STRAIN (IN/IN)

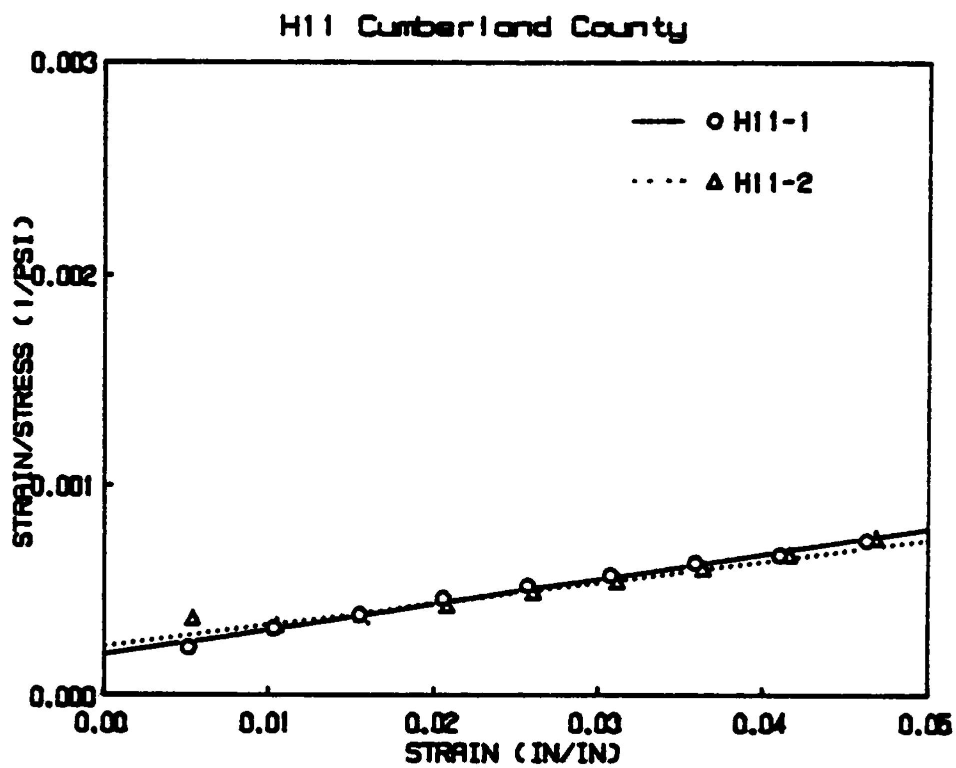
H11 Cumberland County
H11-1
H11-2
STRAIN/STRESS (1/PSI)
0.003
0.002
0.001
0.000
0.00
0.01
0.02
0.03
0.04
0.05
STRAIN (IN/IN)

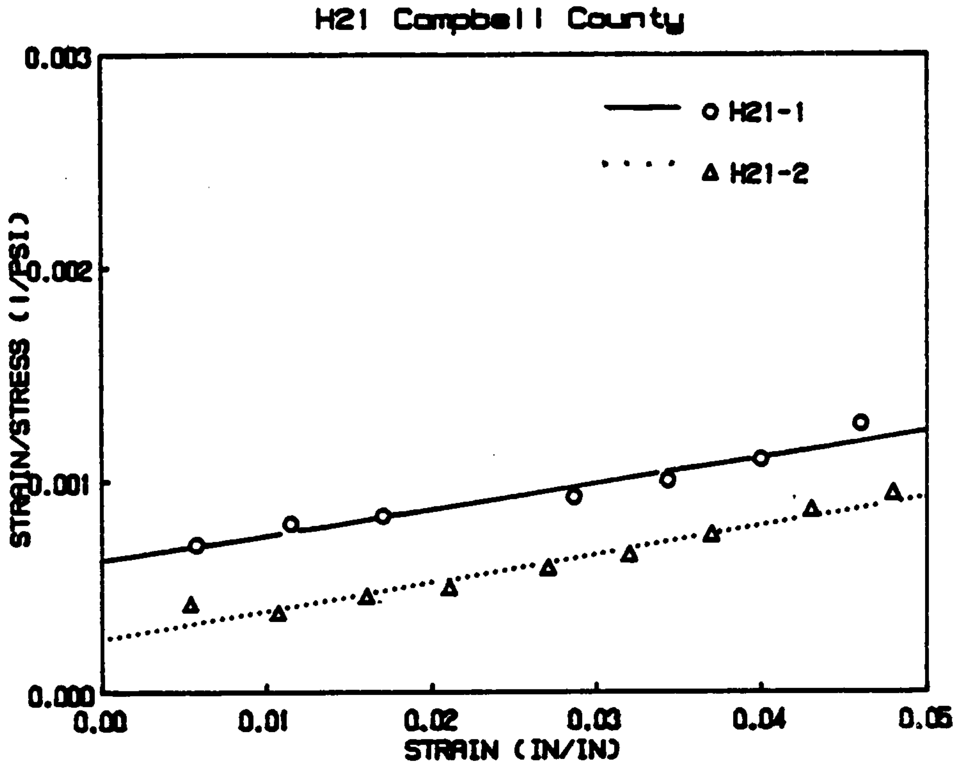
H21 Campbell County
0.003
0.002
0.001
0.000
STRAIN/STRESS (1/PSI)
0.00
0.01
0.02
0.03
0.04
0.05
STRAIN (IN/IN)
H21-1
H21-2

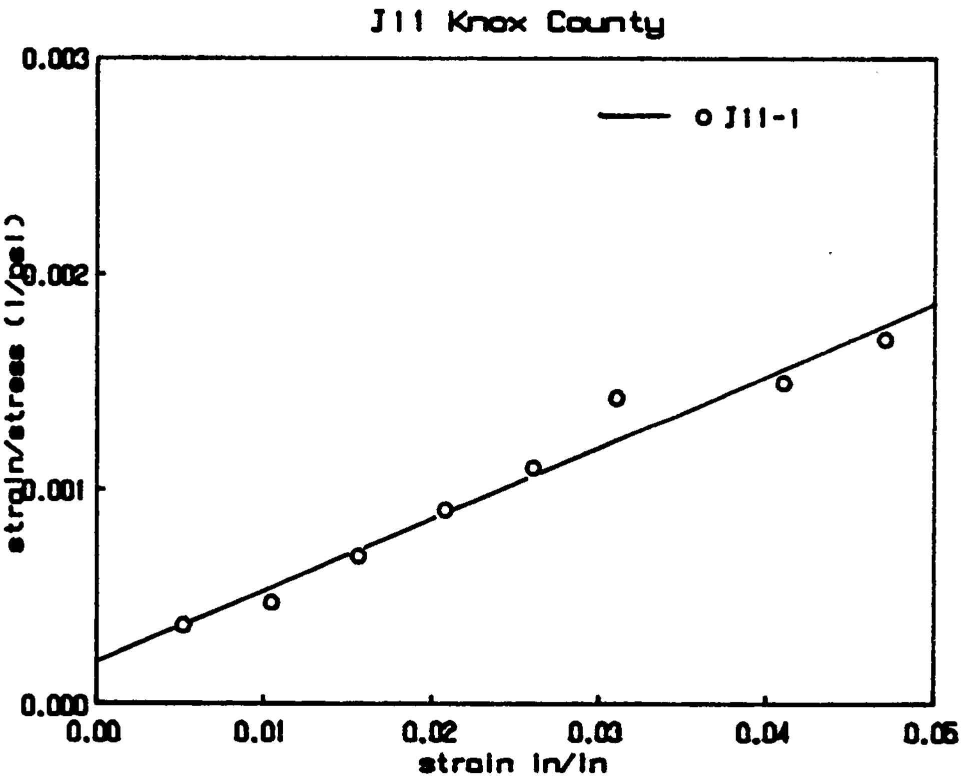
J11 Knox County
0.003
0.002
0.001
0.000
strain/stress (1/psi)
0.00
0.01
0.02
0.03
0.04
0.05
strain in/in
J11-1

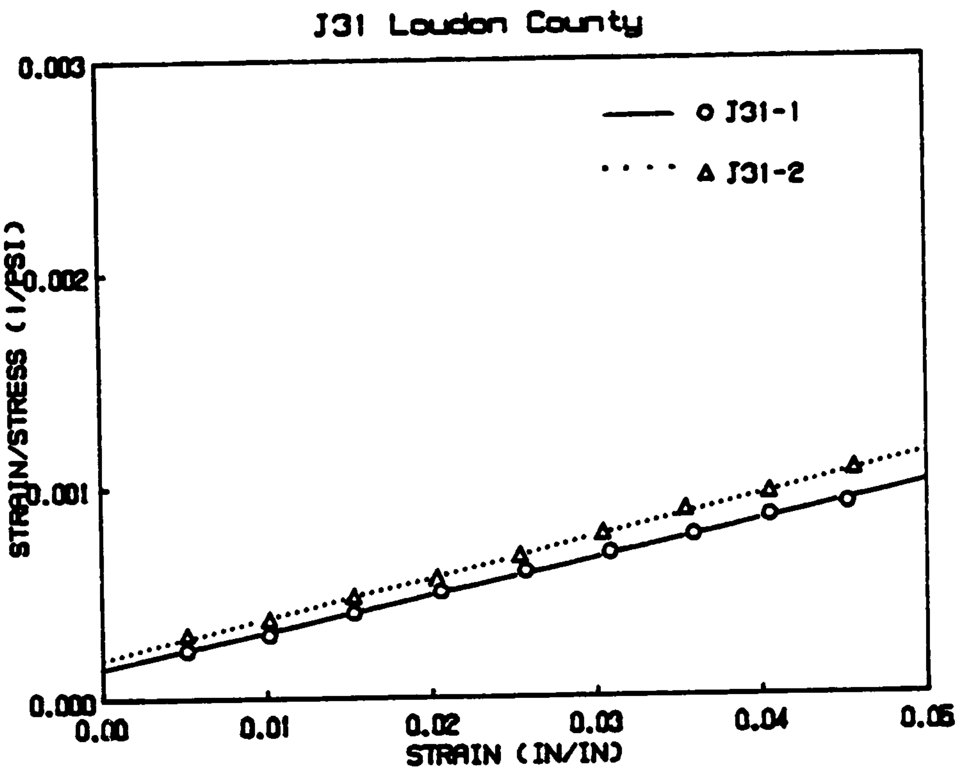
J31 Loudon County
J31-1
J31-2
STRAIN/STRESS (1/PSI)
0.003
0.002
0.001
0.000
0.00
0.01
0.02
0.03
0.04
0.05
STRAIN (IN/IN)

APPENDIX D

APPENDIX D1

MEASURED AND PREDICTED RESILIENT MODULUS
VERSUS DEVIATOR STRESS

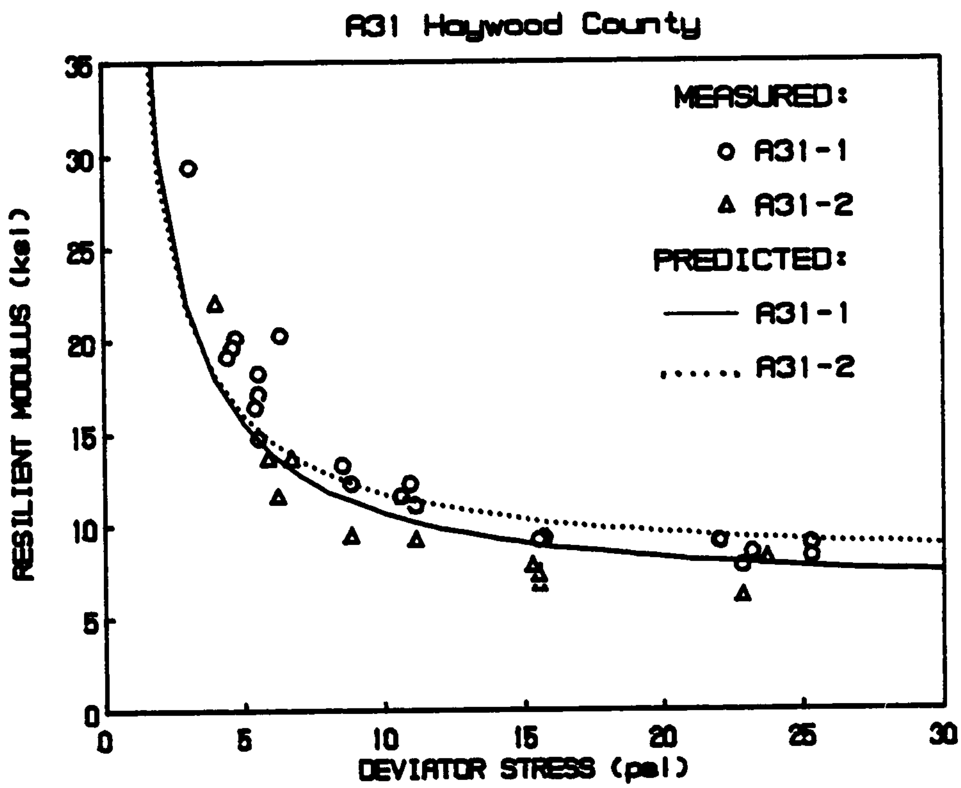

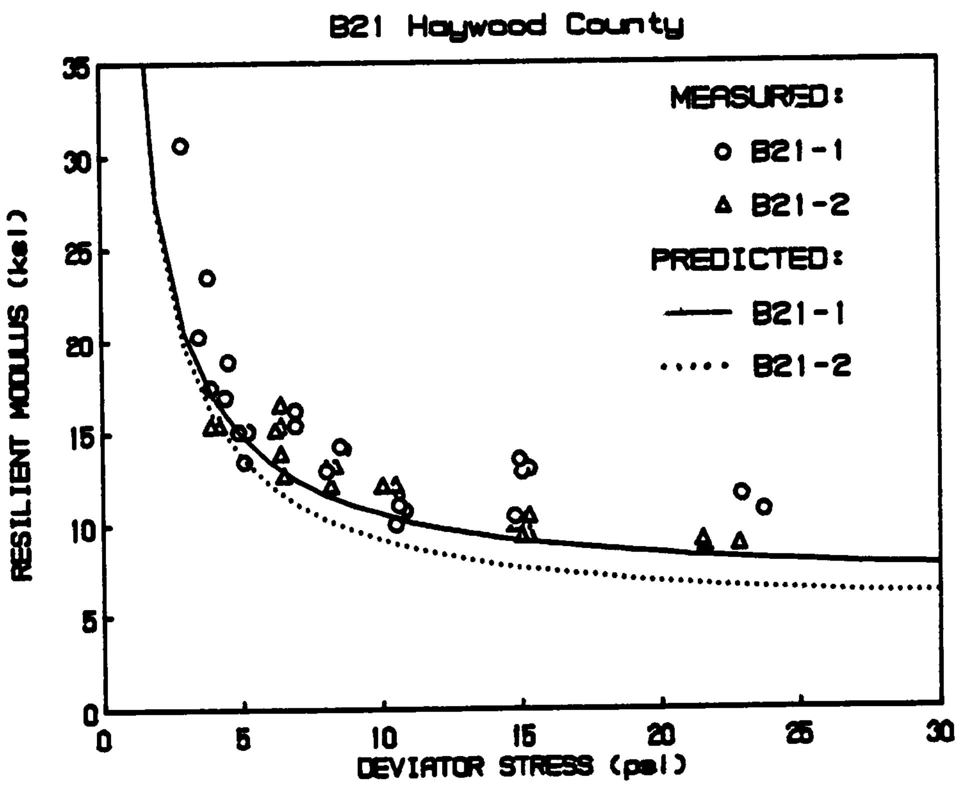

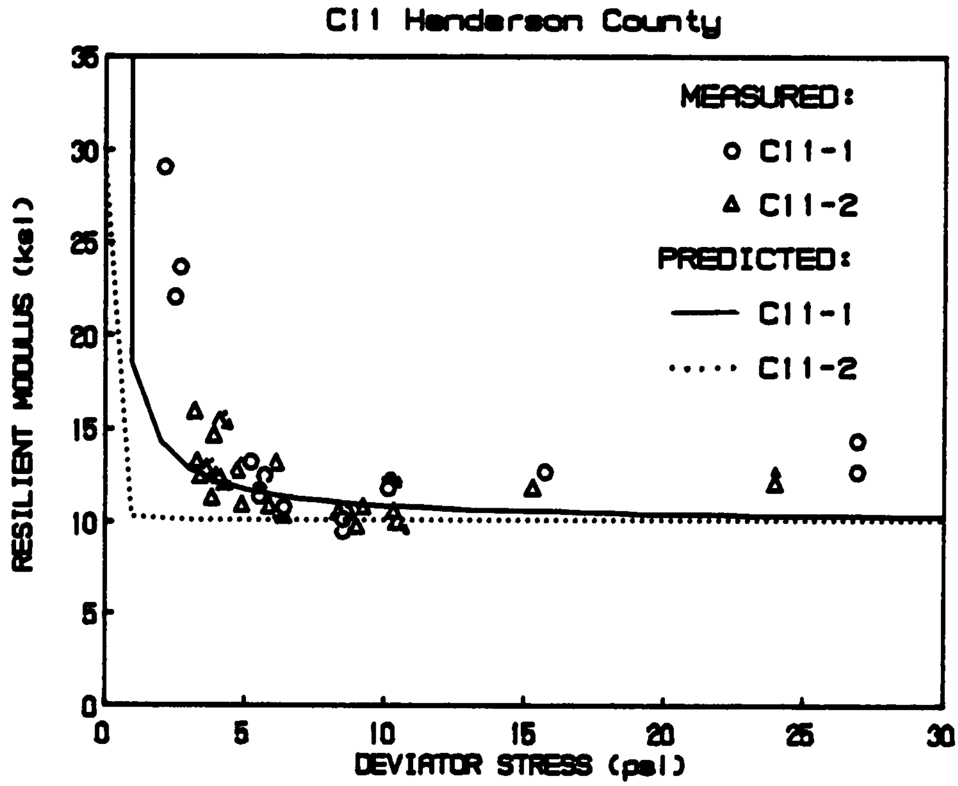

C11 Henderson County
MEASURED:
C11-1
C11-2
PREDICTED:
C11-1
C11-2
RESILIENT MODULUS (ksi)
DEVIATOR STRESS (psi)
0
5
10
15
20
25
30
35

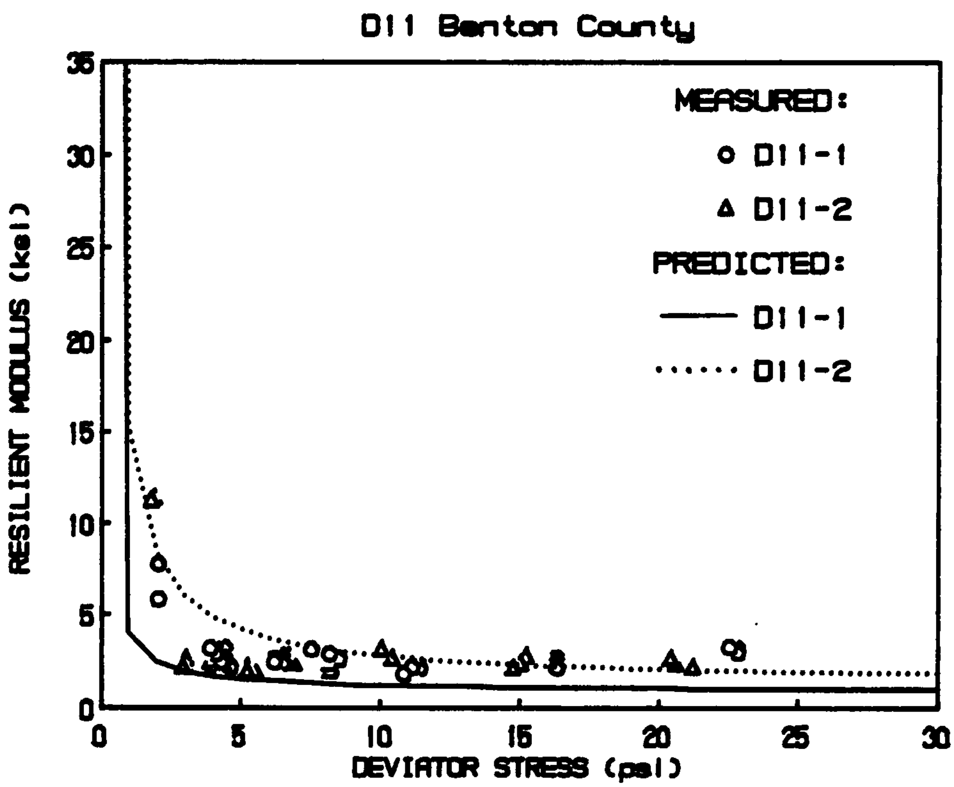

D11 Benton County
MEASURED:
D11-1
D11-2
PREDICTED:
D11-1
D11-2
RESILIENT MODULUS (ksi)
DEVIATOR STRESS (psi)
0
5
10
15
20
25
30
35

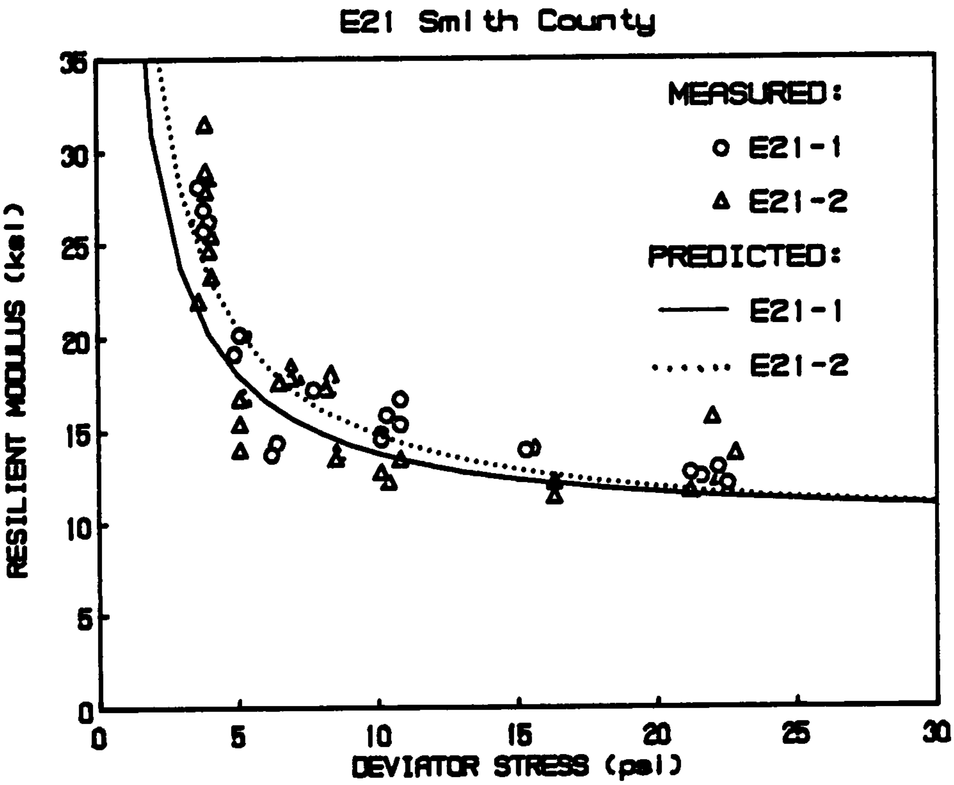
E21 Smith County
MEASURED:
E21-1
E21-2
PREDICTED:
E21-1
E21-2
RESILIENT MODULUS (ksi)
DEVIATOR STRESS (psi)
0
5
10
15
20
25
30
35

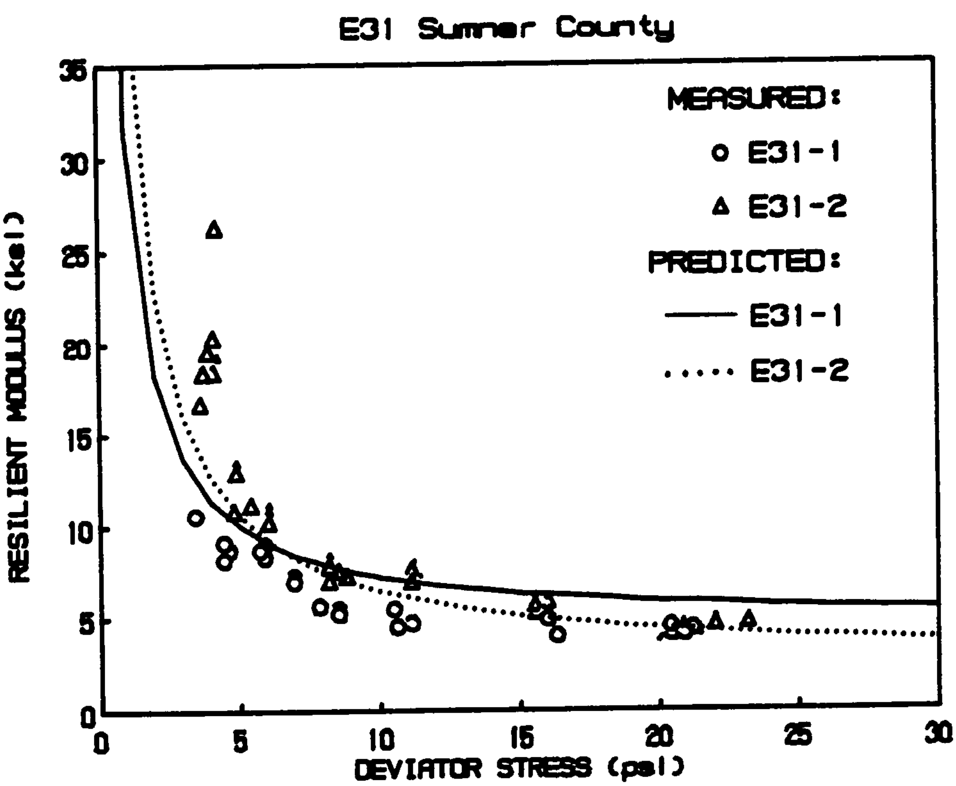
E31 Sumner County
MEASURED:
E31-1
E31-2
PREDICTED:
E31-1
E31-2
RESILIENT MODULUS (ksi)
DEVIATOR STRESS (psi)
0
5
10
15
20
25
30
35

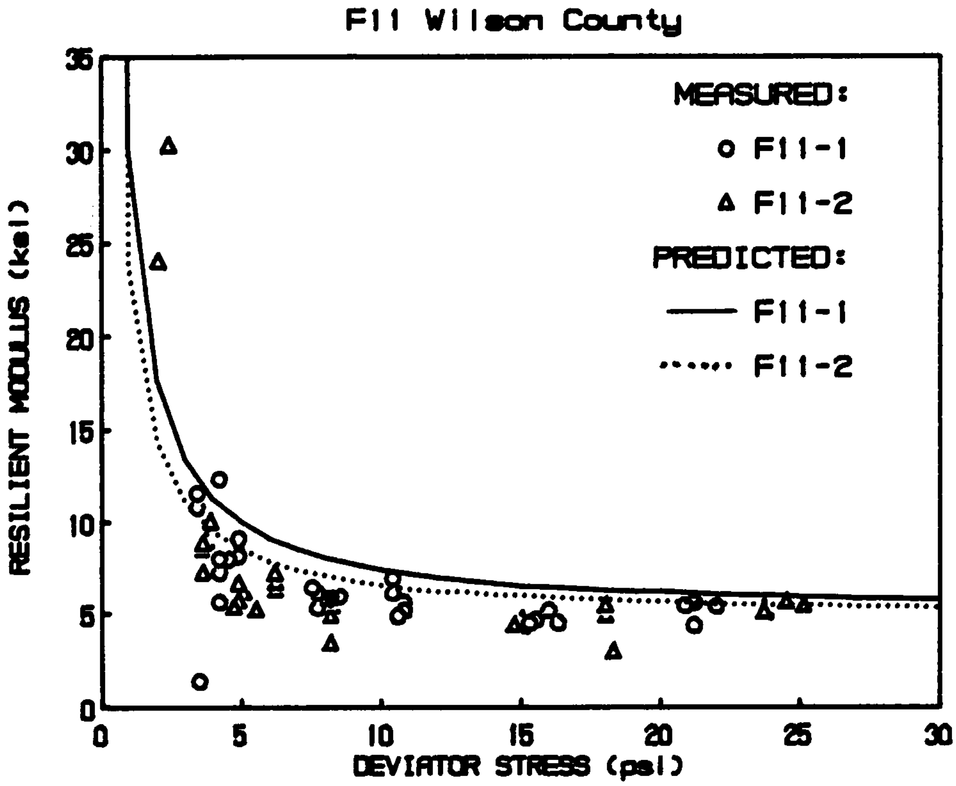

F11 Wilson County
MEASURED:
F11-1
F11-2
PREDICTED:
F11-1
F11-2
RESILIENT MODULUS (ksi)
DEVIATOR STRESS (psi)
0
5
10
15
20
25
30
35

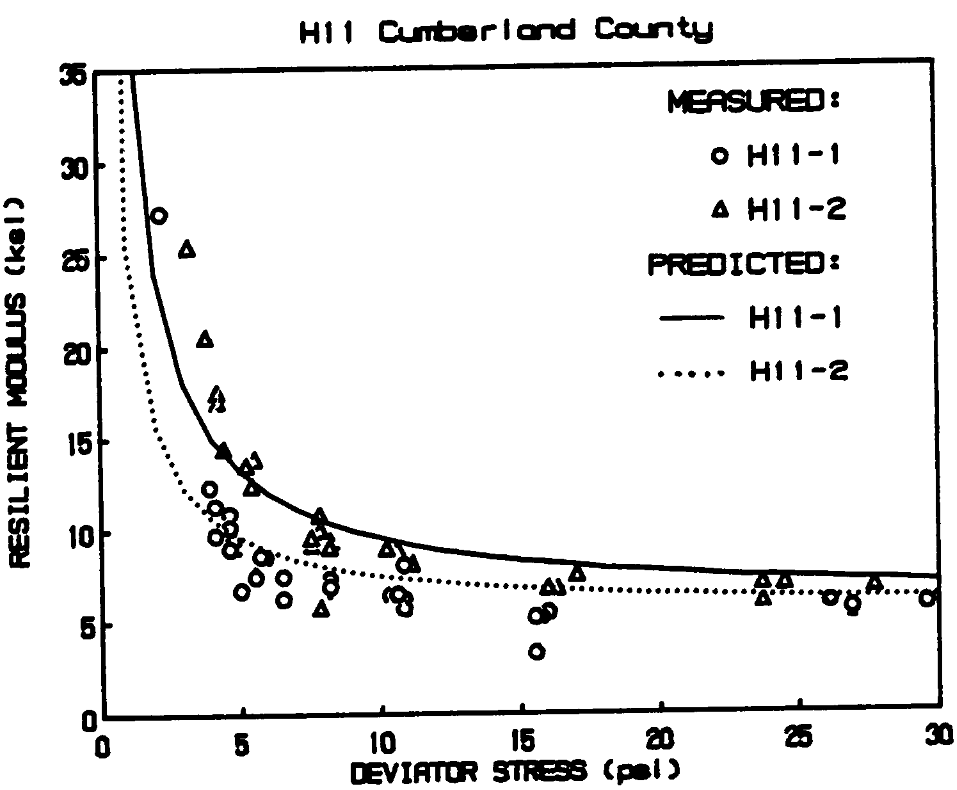

H11 Cumberland County
MEASURED:
H11-1
H11-2
PREDICTED:
H11-1
H11-2
RESILIENT MODULUS (ksi)
DEVIATOR STRESS (psi)
0
5
10
15
20
25
30
35

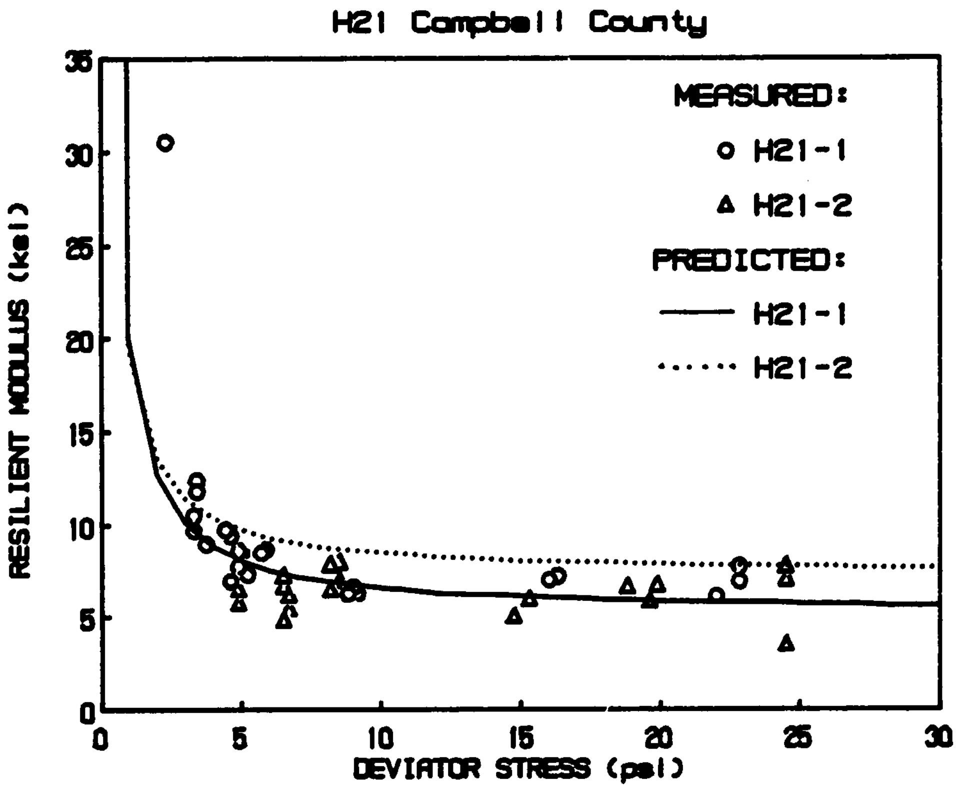

H21 Campbell County
RESILIENT MODULUS (ksi)
DEVIATOR STRESS (psi)
MEASURED:
H21-1
H21-2
PREDICTED:
H21-1
H21-2
0
5
10
15
20
25
30
35

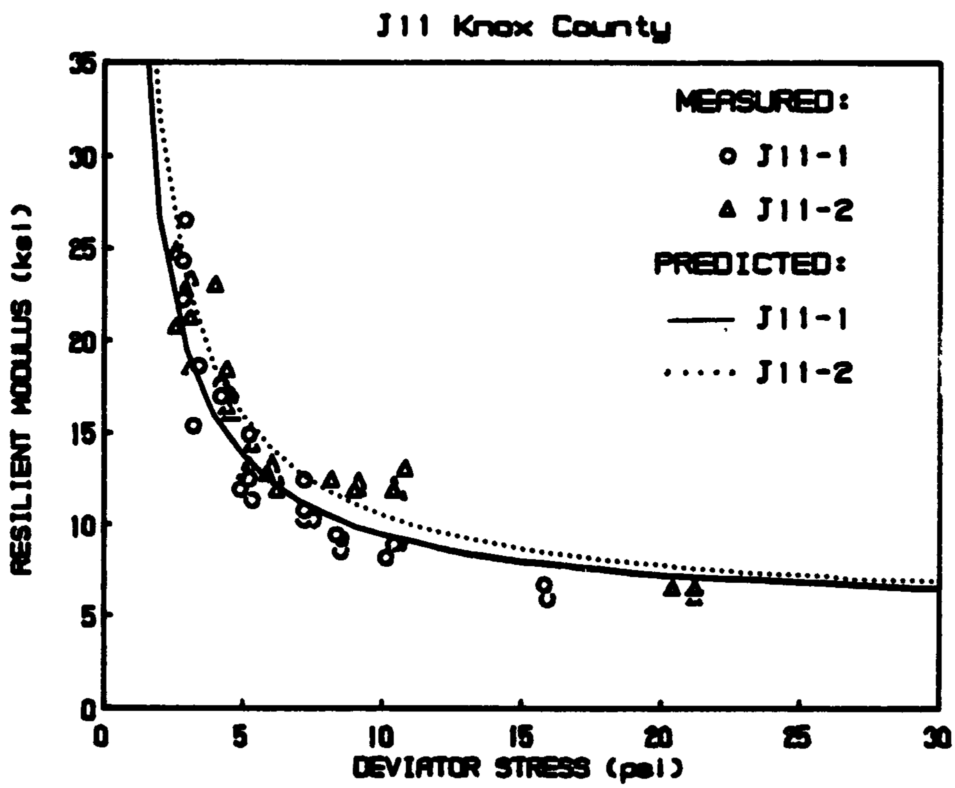

J11 Knox County
RESILIENT MODULUS (ksi)
DEVIATOR STRESS (psi)
MEASURED:
J11-1
J11-2
PREDICTED:
J11-1
J11-2
0
5
10
15
20
25
30
35

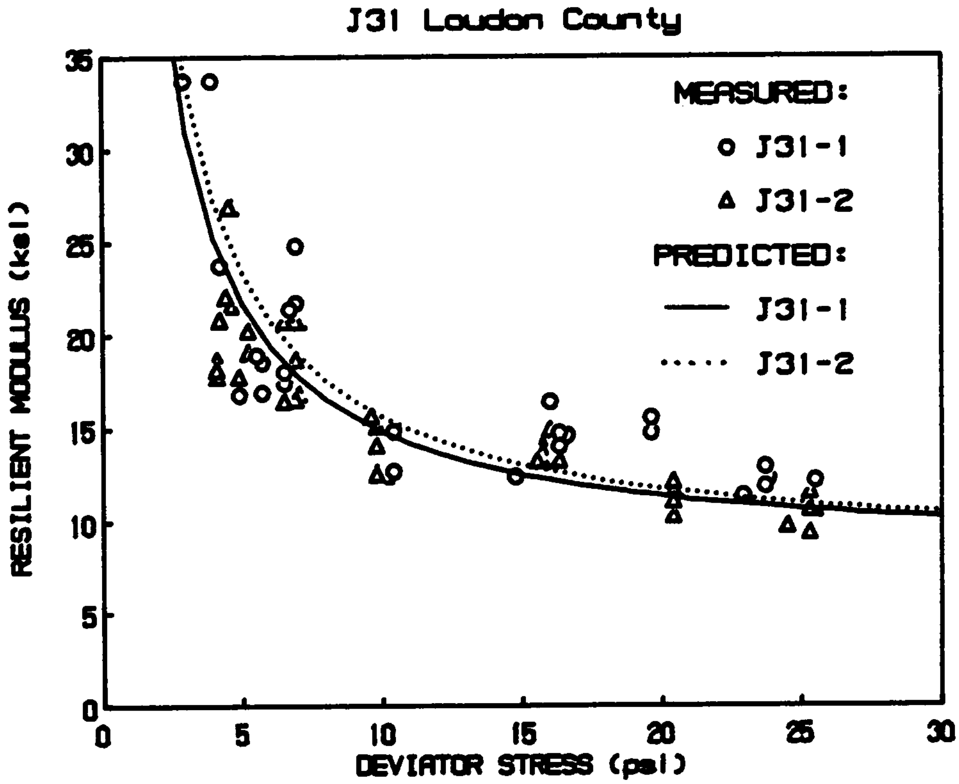

J31 Loudon County
MEASURED:
J31-1
J31-2
PREDICTED:
J31-1
J31-2
RESILIENT MODULUS (ksi)
DEVIATOR STRESS (psi)
0
5
10
15
20
25
30
35

APPENDIX D2

MEASURED AND PREDICTED STRESS VERSUS STRAIN OF UNCONFINED COMPRESSION TEST

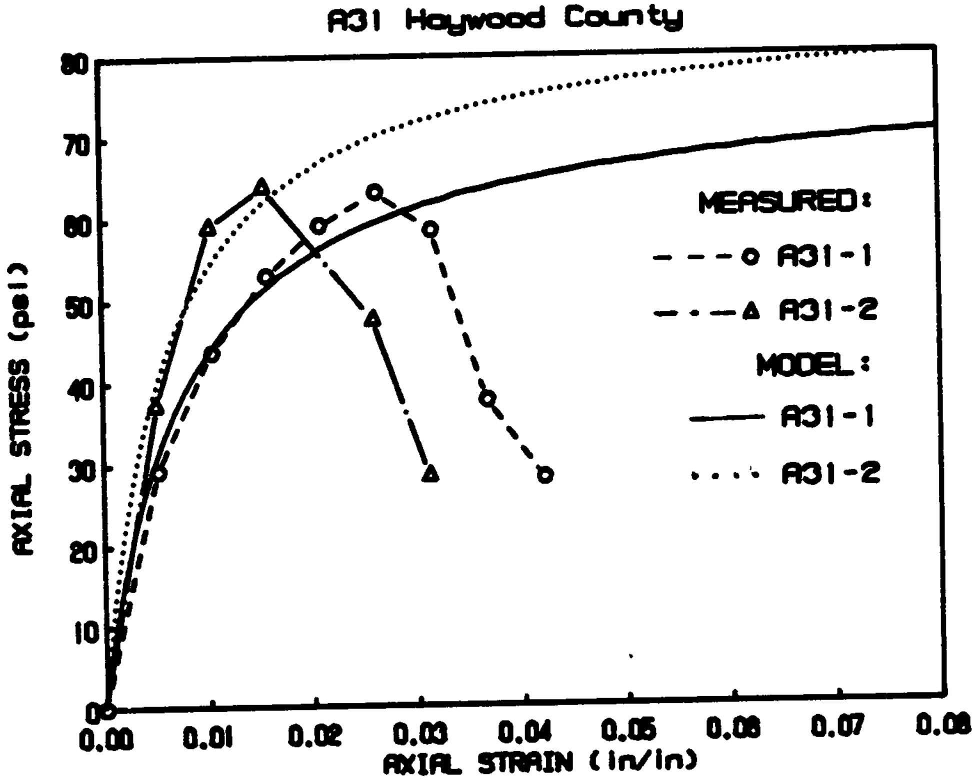

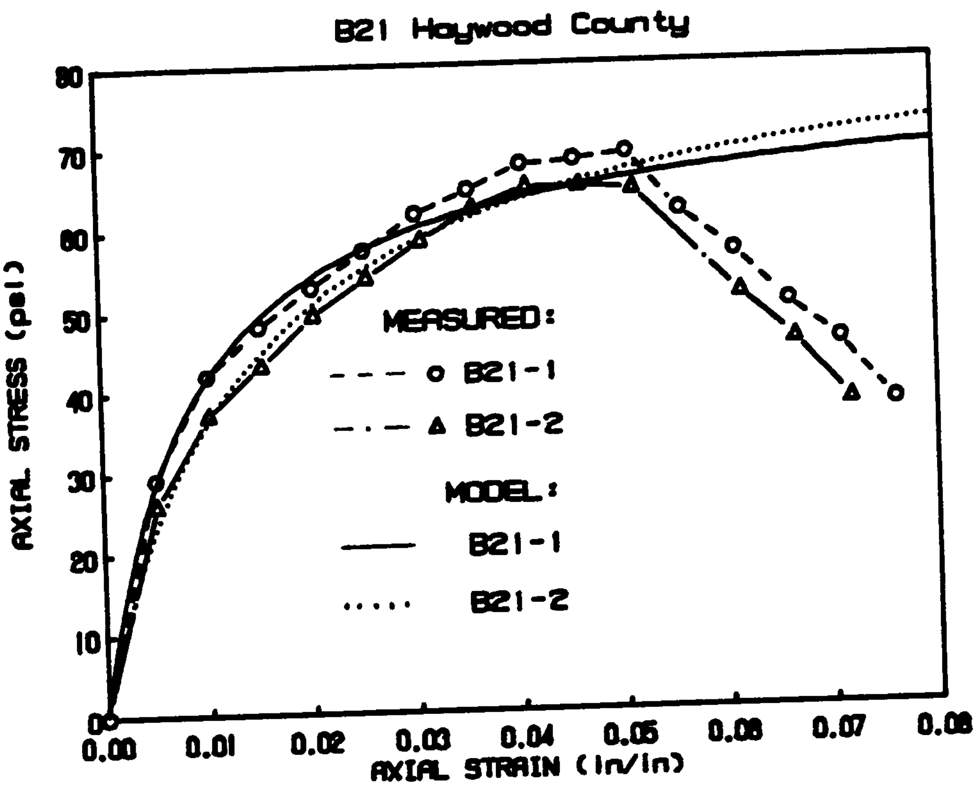

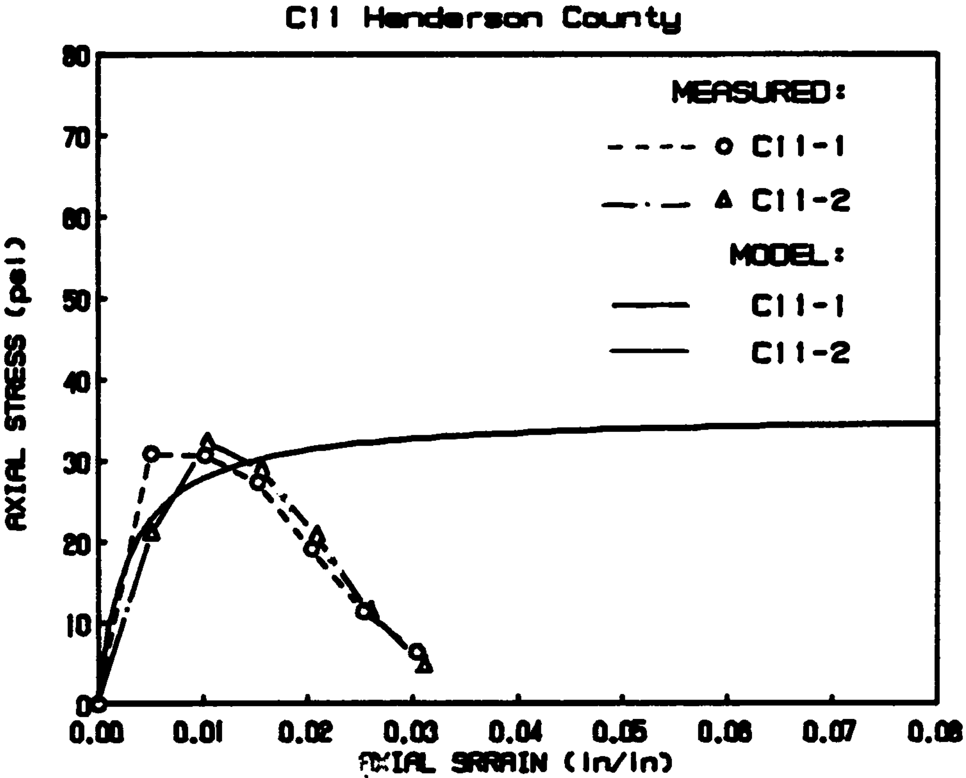
C11 Henderson County
MEASURED:
C11-1
C11-2
MODEL:
C11-1
C11-2
AXIAL STRESS (psi)
AXIAL SRRAIN (in/in)
0
10
20
30
40
50
60
70
80
0.00
0.01
0.02
0.03
0.04
0.05
0.06
0.07
0.08

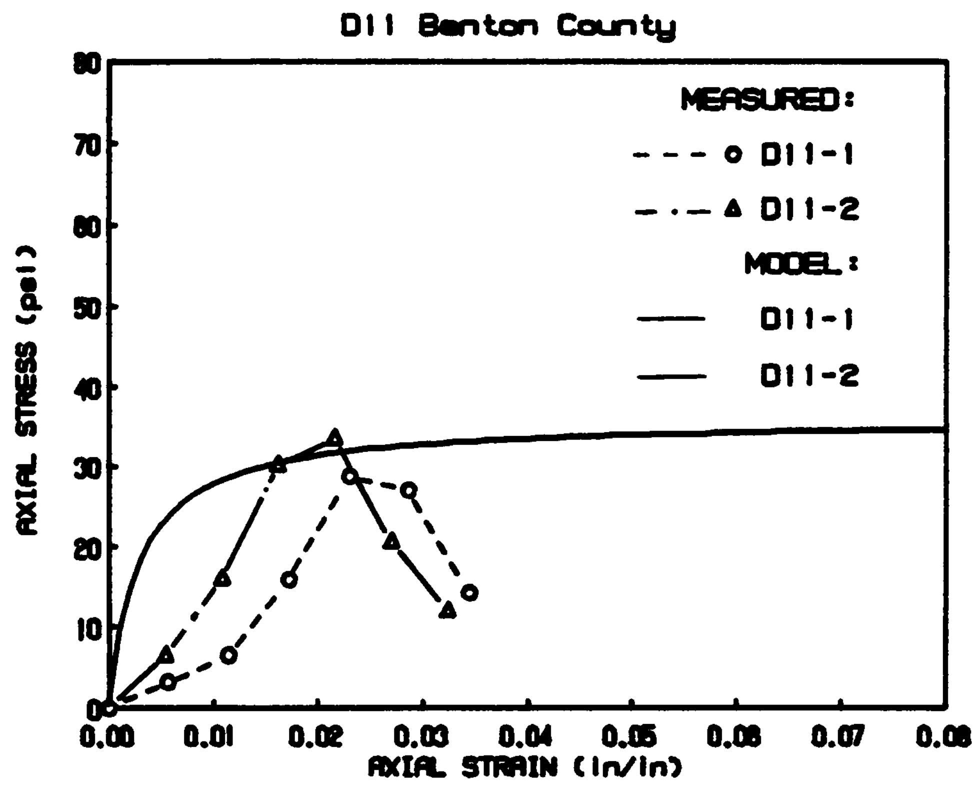
D11 Benton County
MEASURED:
D11-1
D11-2
MODEL:
D11-1
D11-2
AXIAL STRESS (psi)
AXIAL STRAIN (in/in)
0
10
20
30
40
50
60
70
80
0.00
0.01
0.02
0.03
0.04
0.05
0.06
0.07
0.08

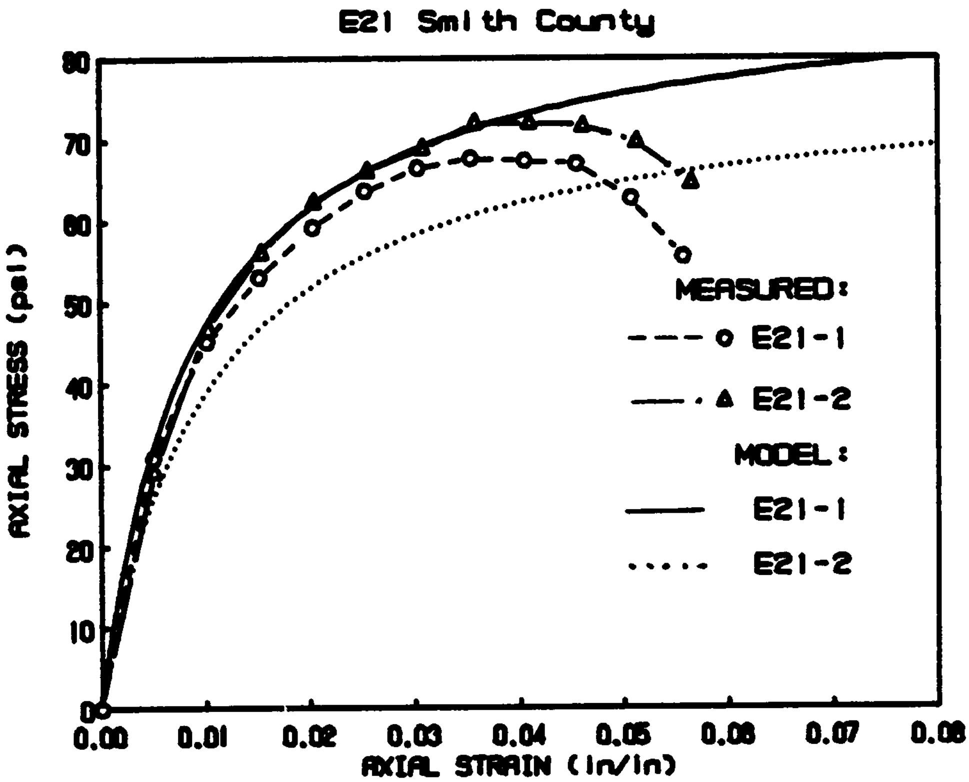
E21 Smith County
AXIAL STRESS (psi)
AXIAL STRAIN (in/in)
0
10
20
30
40
50
60
70
80
0.00
0.01
0.02
0.03
0.04
0.05
0.06
0.07
0.08
MEASURED:
E21-1
E21-2
MODEL:
E21-1
E21-2

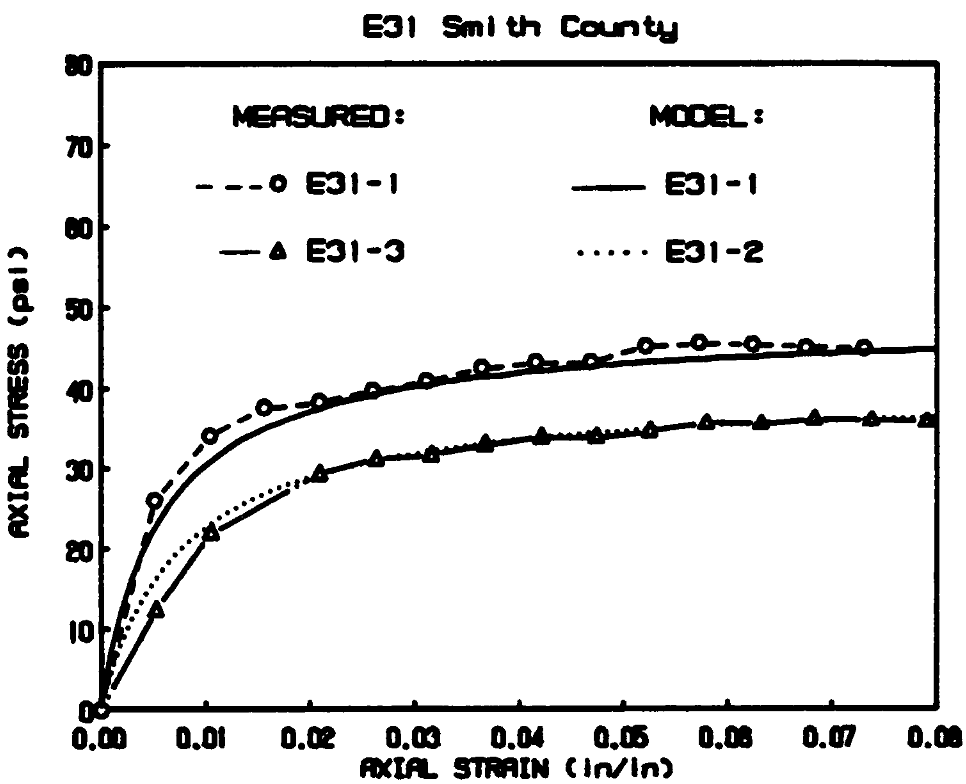
E31 Smith County
AXIAL STRESS (psi)
AXIAL STRAIN (in/in)
0
10
20
30
40
50
60
70
80
0.00
0.01
0.02
0.03
0.04
0.05
0.06
0.07
0.08
MEASURED:
E31-1
E31-3
MODEL:
E31-1
E31-2

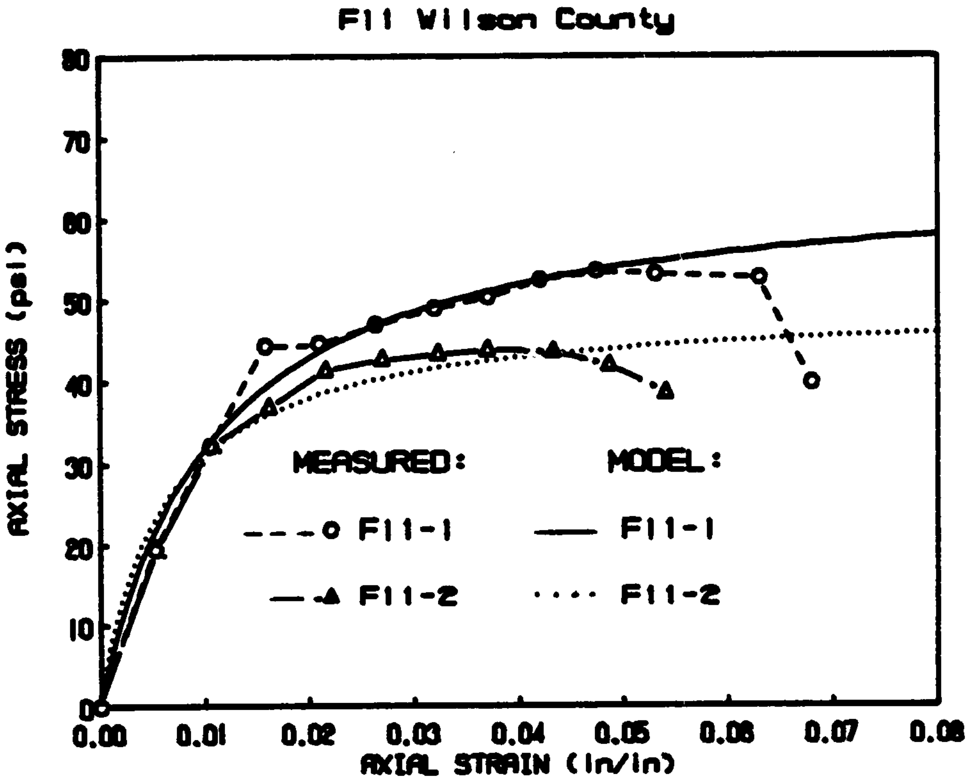
F11 Wilson County
AXIAL STRESS (psi)
AXIAL STRAIN (in/in)
0.00
0.01
0.02
0.03
0.04
0.05
0.06
0.07
0.08
0
10
20
30
40
50
60
70
80
MEASURED:
MODEL:
F11-1
F11-1
F11-2
F11-2

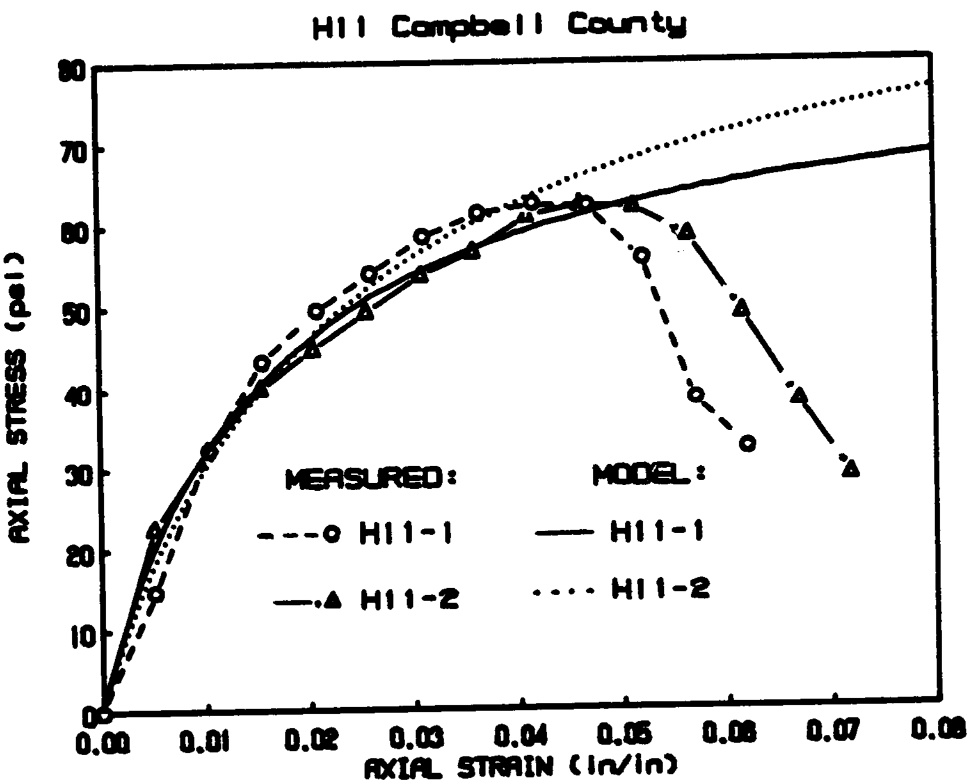
H11 Campbell County
AXIAL STRESS (psi)
AXIAL STRAIN (in/in)
0.00
0.01
0.02
0.03
0.04
0.05
0.06
0.07
0.08
0
10
20
30
40
50
60
70
80
MEASURED:
MODEL:
H11-1
H11-1
H11-2
H11-2

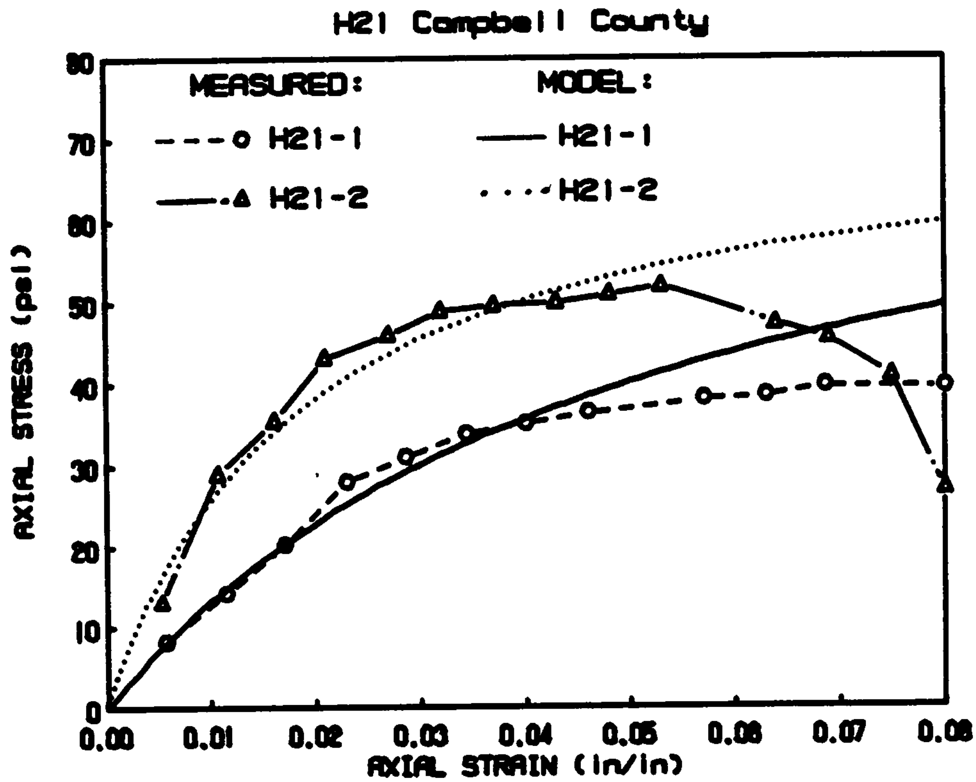
H21 Campbell County
MEASURED:
H21-1
H21-2
MODEL:
H21-1
H21-2
AXIAL STRESS (psi)
AXIAL STRAIN (in/in)
0
10
20
30
40
50
60
70
80
0.00
0.01
0.02
0.03
0.04
0.05
0.06
0.07
0.08

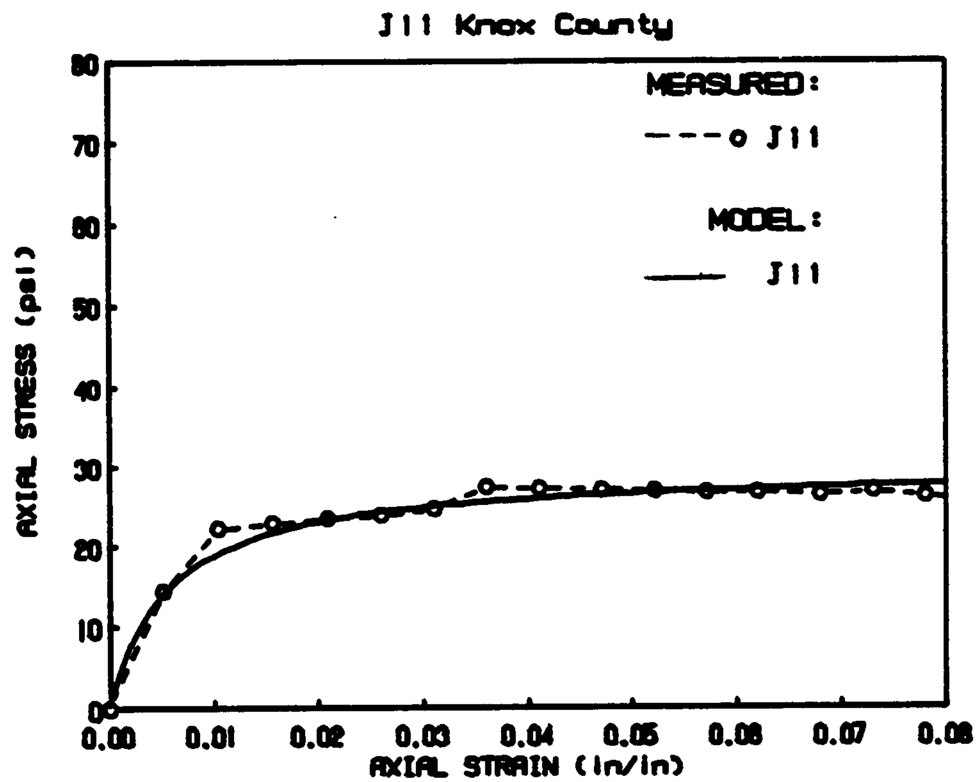
J11 Knox County
MEASURED:
J11
MODEL:
J11
AXIAL STRESS (psi)
AXIAL STRAIN (in/in)
0
10
20
30
40
50
60
70
80
0.00
0.01
0.02
0.03
0.04
0.05
0.06
0.07
0.08

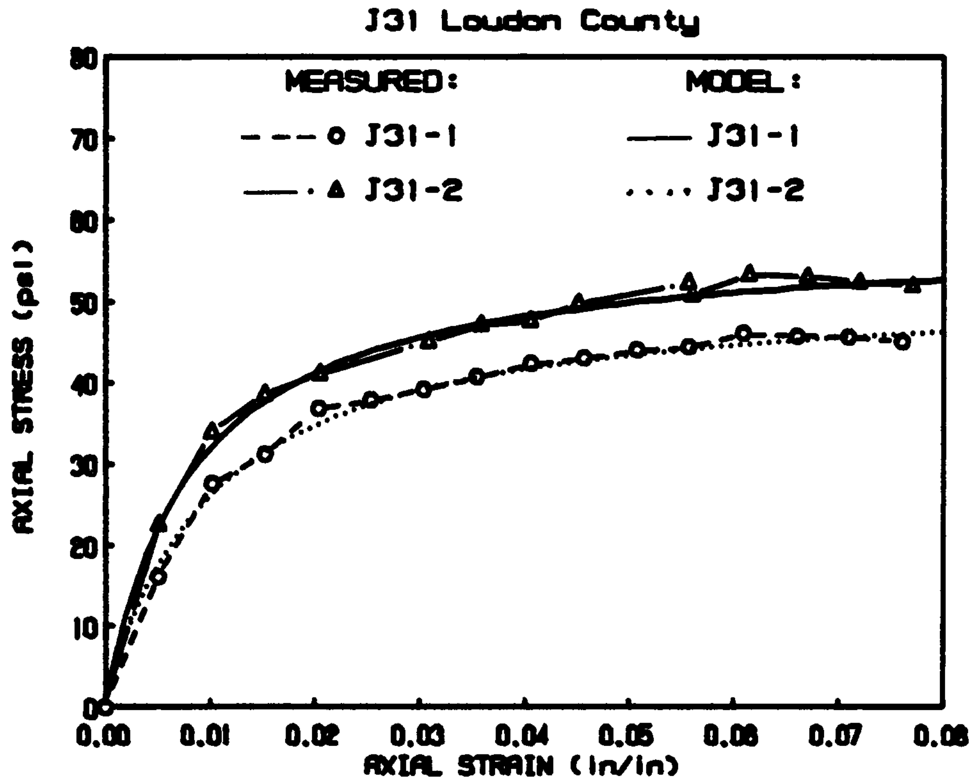

J31 Loudon County
MEASURED:
J31-1
J31-2
MODEL:
J31-1
J31-2
AXIAL STRESS (psi)
AXIAL STRAIN (in/in)
0
10
20
30
40
50
60
70
80
0.00
0.01
0.02
0.03
0.04
0.05
0.06
0.07
0.08

APPENDIX E

APPENDIX E1

TRANSFORMED REPEATED LOAD TEST DATA

A31 Haywood County: Specimen 1 Data

σ_d (psi)	E_r (ksi)	$\sigma_d \times E_r$ (ksi)	σ_d (psi)	E_r (ksi)	$\sigma_d \times E_r$ (ksi)
3.1	29.4	91.1	10.9	12.3	134.1
4.4	19.1	84.0	11.1	11.1	123.2
4.6	19.6	90.2	15.5	9.2	142.6
4.7	20.1	94.5	15.7	9.3	146.0
5.4	16.4	88.4	22.0	9.1	200.9
5.5	18.2	100.1	22.8	7.8	178.0
5.5	14.7	80.9	23.2	8.5	197.2
5.5	17.1	94.1	25.3	8.3	210.0
10.6	11.6	123.0	25.3	8.3	210.0
6.3	20.3	127.9	25.3	8.3	210.0
8.5	13.3	113.1	25.3	9.0	228.9
8.8	12.3	108.2	25.3	8.7	221.8

A31 Haywood County: Specimen 2 Data

σ_d (psi)	E_r (ksi)	$\sigma_d \times E_r$ (ksi)	σ_d (psi)	E_r (ksi)	$\sigma_d \times E_r$ (ksi)
5.9	13.6	82.0	15.3	7.8	119.8
6.2	11.5	71.0	15.5	7.3	109.9
6.7	13.6	91.1	15.5	6.8	105.4
11.1	9.2	102.1	23.7	8.2	194.5
8.8	9.4	82.7	22.8	6.1	139.1

B21 Haywood County: Specimen 1 Data

σ_d (psi)	E_r (ksi)	$\sigma_d \times E_r$ (ksi)	σ_d (psi)	E_r (ksi)	$\sigma_d \times E_r$ (ksi)
2.9	30.6	88.7	8.6	14.1	12.1.3
3.5	20.3	71.0	8.8	14.1	120.7
3.8	23.5	89.3	10.5	10.0	105.0
3.9	17.4	67.9	10.6	11.0	116.6
4.4	16.9	74.4	10.6	9.9	105.0
4.5	18.8	84.6	10.6	10.8	115.0
4.9	15.0	73.6	10.8	10.7	115.6
5.1	13.4	68.3	14.7	14.1	207.3
5.2	15.1	78.5	14.9	13.5	201.0
6.9	15.5	107.0	15.0	13.1	196.3
6.9	15.4	106.0	15.1	12.8	193.5
6.9	16.2	111.8	15.1	12.8	193.5
8.0	12.9	103.2	15.3	13.0	202.0
8.5	14.2	120.7	22.9	11.6	265.6
8.6	14.1	121.3	23.7	10.7	253.6

B21 Haywood County: Specimen 2 Data

σ_d (psi)	E_r (ksi)	$\sigma_d \times E_r$ (ksi)	σ_d (psi)	E_r (ksi)	$\sigma_d \times E_r$ (ksi)
3.9	15.3	59.7	10.0	12.0	102.0
4.2	15.3	64.3	10.5	12.1	127.0
6.4	16.5	75.9	10.6	11.5	122.0
6.2	15.1	93.6	14.7	9.9	145.5
6.4	15.3	98.0	15.0	9.3	139.5
6.4	13.8	88.3	15.3	10.4	159.1
6.5	12.6	82.0	15.3	9.3	142.3
8.0	12.9	103.2	21.5	9.1	195.5
8.3	13.1	108.7	21.6	8.8	190.1
8.4	12.0	100.8	22.8	8.9	202.9

C11 Henderson County: Specimen 1 Data

σ_d (psi)	E_r (ksi)	$\sigma_d \times E_r$ (ksi)	σ_d (psi)	E_r (ksi)	$\sigma_d \times E_r$ (ksi)
2.1	29.0	61.5	8.5	9.5	80.8
2.5	22.0	57.2	10.1	11.8	119.2
2.7	23.6	63.7	10.1	12.0	129.9
5.2	13.2	69.1	10.2	12.2	124.4
5.5	11.4	63.4	10.3	12.1	124.7
5.5	11.7	64.4	15.7	12.5	196.3
5.7	12.5	71.3	26.9	12.7	341.6
6.4	10.8	69.1	26.9	14.4	387.4
8.5	10.1	85.8			

C11 Henderson County: Specimen 2 Data

σ_d (psi)	E_r (ksi)	$\sigma_d \times E_r$ (ksi)	σ_d (psi)	E_r (ksi)	$\sigma_d \times E_r$ (ksi)
3.2	15.9	50.9	4.9	10.9	53.4
3.3	13.2	43.5	5.9	10.8	63.7
3.4	12.4	42.2	6.1	13.1	79.9
3.6	12.8	46.0	6.3	10.5	66.2
3.6	12.8	46.1	6.4	10.3	65.9
3.8	11.2	42.6	8.3	10.5	87.2
3.9	14.6	56.9	8.7	10.5	91.4
4.1	15.4	63.1	9.0	9.7	87.3
4.1	12.4	50.8	9.2	10.8	99.4
4.3	12.0	51.6	10.3	10.5	108.2
4.3	15.3	65.8	10.4	9.9	103.0
4.7	12.7	59.6	10.6	9.7	102.8
4.9	13.0	63.7	15.3	11.8	180.5

D11 Benton County: Specimen 1 Data

σ_d (psi)	E_r (ksi)	σ_d x E_r (ksi)	σ_d (psi)	E_r (ksi)	σ_d x E_r (ksi)
2.0	5.8	11.6	7.5	3.1	23.3
2.0	7.8	15.6	8.2	2.9	23.3
3.9	3.2	12.5	8.5	2.6	21.3
4.1	2.9	11.9	10.8	1.8	19.4
4.1	3.1	12.7	11.1	2.2	24.4
4.3	2.5	10.8	11.4	2.1	23.9
4.4	2.6	11.4	16.3	2.2	35.9
4.4	2.3	10.1	16.3	2.5	40.8
4.4	3.2	14.1	16.3	2.7	44.0
4.6	2.2	10.1	16.3	2.5	40.8
6.2	2.5	15.5	22.5	3.3	74.3
6.2	2.6	16.1	22.8	3.0	68.4
6.5	2.4	14.9	22.8	3.2	73.0
6.5	2.6	16.9			

D11 Benton County: Specimen 2 Data

σ_d (psi)	E_r (ksi)	σ_d x E_r (ksi)	σ_d (psi)	E_r (ksi)	σ_d x E_r (ksi)
1.8	11.2	20.2	6.7	2.8	18.8
1.9	11.4	21.7	6.9	2.3	15.9
2.1	12.2	25.6	8.2	2.6	21.3
2.9	2.2	6.4	8.2	2.3	18.9
3.0	2.6	7.8	8.2	2.5	20.5
3.0	3.0	9.0	8.2	2.0	16.4
3.2	2.2	7.0	8.5	2.2	18.7
3.9	2.5	9.8	10.0	3.1	31.0
4.0	2.2	8.8	10.4	2.6	27.0
4.1	2.1	8.6	14.7	2.4	35.3
5.2	2.0	10.4	14.7	2.1	30.9
5.2	2.2	11.4	15.0	2.4	36.0
5.5	2.0	11.0	15.2	2.8	42.6
6.5	2.6	16.9	20.4	2.6	53.0
6.5	2.3	15.0	20.6	2.3	47.4
6.7	2.4	16.1	21.2	2.2	46.9

E21 Smith County: Specimen 1 Data

σ_d (psi)	E_r (ksi)	$\sigma_d \times E_r$ (ksi)	σ_d (psi)	E_r (ksi)	$\sigma_d \times E_r$ (ksi)
3.6	28.1	101.2	10.1	14.8	149.5
3.7	26.0	96.2	10.3	15.8	162.7
3.8	25.7	97.7	10.8	16.7	180.4
3.8	26.8	101.8	10.8	15.3	165.2
4.0	26.2	104.8	15.3	13.9	212.7
4.9	19.1	93.6	15.5	14.0	217.0
5.1	20.1	102.0	15.5	14.0	217.0
5.2	20.1	104.5	21.2	12.7	269.2
6.2	13.7	85.0	21.6	12.5	270.0
6.4	14.4	92.2	22.2	13.0	288.6
7.7	17.2	132.4	22.5	12.1	272.3
10.1	14.5	146.5			

E21 Smith County: Specimen 2 Data

σ_d (psi)	E_r (ksi)	$\sigma_d \times E_r$ (ksi)	σ_d (psi)	E_r (ksi)	$\sigma_d \times E_r$ (ksi)
3.6	26.4	95.0	7.1	17.9	127.1
3.6	21.9	78.8	8.2	17.2	141.0
3.8	26.8	101.8	8.2	17.3	141.9
3.9	31.4	122.5	8.3	18.0	149.4
3.9	27.8	108.4	8.5	13.4	113.9
3.9	28.9	112.7	8.5	13.8	117.3
4.0	24.6	98.4	10.1	12.7	128.3
4.0	28.5	114.0	10.4	12.2	126.9
4.1	25.4	104.1	10.8	13.4	144.7
4.1	23.2	95.1	16.3	11.4	185.8
5.1	15.3	78.0	16.3	12.2	198.9
5.1	13.9	70.9	21.2	11.7	248.0
5.1	16.7	85.2	21.2	11.7	248.0
5.2	16.8	87.4	22.0	15.7	304.0
6.5	17.6	114.4	22.2	12.3	273.1
6.9	17.8	122.8	22.8	13.7	312.4
6.9	18.4	127.0			

E31 Sumner County: Specimen 1 data

σ_d (psi)	E_r (ksi)	$\sigma_d \times E_r$ (ksi)	σ_d (psi)	E_r (ksi)	$\sigma_d \times E_r$ (ksi)
3.4	10.6	36.0	8.5	5.5	43.7
4.4	8.2	36.0	10.5	5.5	57.8
4.4	9.1	40.0	10.6	4.5	47.7
4.6	8.7	36.0	11.1	4.7	52.2
5.7	8.7	49.6	16.0	4.9	78.4
5.9	8.3	49.0	16.0	5.0	80.0
5.9	9.0	53.1	16.3	4.0	65.2
6.9	7.0	48.3	20.4	4.5	91.8
6.9	7.3	50.4	20.4	4.1	83.6
6.9	7.3	50.4	20.9	4.1	86.5
6.9	7.2	49.7	20.9	4.1	86.5
7.8	5.6	43.7	21.2	4.4	93.3
8.5	5.2	44.2			

E31 Sumner County: Specimen 2 Data

σ_d (psi)	E_r (ksi)	$\sigma_d \times E_r$ (ksi)	σ_d (psi)	E_r (ksi)	$\sigma_d \times E_r$ (ksi)
3.6	16.6	59.8	8.5	7.5	63.8
3.7	18.3	67.7	8.8	7.2	63.4
3.9	19.5	76.0	11.1	6.9	76.6
4.1	20.3	83.2	11.1	7.6	84.4
4.1	19.3	79.1	11.2	7.6	85.1
4.1	18.3	75.0	15.5	5.6	86.4
4.2	26.2	111.7	15.5	5.2	86.8
4.9	12.8	62.7	15.5	5.8	89.9
4.9	10.7	52.4	15.7	5.5	86.4
4.9	13.1	64.2	16.0	5.8	92.8
5.4	11.1	59.9	20.2	4.0	80.8
6.0	10.1	60.6	20.9	4.3	89.9
6.0	10.5	63.0	21.2	4.3	91.2
6.0	10.8	64.8	22.0	4.6	101.2
8.2	7.0	57.4	22.0	4.6	101.2
8.2	7.8	64.0	23.2	4.7	109.0
8.2	8.1	66.4			

F11 Wilson County: Specimen 1 Data

σ_d (psi)	E_r (ksi)	$\sigma_d \times E_r$ (ksi)	σ_d (psi)	E_r (ksi)	$\sigma_d \times E_r$ (ksi)
3.4	11.5	39.1	8.2	5.8	47.6
3.4	10.8	36.7	8.5	6.0	51.0
3.5	10.4	36.4	10.4	7.0	72.8
4.2	8.0	33.6	10.4	6.1	63.4
4.2	12.3	51.7	10.6	4.9	51.9
4.2	5.6	23.5	10.8	5.2	56.2
4.2	7.3	30.7	10.8	5.6	60.5
4.5	8.0	36.0	15.3	4.5	68.9
4.9	8.2	40.1	15.5	4.7	72.9
4.9	8.3	40.8	16.0	5.2	83.2
4.9	9.1	44.6	16.3	4.5	73.4
7.5	6.4	49.3	20.9	5.5	115.0
7.7	6.1	47.0	21.2	4.4	93.3
7.7	5.3	40.8	21.2	5.6	118.7
7.8	5.7	44.5	22.0	5.4	118.8
8.0	5.7	45.6			

F11 Wilson County: Specimen 2 Data

σ_d (psi)	E_r (ksi)	$\sigma_d \times E_r$ (ksi)	σ_d (psi)	E_r (ksi)	$\sigma_d \times E_r$ (ksi)
2.4	30.2	72.5	6.2	6.5	40.3
3.6	7.5	27.0	7.7	5.7	43.9
3.6	7.5	28.5	8.2	3.4	27.9
3.6	8.8	31.7	8.2	4.9	40.2
3.6	7.2	25.9	8.2	5.4	44.3
3.6	8.5	30.6	14.7	4.4	64.7
3.7	9.0	33.3	15.0	4.3	64.5
3.9	10.0	39.0	15.0	4.7	70.5
4.1	7.2	29.5	18.0	5.5	99.0
4.7	5.3	24.9	18.0	4.9	88.2
4.9	5.7	27.9	18.0	5.0	90.0
4.9	6.6	32.3	18.3	3.0	54.9
5.1	6.1	31.1	23.7	5.1	120.9
5.2	5.2	27.0	23.7	5.2	123.2
6.2	7.2	44.6	23.7	5.2	123.2
6.2	6.7	41.5	24.5	5.6	137.2
6.2	6.3	39.1	23.7	5.0	118.5
6.2	6.1	37.8	25.1	5.4	135.5

H11 Cumberland County: Specimen 1 Data

σ_d (psi)	E_r (ksi)	$\sigma_d \times E_r$ (ksi)	σ_d (psi)	E_r (ksi)	$\sigma_d \times E_r$ (ksi)
2.2	27.2	59.8	8.2	7.4	60.7
3.9	12.3	48.0	8.2	6.9	56.6
4.1	9.7	39.8	8.2	6.8	55.8
4.1	11.3	46.3	10.6	6.5	68.9
4.6	10.1	46.5	10.8	5.7	61.6
4.6	9.0	41.4	10.8	6.2	67.0
4.6	10.9	50.1	10.8	8.1	87.5
4.7	9.4	44.2	10.3	6.4	72.3
4.7	8.9	41.8	15.5	3.3	51.2
5.0	6.8	34.0	15.5	5.2	80.6
5.5	7.5	41.3	15.7	5.2	81.6
5.5	7.6	41.8	16.0	5.5	88.0
5.7	8.6	49.0	16.0	5.3	84.8
5.9	8.5	50.2	26.1	6.0	156.6
6.5	7.5	48.8	26.9	5.6	150.6
6.5	6.3	41.0	26.9	5.4	145.3
8.2	6.9	56.6	29.6	5.8	156.0

H11 Cumberland County: Specimen 2 Data

σ_d (psi)	E_r (ksi)	$\sigma_d \times E_r$ (ksi)	σ_d (psi)	E_r (ksi)	$\sigma_d \times E_r$ (ksi)
3.2	25.4	81.3	8.2	9.0	73.8
3.8	20.5	77.9	8.2	9.3	76.3
4.2	17.4	73.1	10.2	8.9	90.8
4.2	16.9	71.0	10.6	8.8	93.3
4.4	14.4	63.4	11.1	8.1	89.9
5.2	13.4	69.7	11.1	8.2	91.0
5.4	12.3	66.4	16.0	6.8	108.8
5.5	13.8	75.9	16.3	6.7	109.2
7.5	9.6	72.0	17.0	7.5	127.5
7.5	9.5	71.2	17.0	7.5	127.5
7.5	9.1	68.3	23.7	7.0	166.0
7.8	10.7	83.5	23.7	6.0	142.2
7.8	5.7	44.5	24.5	7.0	171.5
7.8	9.9	77.2	27.7	6.8	188.4

H21 Campbell County: Specimen 1 Data

σ_d (psi)	E_r (ksi)	$\sigma_d \times E_r$ (ksi)	σ_d (psi)	E_r (ksi)	$\sigma_d \times E_r$ (ksi)
2.3	30.5	70.2	4.9	7.8	38.2
2.3	35.5	81.7	4.9	8.6	42.1
2.3	35.1	80.7	5.0	8.5	42.5
2.3	35.1	80.7	5.2	7.4	42.2
2.3	36.9	84.9	5.7	8.5	48.5
3.3	9.7	32.0	5.9	8.7	51.3
3.3	10.5	34.7	8.8	6.3	55.4
3.4	11.8	40.1	9.0	6.6	59.4
3.4	12.4	42.2	9.1	6.3	57.3
3.7	9.0	33.3	16.0	7.1	113.6
4.4	9.8	43.1	16.3	7.3	119.0
4.6	7.0	32.2	22.0	6.1	134.2
4.6	9.4	43.2	22.8	7.0	159.6
4.9	7.8	38.2	22.8	7.8	159.6

H21 Campbell County: Specimen 2 Data

σ_d (psi)	E_r (ksi)	$\sigma_d \times E_r$ (ksi)	σ_d (psi)	E_r (ksi)	$\sigma_d \times E_r$ (ksi)
4.6	7.0	32.2	8.2	6.4	52.5
4.9	6.4	31.4	8.5	6.2	52.7
4.9	5.7	27.9	8.5	7.0	59.5
4.9	6.6	32.3	8.5	8.0	68.0
4.9	5.7	27.9	14.7	5.0	73.5
4.9	6.4	31.3	15.3	6.0	91.8
6.5	7.3	47.5	18.8	6.6	124.1
6.5	4.8	31.2	19.6	5.8	113.7
6.5	6.6	42.9	19.9	6.8	135.3
6.7	6.1	40.9	24.5	7.8	191.1
6.7	5.4	36.2	24.5	3.5	85.7
8.2	7.9	64.8	24.5	7.1	174.0

J11 Knox County: Specimen 1 Data

σ_d (psi)	E_r (ksi)	$\sigma_d \times E_r$ (ksi)	σ_d (psi)	E_r (ksi)	$\sigma_d \times E_r$ (ksi)
2.8	22.2	62.2	7.2	10.7	77.0
2.8	24.3	68.0	7.2	10.2	77.0
2.9	26.5	76.9	7.2	10.2	73.4
3.2	15.3	45.0	7.2	12.4	89.3
3.4	18.6	63.2	7.3	10.7	78.1
4.2	17.0	71.4	7.5	10.3	77.3
4.2	17.6	73.9	8.3	9.4	78.0
4.4	17.1	75.2	8.5	9.2	78.2
4.5	16.9	76.1	8.5	8.5	72.3
4.9	11.9	56.3	10.1	8.2	82.8
5.2	12.5	65.0	10.4	8.9	92.6
5.2	14.9	77.5	10.6	8.9	94.3
5.2	14.9	77.5	15.8	6.7	105.9
5.3	11.3	59.9	15.9	5.9	93.8

J11 Knox County: Specimen 2 Data

σ_d (psi)	E_r (ksi)	$\sigma_d \times E_r$ (ksi)	σ_d (psi)	E_r (ksi)	$\sigma_d \times E_r$ (ksi)
2.6	24.7	64.2	6.0	13.0	78.0
2.6	20.7	53.8	6.0	13.2	79.2
2.6	24.7	64.2	6.2	12.5	77.5
2.9	22.7	65.8	6.2	11.8	73.2
3.1	18.5	65.8	8.2	12.4	101.7
3.1	21.2	65.7	9.0	11.8	110.7
3.1	23.3	72.2	9.1	12.3	111.9
4.4	16.3	71.7	9.1	11.9	108.3
4.4	18.4	81.0	9.1	12.1	110.1
4.5	16.0	81.0	10.4	11.8	122.7
4.6	16.0	72.0	10.4	12.1	125.8
5.1	12.8	65.3	10.6	11.6	123.0
5.1	12.3	62.7	10.8	13.0	140.4
5.2	13.1	68.1	20.4	6.5	132.6
5.2	12.5	65.0	21.2	6.5	137.8
5.3	14.3	75.8	21.2	6.0	127.2
5.9	12.7	74.9	21.2	6.6	127.2
6.0	13.2	79.2			

J31 Loudon County: Specimen 1 Data

σ_d (psi)	E_r (ksi)	$\sigma_d \times E_r$ (ksi)	σ_d (psi)	E_r (ksi)	$\sigma_d \times E_r$ (ksi)
2.9	33.7	97.7	16.3	14.0	228.2
3.9	33.7	131.4	16.3	14.7	239.6
4.2	23.7	99.5	16.3	14.2	231.5
4.9	16.8	82.3	16.6	14.6	242.4
5.5	18.9	105.5	19.6	15.5	274.0
5.7	16.9	96.3	19.6	14.7	289.0
5.7	18.5	105.5	22.9	11.4	261.0
6.5	18.0	117.0	22.9	11.4	261.0
6.5	17.4	113.1	23.7	12.9	305.0
6.7	21.4	143.4	23.7	12.9	305.0
6.9	21.7	149.7	23.7	11.9	305.0
6.9	24.8	171.1	23.7	11.9	282.0
10.4	14.8	154.0	23.8	12.3	292.0
10.4	12.7	132.1	23.8	12.3	292.0
14.7	12.4	182.3	25.5	12.2	310.0
16.0	16.4	262.4	25.5	12.2	310.0

J31 Loudon County: Specimen 2 Data

σ_d (psi)	E_r (ksi)	$\sigma_d \times E_r$ (ksi)	σ_d (psi)	E_r (ksi)	$\sigma_d \times E_r$ (ksi)
4.1	18.1	74.2	9.8	15.1	150.0
4.1	18.7	76.7	9.8	12.5	122.5
4.1	17.7	72.6	9.8	14.7	144.1
4.2	20.8	87.4	10.1	12.4	125.2
4.4	22.0	96.8	15.5	13.2	204.6
4.5	26.8	123.3	15.7	13.1	205.7
4.6	21.5	98.9	15.7	13.6	213.5
4.6	26.8	123.3	15.7	14.0	219.8
4.9	17.7	86.7	16.0	14.9	238.4
5.2	19.0	86.7	16.3	13.2	215.2
5.2	20.2	105.0	20.4	11.0	224.4
6.5	16.4	106.6	20.4	10.2	208.1
6.5	20.7	134.6	20.4	12.1	246.8
6.9	16.5	113.9	20.4	11.6	263.6
6.9	18.7	129.0	24.5	9.7	237.7
6.9	20.7	142.8	25.3	11.5	291.0
7.0	16.8	117.6	25.3	10.6	238.2
9.6	15.6	149.8	25.3	9.3	235.3
9.8	14.0	137.2	25.5	10.6	270.3

APPENDIX E2

TRANSFORMED UNCONFINED COMPRESSION TEST DATA

Transformed Unconfined Compression Test Data for A31-1.

σ (psi)	ε (in/in)	ε/σ (1/psi)
29.22	0.0053	0.00018
43.60	0.0105	0.00024
53.00	0.0158	0.00030
59.11	0.0210	0.00036
63.25	0.0263	0.00042
58.50	0.0316	0.00054
37.73	0.0368	0.00098
28.14	0.0421	0.00150

Transformed Unconfined Compression Test Data for A31-2.

σ (psi)	ε (in/in)	ε/σ (1/psi)
37.34	0.0052	0.00014
59.11	0.0104	0.00018
63.95	0.0156	0.00024
65.53	0.0208	0.00032
47.70	0.0260	0.00054
28.46	0.0312	0.00110

Transformed Unconfined Compression Test for B21-1.

σ (psi)	ε (in/in)	ε/σ (1/psi)
29.23	0.0051	0.00017
42.00	0.0101	0.00024
48.22	0.0152	0.00032
52.77	0.0203	0.00039
57.27	0.0253	0.00044
61.72	0.0304	0.00050
64.54	0.0354	0.00055
67.34	0.0405	0.00060
67.92	0.0456	0.00067
68.80	0.0506	0.00074
61.65	0.0557	0.00090
56.72	0.0608	0.00107
50.31	0.0660	0.00131
45.50	0.0709	0.00156
37.70	0.0760	0.00200

Transformed Unconfined Compression Test Data for B21-2.

σ (psi)	ε (in/in)	ε/σ (1/psi)
25.98	0.0051	0.00020
37.15	0.0103	0.00028
43.40	0.0154	0.00036
49.56	0.0205	0.00040
54.07	0.0256	0.00047
58.53	0.0308	0.00053
62.30	0.0359	0.00058
64.80	0.0410	0.00063
64.76	0.0462	0.00070
64.41	0.0513	0.00080
56.98	0.0564	0.00090
50.54	0.0615	0.00012
45.70	0.0666	0.00014
37.87	0.0718	0.00190

Transformed Unconfined Compression Test Data for C11-1.

σ (psi)	ε (in/in)	ε/σ (1/psi)
30.85	0.0051	0.00016
30.70	0.0101	0.00033
27.32	0.0152	0.00056
19.20	0.0203	0.00106
11.40	0.0253	0.00222
6.33	0.0304	0.00480

Transformed Unconfined Compression Test Data for C11-2.

σ (psi)	ε (in/in)	ε/σ (1/psi)
21.10	0.0052	0.00025
32.30	0.0104	0.00032
28.92	0.0156	0.00054
20.78	0.0208	0.00100
11.13	0.0260	0.00234
4.74	0.0311	0.00650

Transformed Unconfined Compression Test Data for D11-1.

σ (psi)	ε (in/in)	ε/σ (1/psi)
3.25	0.0057	0.00176
6.45	0.0114	0.00177
16.04	0.0171	0.00107
28.71	0.0229	0.00080
26.95	0.0286	0.00106
14.20	0.0343	0.00242

Transformed Unconfined Compression Test Data for D11-2.

σ (psi)	ε (in/in)	ε/σ (1/psi)
6.50	0.0054	0.00083
16.14	0.0108	0.00067
30.19	0.0162	0.00054
33.53	0.0216	0.00064
20.64	0.0270	0.00131
12.00	0.0324	0.00270

Transformed Unconfined Compression Test Data for E21-1.

σ (psi)	ε (in/in)	ε/σ (1/psi)
30.85	0.0051	0.00016
45.24	0.0101	0.00022
53.04	0.0152	0.00029
59.16	0.0203	0.00034
63.63	0.0253	0.00040
66.47	0.0304	0.00046
67.70	0.0354	0.00052
67.34	0.0405	0.00060
66.98	0.0455	0.00068
62.60	0.0506	0.00081
55.50	0.0557	0.00100

Tranformed Unconfined Compression Test Data for E21-2.

σ (psi)	ε (in/in)	ε/σ (1/psi)
29.23	0.0051	0.00018
46.90	0.0103	0.00022
56.24	0.0154	0.00027
62.35	0.0205	0.00033
66.15	0.0256	0.00039
68.97	0.0308	0.00045
72.07	0.0359	0.00048
72.00	0.0410	0.00057
71.61	0.0462	0.00064
69.68	0.0513	0.00074
64.68	0.0564	0.00087

Transformed Unconfined Compression Test Data for E31-1.

σ (psi)	ε (in/in)	ε/σ (1/psi)
25.98	0.0052	0.00020
33.92	0.0104	0.00031
37.60	0.0156	0.00042
38.36	0.0208	0.00073
39.74	0.0260	0.00065
40.80	0.0311	0.00076
42.46	0.0364	0.00086
43.17	0.0415	0.00096
43.25	0.0468	0.00110
45.18	0.0520	0.00115
45.55	0.0571	0.00113
45.30	0.0623	0.00138
45.05	0.0675	0.00150
44.80	0.0730	0.00163

Transformed Unconfined Compression Test Data for E31-2.

σ (psi)	ε (in/in)	ε/σ (1/psi)
12.34	0.0053	0.00043
21.96	0.0105	0.00048
26.34	0.0158	0.00060
29.40	0.0210	0.00071
31.15	0.0263	0.00084
31.61	0.0316	0.00100
33.01	0.0368	0.00110
33.77	0.0421	0.00125
33.89	0.0474	0.00140
34.63	0.0526	0.00152
35.67	0.0579	0.00162
35.47	0.0632	0.00178
36.20	0.0684	0.00189
35.98	0.0737	0.00205
35.77	0.0790	0.00220
35.57	0.0842	0.00236

Transformed Unconfined Compression Test Data for F11-1.

σ (psi)	ε (in/in)	ε/σ (1/psi)
19.48	0.0053	0.00027
32.30	0.0105	0.00036
44.74	0.0210	0.00047
47.04	0.0263	0.00056
49.00	0.0320	0.00065
50.30	0.0370	0.00074
52.53	0.0420	0.00080
53.48	0.0474	0.00089
53.20	0.0530	0.00100
52.90	0.0580	0.00110
52.60	0.0630	0.00120
39.86	0.0680	0.00171

Transformed Unconfined Compression Test Data for F11-2.

σ (psi)	ε (in/in)	ε/σ (1/psi)
19.48	0.0054	0.00028
32.29	0.0108	0.00033
36.93	0.0162	0.00044
41.52	0.0216	0.00052
42.88	0.0270	0.00063
43.58	0.0324	0.00074
43.97	0.0370	0.00084
43.72	0.0432	0.00099
41.92	0.0486	0.00116
38.60	0.0540	0.00140

Transformed Unconfined Compression Test Data for H11-1.

σ (psi)	ε (in/in)	ε/σ (1/psi)
14.61	0.0052	0.00036
32.30	0.0104	0.00032
43.38	0.0156	0.00036
49.54	0.0208	0.00042
54.05	0.0260	0.00048
58.50	0.0311	0.00053
61.34	0.0364	0.00060
62.57	0.0416	0.00066
62.23	0.0468	0.00075
55.70	0.0520	0.00090
38.47	0.0570	0.00148
32.14	0.0620	0.00193

Transformed Unconfined Compression Test Data for H11-2.

σ (psi)	ε (in/in)	ε/σ (1/psi)
22.73	0.0051	0.00023
32.30	0.0103	0.00032
40.17	0.0154	0.00038
44.76	0.0205	0.00046
49.30	0.0256	0.00052
53.78	0.0308	0.00057
56.65	0.0359	0.00063
61.04	0.0410	0.00067
62.30	0.0462	0.00074
61.94	0.0513	0.00083
58.52	0.0564	0.00096
49.01	0.0615	0.00125
38.10	0.0666	0.00175
28.78	0.0718	0.00250

Transformed Unconfined Compression Test Data for H21-1.

σ (psi)	ε (in/in)	ε/σ (1/psi)
8.11	0.0057	0.00070
14.16	0.0114	0.00080
20.34	0.0170	0.00084
28.00	0.0230	0.00082
30.92	0.0286	0.00093
33.81	0.0343	0.00100
35.14	0.0400	0.00110
36.45	0.0460	0.00126
38.12	0.0570	0.00150
38.48	0.0630	0.00164
39.73	0.0686	0.00173
32.61	0.0743	0.00228
39.53	0.0800	0.00202
37.83	0.0860	0.00230
26.63	0.0910	0.00340

Transformed Unconfined Compression Test Data for H21-2.

σ (psi)	ε (in/in)	ε/σ (1/psi)
12.98	0.0053	0.00041
29.06	0.0107	0.00037
35.43	0.0160	0.00045
43.13	0.0210	0.00049
46.07	0.0270	0.00059
48.97	0.0320	0.00065
49.65	0.0370	0.00075
50.00	0.0430	0.00086
50.96	0.0480	0.00094
51.93	0.0530	0.00102
51.62	0.0590	0.00114
47.35	0.0640	0.00135
45.57	0.0690	0.00150
40.77	0.0750	0.00185
26.96	0.0800	0.00297

Transformed Unconfined Compression Test
Data for J11 (only 1 specimen tested).

σ (psi)	ε (in/in)	ε/σ (1/psi)
22.90	0.0052	0.00036
22.10	0.0104	0.00047
22.75	0.0156	0.00069
23.44	0.0208	0.00090
23.79	0.0260	0.00110
27.31	0.0360	0.00132
27.20	0.0410	0.00150
27.00	0.0470	0.00170
26.90	0.0520	0.00190
26.70	0.0570	0.00214
26.60	0.0620	0.00230
26.40	0.0680	0.00260
26.80	0.0730	0.00270
26.10	0.0780	0.00300
25.70	0.0830	0.00320
24.70	0.0880	0.00356
24.30	0.0930	0.00383
23.80	0.0990	0.00400
23.90	0.1040	0.00450

Transformed Unconfined Compression Test
Data for J31-1.

σ (psi)	ε (in/in)	ε/σ (1/psi)
16.24	0.0051	0.00030
27.50	0.0101	0.00037
32.15	0.0152	0.00047
36.78	0.0203	0.00056
37.86	0.0253	0.00067
39.25	0.0304	0.00077
40.62	0.0354	0.00088
42.28	0.0405	0.00096
42.99	0.0456	0.00106
44.00	0.0506	0.00115
44.39	0.0557	0.00125
46.00	0.0608	0.00132
45.74	0.0660	0.00144
45.50	0.0709	0.00156
44.94	0.0760	0.00170

Transformed Unconfined Compression Test
Data for J31-2.

σ (psi)	ε (in/in)	ε/σ (1/psi)
22.73	0.0051	0.00023
33.93	0.0101	0.00030
38.60	0.0152	0.00040
41.24	0.0205	0.00050
42.94	0.0256	0.00060
45.24	0.0308	0.00068
47.20	0.0359	0.00076
47.63	0.0405	0.00085
49.85	0.0452	0.00091
50.82	0.0560	0.00110
52.40	0.0557	0.00106
53.30	0.0615	0.00115
53.01	0.0666	0.00126
52.40	0.0718	0.00137
51.83	0.0770	0.00149

VITA

Yaw Boateng-Poku was born in Ntonso, Ashanti Region of Ghana on July, 10, 1956. He attended a Catholic elementary school in Sunyani in the Brong-Ahafo Region. He was then accepted to Prempeh College from 1970 to 1975 and the Science College, Legon from 1975 to 1977 and successively passed all required examinations.

After a three-year break, within which he toured some West African nations, he came to the United States and entered Knoxville College in 1980. He transferred to The University of Tennessee in 1982, and received a Bachelor of Science in Civil Engineering in June 1986. In June of 1986 he accepted a graduate research assistantship at The University of Tennessee, Knoxville, and began study towards a Master's degree in Geotechnical Engineering. This degree was awarded in August 1988.

The author is a member of Chi Epsilon and the American Society of Civil Engineers.